Evaluations of Porous Burner Characteristic Diagrams and Process Water Production Possibilities

By

Fatih BACAKSIZ

**A Dissertation Submitted to the
Graduate School in Partial Fulfillment of the
Requirements for the Degree of**

MASTER OF SCIENCE

**Department: Energy Engineering
Major: Energy Engineering
(Energy and Power Systems)**

İzmir Institute of Technology

İzmir, Turkey

October, 2002

We approve the thesis of **Fatih BACAKSIZ**

Date of Signature

..... **18.10.2002**

Prof. Dr. Ing. Gürbüz ATAGÜNDÜZ

Supervisor
Department of Mechanical Engineering

..... **18.10.2002**

Assist. Prof. Dr. Fikret İNAL

Co-Supervisor
Department of Chemical Engineering

..... **18.10.2002**

Prof. Dr. Ali GÜNGÖR

Department of Mechanical Engineering

..... **18.10.2002**

Assoc. Prof. Dr. Barış ÖZERDEM

Department of Mechanical Engineering

..... **18.10.2002**

Assist. Prof. Dr. Gülden Gökçen GÜNERHAN

Department of Mechanical Engineering

..... **18.10.2002**

Prof. Dr. Ing. Gürbüz ATAGÜNDÜZ

Head of Interdisciplinary
Energy Engineering (Energy and Power Systems)

ACKNOWLEDGEMENTS

The author would like to express his sincere gratitude to his supervisor, Prof. Dr.-Ing. Gürbüz Atagündüz for his effort, encouragement and his invaluable guidance. The author is grateful to Assist. Prof. Fikret Inal for his suggestions and comments. It is a pleasure for the author to express their appreciation to Prof. Dr. Dr. h.c. F. Durst, without his kind invitation and support; this thesis could not be completed. Further the author very much appreciates the work by Dipl.-Ing. F. Avdic during the experimental work in Erlangen. One can remind that the burner was denoted by Alexander von Humboldt Foundation and the burner was manufactured by the "Lehrstuhl für Strömungsmechanik" of the University Erlangen under the supervision of Prof.Dr.Dr.h.c. Franz Durst. The author is thankful to Alexander von Humboldt Foundation and Faculty of Engineering, Izmir Institute of Technology for their support to fulfil this research work. The author would like to thank ELSEL Gaz Armatürleri A.Ş., Turkey for providing the gas flow meter used for experiments in Izmir. Finally, the author wishes to express his thanks to his family for their help and support during his studies.

ABSTRACT

In recent years, there has been a trend to new developments in gas and oil burners, which have been dominated by the aim of reducing pollutant emissions, reducing burner size and increasing the power modulation range. Several methods have been proposed in order to obtain more efficient combustion systems with low pollutant emissions. Over the past few years, a great deal of investigation on combustion in porous medium has been performed. In its efforts to optimize combustion processes, the Institute of Fluid Dynamics in Friedrich-Alexander University, Erlangen (LSTM-Nürnberg/Germany) has succeeded in developing the technology of combustion in porous media and this burner was used in this study.

This thesis was focused on the evaluation of the porous burner characteristic diagrams and determined the possibility of the process water production. The experimental works were consisted of two main parts. One of them was carried out at the Institute of Fluid Dynamics in Erlangen. The second was performed at Izmir Institute of Technology. The aim of the experimental work for 25 kW porous burner was to analyse temperature distribution of exhaust gases close to the outer surface of ceramic matrix as well as pollutant emissions as a function of the burner surface. The aim of the second part was to investigate pollutant emissions as a function of the burner power and excess air ratio numbers, analyse the exhaust gases and cooling water temperature distribution with respect to burner power. Liquefied Petroleum Gas (%70 Butane + %30 Propane) was used as a fuel, which is utility gas in Turkey.

It was concluded that the 25 kW burner allow very stable combustion with turn down ratio of around 6:1, and 4:1 for 10 kW burner, and excess air ratio numbers in the range 1.40 - 2.0. The exhaust gas temperature could easily reach 1100°C with a more and less uniform distribution over the 25 kW burner's exit surface area. It was noticeable that the emission values lie lower than the values given by both German Norm 4702 and International Energy Agency, for 25 kW porous burner. CO an NO_X emission values for 10 kW porous burner were quite lower than the emission limits for large new combustion facilities in Turkey. The burner showed that considerable amount of heat was transferred from exhaust gas to cooling water. Finally, porous burner can be used for process water production in various fields of energy engineering.

ÖZ

Son yıllarda gaz ve sıvı yakıtlı brülörlerin gelişmesinde, emisyon değerlerinin düşürülmesi, brülörlerin çalışma güç aralıklarının genişletilmesi ve hacimlerinin azaltılmasına yönelik çalışmalar yapılmış ve önemli gelişmeler sağlanmıştır. Verimli ve düşük emisyon ürünlü yanma yapabilmek için bir çok araştırma yapılmaktadır. Poröz ortamda yanma bu araştırma konularından biridir. Bu tezde Friedrich-Alexander Üniversitesi, Erlangen-Nürnberg/Almanya, Akışkanlar Mekaniği Kürsüsü'nde geliştirilen ve endüstride kullanılan brülörlere göre daha verimli bir yanma yapabilen poröz başlıklı brülörler incelenmiştir.

Bu çalışmada poröz brülörün çalışma karakteristiklerinin değerlendirilmesi ve proses suyu üretimine uygulanabilirliği araştırılmıştır. Bu amaçla deneysel çalışma iki ana kısımdan oluşmuştur. Birinci kısımdaki deneyler Erlangen'de yapılmıştır. Deneylerin amacı poröz malzeme olarak kullanılan seramik matristeki sıcaklık dağılımının, yanma ürünlerinin brülör gücü ve hava fazlalık katsayısı ile değişiminin incelenmesidir. İzmir Yüksek Teknoloji Enstitüsü'nde yapılan deneyler çalışmanın ikinci kısmını oluşturmaktadır. Bu deneysel çalışmadaki amaç ise ülkemizde mutfak gazı olarak kullanılan sıvılaştırılmış petrol gazının yakılarak poröz brülörün davranışının incelenmesidir.

Bu çalışmalar sonunda her iki brülörde de, hava fazlalık katsayısının 1.40–2.0 değerleri arasında daha verimli bir yanma yapıldığı ve 25 kW'lık brülörde çalışma güç aralığının 6 kat, 10 kW brülörde ise 4 kat arttığı gözlenmiştir. 25 kW'lık brülörün çıkışından alınan egzoz gazı sıcaklığının 1100ºC ulaştığı ve brülör çıkışında sıcaklık dağılımının düzgün olduğu görülmüştür. 25 kW'lık brülörden elde edilen emisyon ölçüm değerlerinin Alman normu 4702 ve Uluslararası Enerji Ajansı tarafından verilen emisyon değerlerinden düşük olduğu, 10 kW'lık brülörden elde edilen emisyon değerlerinin de Türkiye'de büyük yanma uygulamaları için istenen değerlerden düşük olduğu görülmüştür. 10 kW'lık poröz brülörde egzoz gazlarından önemli miktarda ısının soğutma suyuna transfer edildiği gözlenmiş ve poröz brülörlerin enerji mühendisliğinin değişik bir çok alanında kullanılabilir olduğu sonucuna varılmıştır.

TABLE OF CONTENTS

LIST OF FIGURES

LIST OF TABLES

CHAPTER 1

INTRODUCTION

In recent years, in order to accept the countries as being developed in the view of technologically and economically, it is necessary to relate with the innovations in the field of technology and their usefulness for the environment. For the countries that achieve the energy demand from the primary fuels, to provide clean combustion is an important problem that has to be solved. In the aspect of this view the burners, which are used for realising combustion, possess important role for this matter.

Porous medium burner technology is a novel combustion technology, which, after initial experiments at the Institute of Fluid Mechanics at the University of Erlangen-Nürnberg, has now been developed to series maturity. In porous medium burners, the combustion process takes place in cavities (several millimetres in size) of an inert porous medium. The intensive heat transfer between the gas phase and the porous medium that this entails gives rise to a unique combination of advantages for combustion technology: the burners are compact, have low pollutant emissions and can be adjusted continuously over a wide range of powers [1].

There has been a recent surge of interest in the combustion of hydrocarbon fuels within porous inert media and the surface of the porous burner. Much research on porous burner has been done in the last decade. An overview of the research of combustion in porous media is given in literature [2]. The differences between catalytic porous media and inert porous media were described in this study. Catalytic porous media have the advantage of a large surface area per unit volume, where the chemical reaction takes place. When a porous inert medium is used as a flame holder, the combustion can take place within the burner, or close to the surface of the burner. Both combustion modes are shown in Figure 1.1.

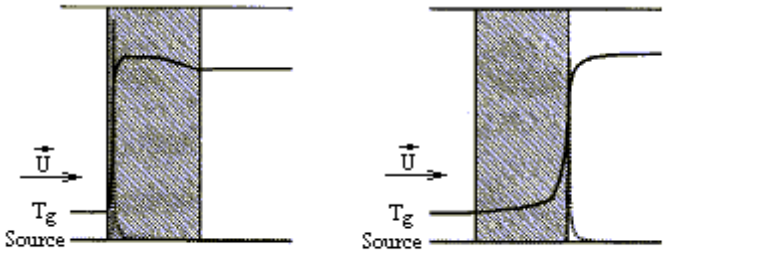

a) Combustion within a porous medium b) Surface combustion on a porous medium

Figure 1.1. Combustion within porous inert medium and combustion stabilised near the surface [3]

Combustion within a porous medium is presented in Figure 1.1.a. The flame stabilises in the first part, near the inlet of the porous burner. The gas temperature Tg reaches its maximum value inside the porous medium, and decreases due to cooling downstream. Surface combustion is shown in Figure 1.1.b. The flame stabilises near the outlet of the burner and the volumetric heat release reaches its maximum near the surface. The gas temperature reaches its maximum value outside the porous medium near the surface and the burner through conduction cools the flame [3].

The surface burners are studied only in the radiant mode in the literature. Radiant burners are divided into many classes and subclasses (Figure 1.2.), [4].

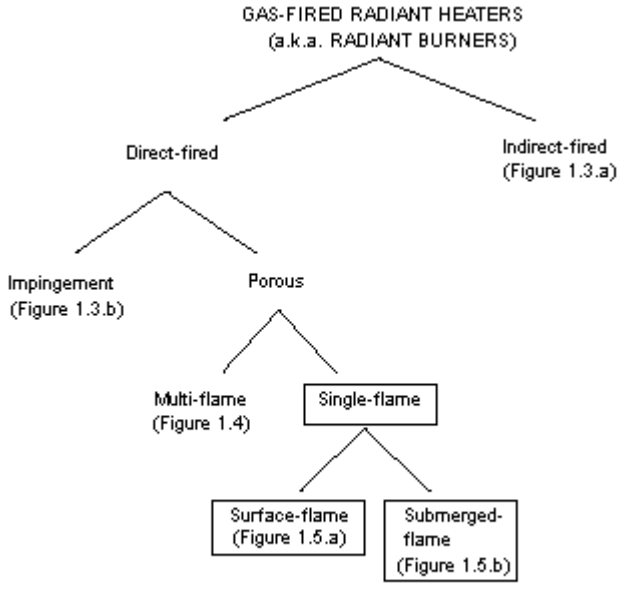

Figure 1.2. Classes of gas-fired radiant heaters [4]

The first division of radiant burners is into indirect-fired burners and direct-fired burners. Indirect-fired burners contain the flame and prevent combustion products from contacting the object being heated (the "load"). In contrast, the combustion products from a direct-fired burner can contact the load. The most common indirect-fired burners enclose a flame inside a tube. They are called radiant-tube burners. The flame - usually a non-premixed jet flame - heats the inside of the tube, which then radiates to the load. Figure 1.3.a, shows a schematic of a radiant-tube burner. Fuel and air enter on the bottom left and burn within the enclosure. The hot combustion products pass through the tube, heating it to incandescence. The inside of the tube is designed to facilitate a high heat transfer rate between the tube and the hot gas flowing through the tube.

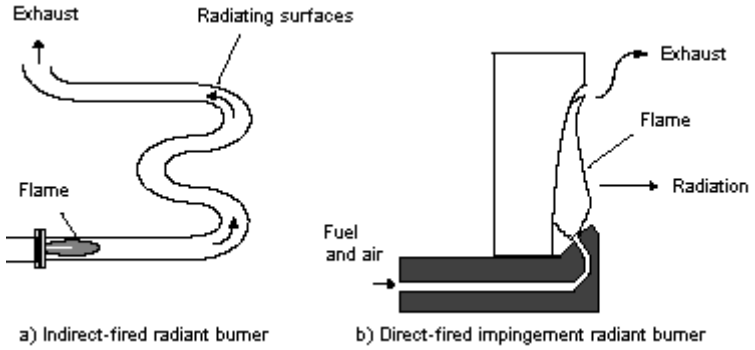

Figure 1.3. Two types of radiant burners [4]

Radiant tube burners have several disadvantages. Emissions of nitrogen oxides ($NO_X \rightarrow NO + NO_2$) can be quite high when a non-premixed flame is used because the non-premixed flame might have hot zones, which can lead to elevated NO_X formation rates. Also, the limited contact between the flame and surface can lead to low radiant efficiency, which may require use of large tubes to achieve the required heat flux. Despite these shortcomings, radiant-tube burners are frequently used in situations where contamination of the load is unacceptable, such as in metal treating.

Depending on the flow path of the gas and the position of the flame, direct fired radiant burners can be divided into two classes: impingement radiant burners and porous radiant burners. Figure 1.3.b, shows an impingement radiant burner in which a flame impinges on a refractory surface. The surface is heated by the flame and radiates to the load. Several features of this design limit its usefulness, such as the small contact area between

solid and gas. The possibility of high refractory temperatures, though, makes these burners a popular choice for high temperature applications such as metal treating.

In porous direct-fired radiant burners the combustion gases pass through the radiating material. Porous direct-fired radiant burners can be further sub-divided into two classes: burners, which consist of multiple flames "multi-flame burner", and burners, which consist of one continuous flame "single-flame burner". The ported-tile burner is a popular multi-flame porous direct-fired radiant burner (see Figure 1.4.). Ported-tile burners are made from a non-porous ceramic block that has been cast with an array of holes. Premixed air and fuel flow through each hole and a small premixed flame from each hole heats the ceramic block. The small contact area between the flame and the ceramic limits the efficiency of ported-tile burners.

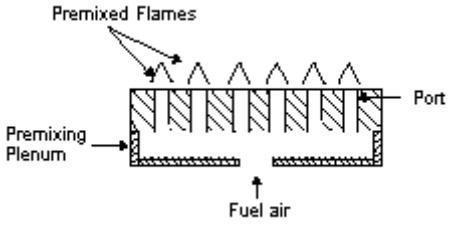

Figure 1.4. Cross-section diagram of a ported-tile burner [4]

Single-flame burners can be further subdivided into two sub-classes: burners in which a single flame is on the surface of the porous medium "surface-flame burner" and burners in which a single flame is entirely within the porous medium "submerged-flame burner". Figure 1.5, shows schematic drawings of a surface-flame burner and a submerged-flame burner. The porous medium can take many forms, with porous media in current designs consisting of metal fibres, ceramic fibres, bonded hollow spheres, and ceramic foam, to name a few [4].

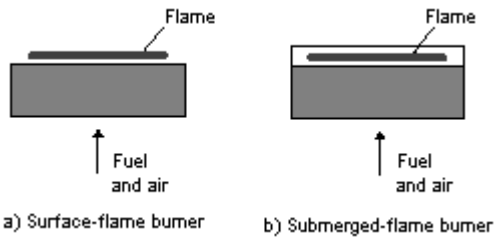

Figure 1.5. Two types of porous direct-fired radiant burners [4]

Chapter 2 describes the porous medium burners in detail; theoretical background and up-to-date review of the porous medium burner technology are presented. Fluid mechanics, combustion in porous media, heat transfers in porous medium, combustion products and emission measurements are briefly mentioned. Basic construction of the porous medium burner is also presented. The porous medium burner technology can be applied to many industrial branches, which are given in Chapter 3, due to the conspicuous properties. In Chapter 4, the experimental works have been described and their discussions are provided in Chapter 5.

CHAPTER 2

POROUS MEDIUM BURNER TECHNOLOGY

In recent years, new and improved burner concepts, especially for gaseous fuel, have been developed and provide the basis for low NO_X and CO-emission combustion systems. In the case of heating applications, the systems consist of separate combustion and heat exchanger section, although both parts are commonly integrated into the housing. It is general practice to build combustors in such a way that they contain free burning flames in an enclosure acting as a combustion chamber. The hot gases from the combustion chamber are subsequently fed through heat exchangers. This concept leads to large heating systems, requiring special heating rooms in household applications. In addition the employed burner concepts result in small operating windows with respect to the power and air to fuel ratio. In general burners can only be regulated in the range of $P_{max}/P_{min} \approx 2$, although a wider dynamic range is generally considered to be of advantage. Hence existing heating systems are considered to be too large in size and have in insufficient dynamic range but most modern burners show a good performance regarding emission products. Nevertheless more stringent requirements on NO_X emissions may be anticipated in the not too distant future and markets requests for smaller and cheaper household heating systems can be foreseen. As a consequence there is a continued interest in low emission burner technology for both gas and liquid fuels and also in more compact systems [5].

Most premixed combustion technologies are characterized by free flame structures, which are very thin. The chemical reactions occur in a small region, while the rest of the combustion chamber is not used as far as main chemical reactions are concerned. The reason for the thin combustion zone lies in the poor heat transfer properties of the gas mixture. Taking into account that these attributes are improved by inserting solid materials within the combustion region, that is the reason why it is named porous burner, using their superior thermal properties (e.g. thermal conductivity, thermal radiation), combustion within porous media has been receiving increased attention and numerous porous burners investigated. In general porous media burners can be classified in two groups;

1. Matrix stabilized porous burners

   Burners with flame stabilized and burning completely inside the porous matrix.

2. Surface stabilized porous burners

   Burners with flame stabilization near or on the porous materials surface with a significant part of the combustion process take place outside of the matrix.

In fact, when compared to conventional combustion process with free flame burners, higher burning rates and increased flame stability characterizes especially porous medium burners with flame stabilization within the porous material. Furthermore, combustion zone temperatures are controllable so that emissions of pollutants such as CO and NO_X are minimized. On account of these qualities, there are diverse fields of application for the porous media combustion such as water or air heaters for industrial and domestic applications, steam generators etc. [6].

2.1. Principle of Porous Medium Burner

Combustion in inert porous media has become a recent subject of interest because it offers higher power densities, higher power dynamic ranges and smaller emissions than free flame combustion. In porous medium combustion, a porous inert medium is used to sustain and enhance combustion within the solid matrix [7]. A simplified scheme of a porous burner is shown in Figure 2.1. This burner does not work as a catalytic combustor but burns with flames within the pores of a porous medium. In this kind of burners, the premix air enters the hotter porous matrix and is heated by convection as it passes through the voids of the porous media. The porous media in this region (pre-heating region) has been heated by conduction and radiation from the combustion region. This energy feedback mechanism that is created is responsible for the good characteristic of inert porous media combustion. Such burners offers an interesting and potentially promising route towards burners with high power density, high power dynamic range, low emission products, enhanced flame stability, extended flammability limits and high efficiencies [8,9].

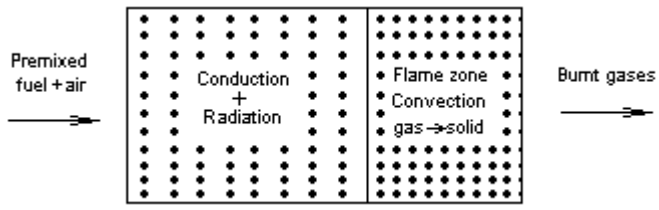

Figure 2.1. Simplified porous burner scheme [8]

2.1.1. Investigations of Porous Medium Burners

Recent research and development in the area of combustion and burner design have been motivated by the desire to preserve a clean environment and to reduce energy consumption. In order to obtain more efficient combustion systems with low pollutant emissions, several methods have been proposed. Many of them use various heat transfer mechanisms to reticulate the product enthalpy to the pre-combustion zone [10].

Over the past few years, a great deal of investigation on combustion in porous medium has been performed, starting with basic experiments by mostly Russian scientists, who found the combustion regimes and the flame propagation criteria for porous medium combustion [11].

Porous inert media burners can be grouped as combustors, combustor-heat exchangers, and combustor-radiant heaters. These three categories are dictated by the main function of the burner. Combustors convert the chemical energy of the fuel to the sensible energy of the products. In addition, the products' energy is transferred to the process fluid circulated through a heat exchanger incorporated in the porous media in the combustor heat exchangers or to radiation in combustor-radiant heater [12].

Burning associated with heat exchangers has diverse applications. Many techniques use various heat transfer mechanisms to recirculate the product enthalpy to the pre-combustion zone. Premixed combustion within a porous medium is a direct application of porous media to an excess enthalpy flame. An accelerated flame in a nozzle packed with 40% porosity material was reported in 1954. Experimental data on combustion within sand of different calibrated sizes presented in 1966 [13]. A simple semi-empirical model to compute flame speed and account for the effect of solid conduction preheating, convection, and heat of reaction was established.

A porous solid of high conductivity was inserted into the flame to conduct the post flame enthalpy to aid in preheating the fresh mixture. By choosing the porosity of the solid to alter the heat transfer coefficient between the solid and gas, so that the excess enthalpy

could be controlled. An iron block with many small, straight, and parallel holes was used as a major component of excess enthalpy burner. When burning methane, the stable burning rate could be extended below the normal lean limit. It is considered that heat flow to surroundings governed the flame stability. As the flow rate increased, heat loss became relatively insignificant; therefore flammability was extended further [14]. Separate energy equations for gas and solid were considered in an improved numerical model. An important result of this analysis was that a maximum critical flow rate exists, above which the system cannot sustain combustion. With heat loss introduced, this maximum critical flow rate was reduced. In addition, there was a minimum flow rate, below which no combustion was possible. In later analyses, it is reported that the flame could be stable only on the positive gradient portion of the flame speed versus flame location solution curves [15].

Many small diameter ceramic tubes in a bundle as the porous medium were tested in a series of experiments with excess enthalpy flames. The experiments showed:

1) Flame could actually be stabilized in three regions, one within the tube bundles,
2) Emissions of NO_X and CO were reduced remarkably when flame was stabilized inside the tubes,
3) With internal and external recirculations, the peak flame temperature was more than twice the adiabatic flame temperature at equivalence ratios around 0,18 for city gas. However, significant drawbacks in these analyses were found. First, the chemical reaction rates were only modeled as an exponentially temperature dependent term in the gas energy and species equation. Second, no radiative heat transfer was considered, which significantly affected the predicted combustion phenomena. Third, the porous material was assumed to have infinite thermal conductivity. This further deviates from reality since the material is a ceramic. Therefore, all analyses are meaningful only for qualitative trends.

Another experiment is similar to that performed in 1954. The results of this study showed that the flame speed exceeded normal values by 1-30 times, and speed grew as the pressure increased. It was found that the flow within the porous medium was turbulent with fine-structure fluctuations. However, the effects of heat recirculation mechanisms within the porous packing were not considered. Later, two distinct flame speeds were reported in a more recent paper. As the pore size was reduced, so was the flame speed. This was confirmed the experiments which were made in 1966 [16].

A new experiment, which consisted of a ceramic block with seven large straight holes that serves as flame holders, was made in 1984 [17]. Thermally stabilized combustion was accomplished within the holes through the action of wall-to-wall radiation, in-wall

conduction, and wall-gas convection and intensification of heat transfer in the laminar-turbulent transition. Utilizing the simple geometry of the burner and neglecting gas radiation and kinetics effects, an analysis showed that as many as seven stable steady flame fronts existed within the holes for a given flow rate [17].

A rigorous model for multi-mode heat transfer, Arrhenius-type one-step reaction kinetics, and exact solution for radiative transfer in the absorbing/emitting medium was presented in another experiment. However, scattering effects and an optical thickness were not considered [18].

In a more recent development reticulated dodecahedral structure ceramic foam as the heat-recirculating medium, which has several advantages over other forms of porous materials, was used. First, except for some metal alloys, it has a higher operating temperature than metallic porous media does. Second, the typical porosity falls in the range of 84-87%, which incurs less pressure loss. Third, it has much larger volumetric surface area than the small tube bundles or the ceramic block with straight-through holes. Hence more convective heat transfer is possible between the gases and solid. However, due to the large optical thickness of the ceramic (on the order of 30-300), the radiative penetration effect is confined to a short distance. Noting the deficiency of one-step kinetics in the analysis, multi-step kinetics for methane flame modeling was used. It is obtained that a maximum temperature lower than that predicted by one-step kinetics. However, due to convergence difficulties, only a limited range of solutions ($0.8 \leq \Phi \leq 1$) were obtained. Experimentally, flame speed exceeded the free laminar flame speed and increased with pore size. Lower NO emissions were also found experimentally within the range of $0.60 \leq \Phi \leq 0.95$ in the porous ceramic burner with a flame holder to stabilize the flame [19].

Another experiment was performed in 1989. Its results showed that the flame can be stabilized in two spatial regimes: one in the upstream half and the other near the downstream end of the porous medium. This analysis modeled scattering effects by using the spherical harmonics approximation and included one-step kinetics. It confirmed the flame stability characteristics they observed experimentally. However, without accurate thermo-physical properties its model could not produce quantitative prediction [20].

It is presented a similar experiment and analysis was made, but honeycomb ceramic used as a burner. In the analysis, the global reaction rate for a propane/air flame and surface radiation feedback were included. Except for the peak flame temperature, the analysis provides reasonable agreement with measurements of burning rate and temperature profile because of the well-defined geometry. Two types of stable flame were observed: a one-

dimensional flame at a higher flame speed and a highly two-dimensional flame at lower flame speed. The two types of flame correspond to the higher and lower burning speed solutions calculated by the one-dimensional flame analysis with an adjustable heat loss term in the solid phase energy equation.

In all previous work, on the theoretical modeling of combustion within porous inert media and detailed chemical kinetics is not considered. Due to the stiffness of the kinetics, the high nonlinearity with temperature of radiation flux, and significant computational requirements that is available only on super computers. With the multi-step kinetics included, the study of pollutant emissions (CO and NO_X) and the effect of radical generation in the preheating zone are possible [21].

A lot of research efforts were dedicated to the numerical modeling of heat transfer and combustion in porous media. Most of the studies are one-dimensional and used averaged heat transfer properties; the most advanced may use a direct discretization of the porous structure. Other criteria are the modeling of flame stabilization, heat transport mechanisms and chemical kinetics. An early work on surface stabilized burners was performed in 1988, which was applied a one-dimensional two-phase model with one-step kinetic to investigate the effects of heat transport parameters on the flame structure and burning velocity. It was found out that one-step kinetic model lead to an over-prediction of peak flame temperatures in 1993. Therefore, a one-dimensional model wherein the detailed chemical kinetics as well as the energy exchange between solid and gas were considered for a porous media with stabilization in the matrix. The influences on temperature and species profiles and flame speed were determined. A similar model was used for prediction of NO emissions in surface stabilized burners. This two-phase model is limited to adiabatic and one-dimensional conditions. It was used a two-dimensional model for numerical simulations on a combustor heater with matrix stabilization in order to predict thermal efficiency, flame location, temperature distributions and pressure drop. The effects of changes in excess air, firing rate, porous size, geometry, activation energy and thermal conductivity were investigated. The model was, however restricted to one-step kinetics.

Another investigation is the combustion in a porous medium made of in-line or staggered arrangements of discrete or connected square cylinders. This two-dimensional numerical simulation differs from volume-averaged methods, but is not necessarily more accurate because it is difficult to transfer a three-dimensional unordered structure into a two-dimensional. Moreover, calculations were made only for adiabatic cases with a simple one-step kinetic model. Although such direct simulations give useful hints about

temperature distribution, flame velocity and interfacial heat transfer, they are not capable of predicting in detail the effects of the processes in the flame.

These models are merely a selection of works. In all these models either the heat transport in the porous medium or the porous medium geometry is modeled very exactly (i.e. by two-phase models, or models with direct discretization of the porous structure) or the chemical kinetics is considered in detail (i.e. by multi-step kinetics). These basic thoughts were taken up and continued by the Institute of Fluid Mechanics/University of Erlangen/Germany. Porous Medium Burners with matrix stabilization were developed. Because of an important influence of lateral heat loss in these burner constructions, which consist of small burner cross-section areas with a remarkable heat removal to the combustor walls, a two-dimensional model is necessary. The porous medium is modeled as pseudo-homogenous and is based on an effective thermal conductivity, which consists of radiative conductive and disperses heat transport mechanisms. The kinetics is modeled with 20 species and 164 reactions. This means a two-dimensional model is used, where in contrast to former models all heat transfer mechanisms and comprehensive kinetics are considered simultaneously. The applied flame stabilization concept is based on a sudden change of the porous size. This corresponds to a change of modified Péclet number and thus flame stabilization is performed at the interface of the porous regions with flame quenching (low porous size) and flame propagation (large porous size) [6,22].

2.1.2. Fluid Mechanics of Porous Media Burners

Studies of flows through porous media have dealt mostly with materials of relatively low porosity. For situations where the flow velocity is low and the particle or pore size of the porous media is small compared with the hydrodynamic length scales, inertial forces are usually negligible. For these types of flows the flow rate is proportional to the applied pressure differential, expressed through Darcy's law in one dimension as

$$u = \frac{K}{\mu}\frac{\partial P}{\partial x} \tag{2.1}$$

where u is the flow velocity, μ is the viscosity of the fluid, P is pressure, and K is the specific permeability of the medium, having dimensions of (length)^2. The permeability can vary many orders of magnitude for different media, and is a measure the medium's resistance to flow. The permeabilities of media used for PIM burners are very large due to their high porosities [23].

Large vortex structures and large friction coefficients, resulting in an extensive momentum and interphase energy exchange between the gas and the solid phase characterize gas flows through porous media. Ceramic pebbles, ceramic foams, metal foils, etc. can be used as porous media, resulting in different properties of the porous matrix. The porosity ε (void fraction) of the porous medium (PM) is defined as:

$$\varepsilon = \frac{free\,volume\,of\ pores}{PM\ volume} \tag{2.2}$$

Typical values for a pebble bed are 0,36<ε<0,45 for any pebble diameter δ. The specific surface 'a' per unit volume of the inner PM is generally large. For example for a packed bed formed from spheres with a diameter δ:

$$a = \frac{6(1-\varepsilon)}{\delta} \tag{2.3}$$

which is much larger than the specific surface of a tube (2/r). The hydraulic diameter d_h of the pores is for a bed of packed spheres:

$$d_h = \frac{\varepsilon\delta}{3(1-\varepsilon)} \tag{2.4}$$

2.1.3. Combustion in Porous Media

Combustion in porous media offers many advantages in comparison to the conventional free flame. A higher burning rate decreases the burner size and increases the combustion stability within a wider power modulation range. The improved heat transfer in the porous medium smoothes the temperature peaks and reduces therefore the production of the waste gas emission of NO_X and CO. Furthermore the combustion chamber geometry can be varied. As the operating temperature is larger than 1300ºC the porous material as well as the shape are a subject in which there are necessary further researches. These numerous advantages and the advanced developments make already possible many applications in household and industry in burners and engines.

It is very important to optimize the burning technique as it is the main technique to release the chemical energy that is in fuel, e.g. oil, natural gas, wood, etc. which is the main energy source mankind uses. The way to release this energy is by burning the fuel, which is an exothermal reaction conventionally in free flames. But free flames have several disadvantages. As the heat conductivity and the radiation of gas is very small the reaction layer is very thin, i.e. that the whole reaction takes place in this small area and therefore the

whole reaction enthalpy is released in this area. This causes high temperature peaks of about 2000 K whereas in other areas there is no reaction and very low temperatures. So the temperature gradient is high. This is also the reason for the high waste gas emissions. High temperature causes the production of nitrous oxides NO_X, which are a big problem in burning processes. This thin reaction zone also determines a large combustion chamber for a useful heat output, which means an unsatisfying space utilization of the burning chamber. Also the stability of the flame is a point to optimize. A flame is stable and self-maintaining if the heat transfer upstream to heat up the cool reactants to the ignition temperature is as fast as the gas velocity. If the flame propagation is slower, the flame will be blown out. If it is too fast, there will be a flashback. To increase the power density an increase of the gas velocity (i.e. by burning more fuel) does not guarantee a stable combustion but at the worst the flame is blown out. The variation of power density is not trivial in free flames. That's why a turbulent movement in the flame is developed. It folds the flame, increases the flame zone and improves the heat transfer. But there are several disadvantages of this turbulence, e.g. the noise and the high-energy consumption.

To improve the heat transfer in the burning chamber from product to reactant it is applied a porous medium that has a higher heat conductivity and radiation than gas. The glow in the porous medium is not a flame but the radiation of the porous medium. The combustion in porous medium proceeds even without flames. The higher heat conductivity in axial and radial direction results in a higher flame velocity (10-30 times faster) and a higher burning rate in comparison to the free flame. The temperature distribution is consistent.

Several scientists have investigated flame propagation through porous media. The experimental work was performed in tubes filled with the PM and the premixed fuel-air mixture. The propagation of the flame front, temperature, pressure etc. was recorded at several places in the tube after ignition at one end. It was found that five steady combustion regimes (steady propagation velocity of the flame front across the tube after a short entrance length) existed for combustion in porous medium with different flame propagation mechanisms. An intermediate rapid combustion regime between the high velocities regime and sound velocities regime was identified [6]. These velocity regimes were presented in Table 2.1.

Table 2.1. Flame propagation regimes in porous media [5]

Regime	Wave velocity (m/s)	Flame propagation mechanism
Low velocities (LVR)	$0\text{-}10^{-4}$	Heat conductivity, interphase heat exchange
High velocities (HVR)	0.1-10	Convective, uniform pressure
Rapid Combustion (RCR)	10-100	Convective, smooth pressure gradient
Sound velocities (SVR)	100-300	Convective, pressure gradient
Low velocity detonation (LVD)	500-1000	Self ignition under shock wave interaction
Normal detonation (ND)	1500-2000	Detonation under heat and pulse losses

In the present work the HVR and RCR are of greatest interest regarding the practical applications of combustion in PM. Babkin et al. was proposed by the following flame propagation mechanism for these regions. A positive feedback between flame acceleration and turbulence production (the flame acceleration causes turbulence, which in turn leads to flame acceleration) is damped by local quenching of the chemical reaction due to intense heat exchange in the turbulent flame zone. If the characteristic time of thermal relaxation becomes less than that of chemical conversion the flame will be quenched. Since turbulent flow contains a spectrum of instantaneous gas velocities those parts of the flame moving with the maximum velocities will be quenched, resulting in a stable velocity of flame propagation. It must be noted that the frictional resistance in the PM greater by several orders of magnitude than that in smooth or rough pipes. Regardless of such high resistance and heat losses, steady combustion and detonation regimes are proven to be possible [6].

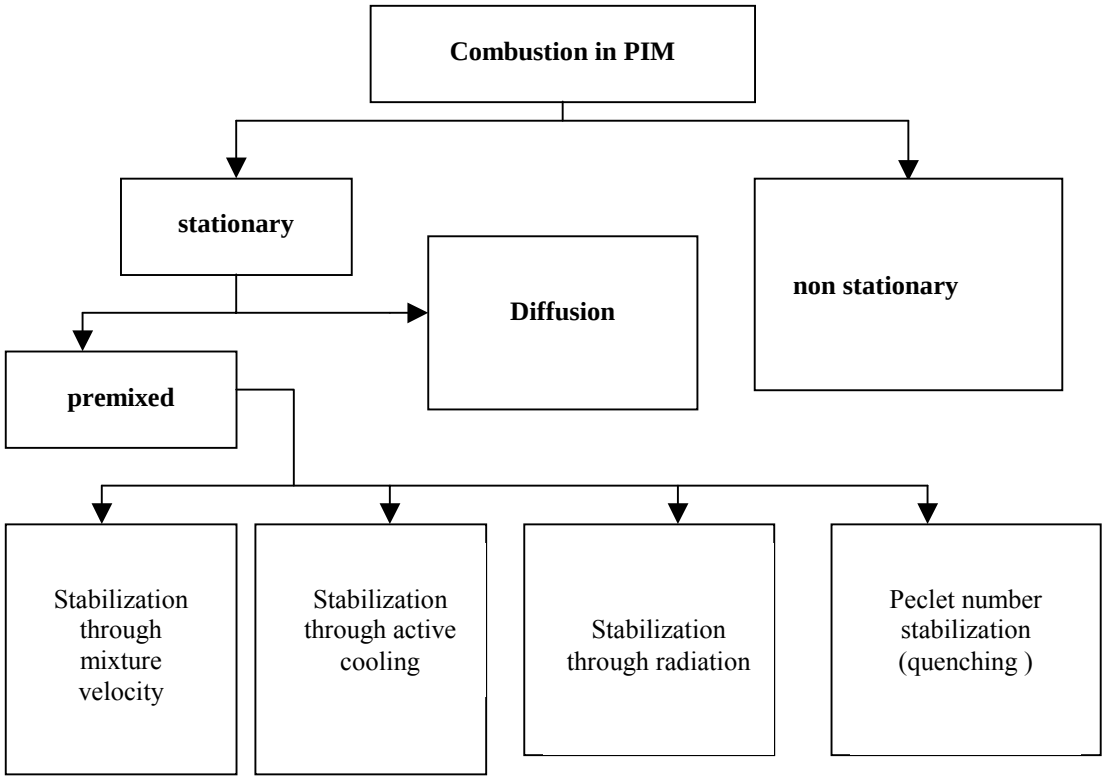

Figure 2.2. Combustion in porous inert media [24]

There are several possibilities to make the flame stable, i.e. there should be no flashback and also no quench of the flame.

In general it is easier to stabilize a flame in a porous medium than in the free space of a conventional burner due to the higher heat capacity of the solid, which accumulates the heat energy. This stabilizes the flame even at fast fluctuations of fuel or air quantities.

It is possible to stabilize the combustion in porous medium through mixture velocity: The gas velocity at the entrance of the PM must be higher than the flame velocity that is in the combustion zone. This can be realized by enlargement of the cross section, or a temperature based controlling of the gas mixture or an increase of porosity.

The second possibility is based on temperature. The temperature influences the reaction. In a colder gas the reaction rate is smaller therefore less fuel reacts. So, active cooling controlled (and stabilized) the reaction rate.

The most common technique nowadays to stabilize the flame is the stabilization through radiation. The premixed gas flows through a porous medium. The reaction takes place partly in and partly close to the PM. As there is only a small distance between reaction zone and surface of the PIM, the PM absorbs the released heat-by-heat conduction. It begins to glow and radiates heat energy. The temperature of the solid and gas decreases. A higher

flow rates increases the distance between PM and reaction zone. There is less heat absorption and therefore less radiation of the PM, more heat energy remains in the PM. This increases the burning rate and the flame velocity upstream. If the flow rate gets too high, the flame behaves like a free flame and is blown out. If the flow rate decreases, the flame takes place in the PM that will absorb and radiate more heat energy and stabilize the flame in this way. If the flow rate gets too small, there can be a flashback or the heat production is smaller than the heat conduction and radiation so that the flame is quenched. These limits to the lower and upper flow rate offer nevertheless a wide range of flow rate and power density.

The fourth possibility to stabilize the combustion in PM is the Péclet number stabilization. It is researched and developed at the department of Fluid Mechanics of the University of Erlangen-Nürnberg. It is based on a combination of a porous material with small pore sizes that quenches the flame and a porous medium with bigger pore sizes where the reaction proceeds. The reason for quenching the flame at a critical pore size is determined by the heat conductivity of the porous medium. If the pore size is smaller than the critical one, the cavity volume is smaller and therefore the inner surface is larger. So the heat conductivity from the gas to porous medium is better. More heat is removed than it is produced by reaction. The flame is extinguished.

A modified Péclet number for the flame propagation in porous media can determine the critical pore size. If the Péclet number of a PM is smaller than 65 there cannot be combustion in this PM.

$$Pe = \frac{S_L \, c_p \, \rho \, d_m}{\lambda} \qquad Pe \geq 65 \tag{2.5}$$

S_L : laminar flame velocity

d : equivalent porous cavity diameter

c : heat capacity of gas mixture

ρ : density of gas mixture

λ : heat conductivity of gas mixture

It can be interpreted as ratio of equivalent porous cavity diameter and the laminar flame thickness. It can also be interpreted as ratio of heat production rate to heat removal rate.

The advantage of this stabilization technique is the more variable power range of 1:20. Furthermore it can be done without any expensive constructions of e.g. cooling elements [24].

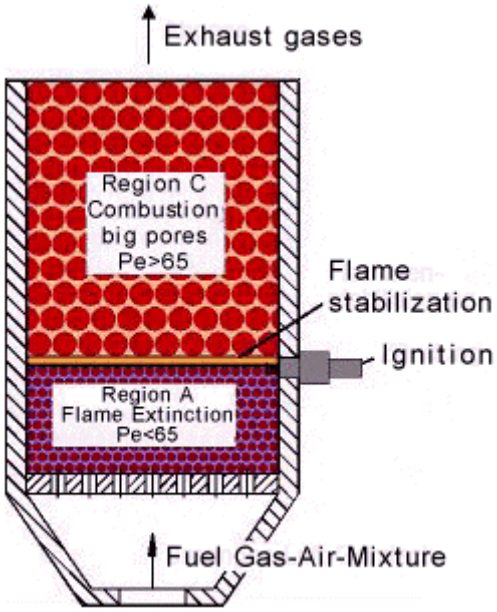

Figure 2.3. Cross-section of the burner with two porous regions [11]

In the case of combustion and heat transfer, the hydraulic diameter d_h is not suitable characteristic dimension for diameter (d_m). Another method was proposed for determining the typical diameter d_m of the pores, in which d_m is the quenching diameter for a cylindrical tube in those cases where the porous matrix acts as a flame trap [5]. It was found that for sphere packing, the equivalent diameter for a PM cavity space is:

$$d_m \approx \frac{\delta}{2.77} \tag{2.6}$$

The characteristic cooling time of the hot gases were calculated as the time in which the temperature of the hot gas in the porous medium diminishes towards the temperature of the porous matrix. The cooling time multiplied by the flame front propagation velocity resulted in a characteristic cooling distance < 5 mm for all known experimental cases. The recorded flame front thickness in the same experiments was several centimeters. This means that the chemical transformation and cooling of the combustion products proceed simultaneously in each section of the PM, if the cooling distance is much less than the reaction region thickness. Cooling of the combustion products terminates in practically the same section where the chemical reactions stop [5].

In order to realize steady combustion in porous media, the heat transport was adjusted in such a way that the combustion process is stabilized at a specific position of the combustion chamber. Practically, this was reached by a steep gradient in the pore size of the porous matrix. This means that there is a preheating region with small pores (region A) behind the combustion region (C), where the cavity space diameter is larger than the quenching one. After ignition, combustion is self-stabilized at the interface between the two regions and a three-dimensionally extended reaction zone appears. A change in the load of the burner does not effect the starting location of the combustion region, but only changes its length. Since the walls of the burner are cooled with water, the combustion region was inserted with 10 mm layer of insulating ceramic material in order to avoid incomplete reactions and CO emissions, but have a controlled heat removal from the combustion zone at the same time.

Quenching in the first region A prevents combustion, if the temperatures are kept low enough. In the combustion region, the effective heat transport processes can be adjusted by selection of suitable structures and materials so that a very high power modulation is possible. These heat transfer properties can be related to the geometry of the matrix and to the heat transport properties of the solid materials being used. The structure of the porous material affects the radiative heat transport by its optical thickness, the conductive heat transport by the contact surfaces and the convective heat transport by the porosity and the resulting flow pattern. The solid material influences the heat transport by its material properties such as thermal conductivity and emissivity. Schematic diagram of the heat fluxes in the porous combustion region is shown in Figure 2.4 [6].

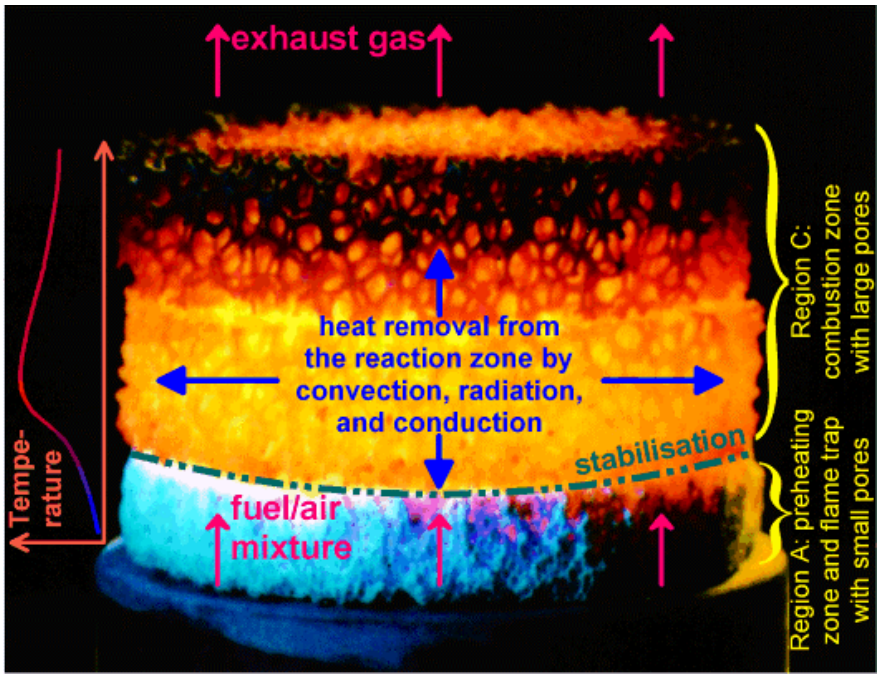

Figure 2.4. Schematic diagram of the heat fluxes in the porous combustion region [25]

The main principal advantages of steady combustion in inert porous media may be summarized as follows;

High flame speeds: Vortex structures are produced through the flow in the porous material. The vortex structures wrinkle the flame front and enhance the combustion process, which can take place at the inner boundaries of the large inner surface.

Low combustion temperatures: The heat transport between gas and solid phase (radiative and convective) is very effective because of the large inner surface. The temperature of the gas phase can be controlled from the temperature of the solid phase. Low flame temperatures resulting in low NO_X emissions can be realized.

Stable combustion: The high heat capacity of the porous medium results in a non-sensitive behavior to external disturbances or changes [5].

2.1.4. Porous Materials and Shapes

Porous medium burner technology has not only perfected the stabilization mechanisms but has, more importantly, made a breakthrough in the development of high temperature ceramics. The porous media in porous burners undergo severe thermal and chemical stress. Not only the corrosive atmosphere but also the high maximum temperatures and the steep temperature gradients over space and time, place the material

under severe stress. For that reason, initial experience was obtained with spherical fillings or filling material based on aluminum oxide. However, the total porosity of these materials is so low that high-pressure losses arise and the burners respond with great inertia. Because these properties are undesirable in most applications of porous medium burner technology, the main materials now used are ceramic foam or structures that resemble the static mixers or regular packing often used in process engineering. The advantages of these structures can be found in the following:

- The open pore structures with good flow through properties keep pressure losses low and low-cost burner blowers with low energy consumption can be used.
- Heat transfer is excellent. The gas is often forced to flow inward and outward, to split and reunite. With the convective heat transfer that this causes, a balanced temperature field is generated on a low level. This is accompanied by low pollutant emissions.
- Finally, the structures are characterized by a very low weight. That means that the thermal inertia is low, which has the effect that the burner heats up quickly on starting and adapts to power changes quickly.

Metallic materials are less suitable for porous media because of their inadequate thermo-stability. For nickel base and Fe-Cr-Al-alloys the upper limit is approximately 1400 ºC. For porous medium burners, typical maximum temperatures can be between 1400 and 1600 ºC, in extreme cases even 1700 ºC. Moreover, metallic materials have a high thermal capacity per unit volume, so those porous medium burners consisting of metallic materials respond with great inertia. Materials based on aluminum oxide; silicon carbide and zirconium oxide are mainly used.

Aluminum oxide can be used up to approximately 1900 ºC under air. High SiO_2 contents between 20 and 40 mass % reduces the application limit to approximately 1650 ºC. Because of its high thermal expansion coefficient and an average thermal conductivity, resistance to temperature changes of Al_2O_3 ceramics is relatively low.

Silicon carbide already noticeably oxidizes to SiO_2 at approximately 600 ºC, which results in surface passivation. As long as this layer remains stable SiC can also be used at very high temperatures, usually up to 1600 ºC. The resistance of SiC ceramics to temperature changes is very good, which is due to the low expansion coefficients and the high thermal conductivity.

Zirconium oxide can be used up to approximately 2300 ºC but a modification change associated with volume increase during cooling can destroy the structure. Adding

various additives stabilizes the high temperature modification. In this way, fully and partially stabilized ZrO_2 can be used up to approximately 1800 ºC. The high thermal expansion and the low thermal conductivity have a negative effect on the resistance to temperature change. A data comparison of the materials relevant for use in porous medium burners is shown in Table 2.2.

Table 2.2. Most important material data of Al_2O_3, SiC, ZrO_2 [1]

Parameter	Dimension	Al_2O_3	SiC	ZrO_2
Maximum use temperature in air	ºC	1900	1600	1800
Thermal Expansion coefficient α (20-1000^{0}C)	10^{-6}*1/K	8	4-5	10-13
Thermal conductivity λ (at 20^{0}C)	W/m*K	20-30	80-150	2-5
Thermal conductivity λ (at 1000^{0}C)	W/m*K	5-6	20-50	2-4
Specific thermal capacity	J/g*K	0.9-1	0.7-0.8	0.5-0.6
Thermal shock resistance, hard shock, R (σ/E*α)	K	100	230	230
Thermal shock resistance, mild shock, R'*(R*λ)	10^{-3}W/m	3	23	1
Total emissivity at 2000 K	-	0.28	0.9	0.31

The requirements on the porous media are very different for the various applications for which porous medium burner technology can be used. Depending on the type of fuel, air

and fuel flow and burner geometry, the temperatures to which the porous media are subjected are very different. Moreover, individual criteria such as costs, lifetime, pollutant emission mechanical stability (very important in automotive industry), pressure loss and thermal inertia will be weighted differently depending on the application. For that reason, a number of manufacturers have developed different porous media, which optimally meet the stringent requirements of porous medium burner technology [1].

It is a special feature of this technology that it is dependent on special high temperature resistant porous components. Therefore, many works also provide a survey of materials and shapes of porous materials, which are suitable for the combustion in porous media.

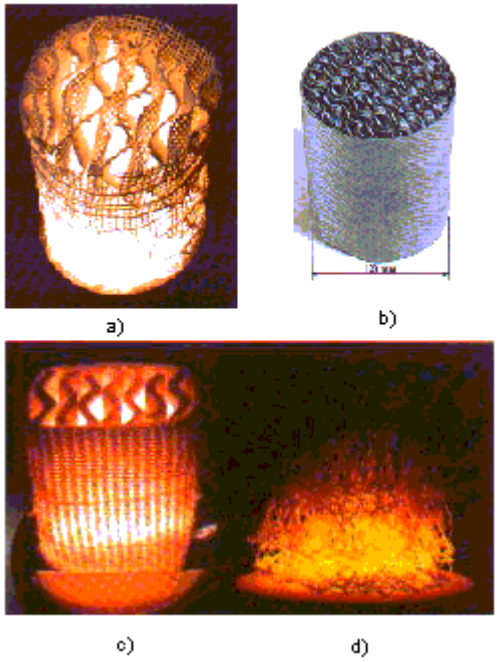

Figure 2.5. Different ceramic porous materials: a) Al_2O_3 fiber structure; b) C/SiC structure; c) static mixer made of zirconia foam; d) Fe-Cr-Al alloy wire mesh [25]

The most important material and forms for porous burners are SiC foams as well as mixer-like structures made of Al_2O_3 fibers, ZrO_2 foams and C/Si structures. For some applications also iron-chromium-aluminum alloys and nickel-base alloys can be used. All of the mentioned materials are substantially different with regard to manufacturing and properties. Al_2O_3 and ZrO_2 materials can be used at temperatures about 1650 ºC. Metals and SiC materials do not meet this qualification; however, they show outstanding characteristics with regard to thermal shock resistance, mechanical strength, and conductive heat transport.

Wire meshes and mixer-like structures have a good start-up behavior and a small pressure drop. In the following paragraphs the properties of four different components, as shown in Figure 2.5, are presented in detail.

The overall performance of the porous body is always a combination of the base material itself and the actual porous structure. Therefore, for both the suitable materials and for the shapes of porous structures the basic properties are given below. However, the emissivity data is not very reliable and is strongly dependent on the actual surface structure.

Aluminum oxide structures (Figure 2.5.a) can be principally used if the maximum process temperatures do not exceed 1950 ºC, although the technical temperature limit of this structure is nowadays at about 1700 ºC. Besides Al_2O_3 based materials show an intermediate heat conductivity ranging from 5 W/(mK) at 1000 ºC to about 30 W/(mK) at 20 ºC. Also, aluminum oxide shows an intermediate thermal expansion, an intermediate resistance to thermal shock and an overall emissivity at 2000 K is about 0.28.

High quality silicon carbide materials (Figure 2.5.b) may be characterized by a maximum usage temperature of about 1600 ºC, a high heat conductivity in the range of 20 W/(mK) at 1000 ºC to about 150 W/(mK) at 20 ºC, a very low thermal expansion, and a very good resistance to thermal shock. The overall emissivity at 2000 K is about 0.8 to 0.9.

Temperature resistant metal alloys (Figure 2.5.d) may be used for temperatures below 1250 ºC. Their properties feature a high heat conductivity ranging from 10 W/(mK) at 20 ºC to about 28 W/(mK) at 1000 ºC, an extreme thermal expansion, and an extremely good resistance to thermal shock. The emissivity of metals varies strongly with the surface finish and the surface itself and stretches at 300 K from 0.045 for polished nickel to about 0.5 for used stainless steal.

Of all presented materials, solid zirconia (Figure 2.5.c) shows the highest temperature resistance up to 2300 ºC. The heat conductivity of solid zirconia is hardly temperature dependent and in the range of 2 W/(mK) and 5 W/(mK). The emissivity at 2000 K is about 0.31. If used as porous zirconia based mixer structures, as shown in Figure 2.5.c, this structure combines the extremely high maximum temperature resistance of solid zirconia with a short start-up phase and an extremely good resistance to thermal shock, due to the high inner porosity of the ZrO_2 lamellas. As a result of the geometrical shape, such structures also show excellent radiation heat transport properties. Excellent dispersion properties and a very low pressure drop.

Another suitable structure for porous media combustion is static mixer (Figure 2.5.a. and b.). They may be characterized by a low conduction heat transport, a short start-up

phase, excellent radiation heat transport, excellent dispersion properties, and by a very low-pressure drop.

Wire meshes as shown in Figure 2.5.d. show poor conduction heat transport and dispersion properties, due to their high porosity. On the other hand, they have a short start-up phase, excellent radiation heat transport properties as well as a very low-pressure drop.

Ceramic foams of different base materials are used for porous burners. Independent on the base material such structures feature good conduction heat transport, a rather long start-up phase, low radiation heat transport properties, intermediate dispersion properties, and a relatively high pressure drop [25].

As the conditions in the combustion zone aren't too easy, there are several requirements on the material and on the shape of the PM.

The adiabatic temperature is about 1600-1800 ºC. Although the good heat transfer of the PM lowers this working temperature, there is still temperature higher than 1300ºC in the combustion chamber. Also the temporal and local temperature gradient stresses the material. So it has to be resistant to thermal shocks. It also must have a moderate thermal expansion. But it is not only the high temperature but also the reactive atmosphere where even the inert nitrogen-molecules react. Furthermore the shape has to guarantee a good flow behavior with open pores to get low-pressure loss and therefore less energy consumption and a compact burner chamber.

The shape also influences the production of eddies and the split and reuniting of the flow which means a good heat convection.

In addition the material has to have a good heat conductivity, which causes a homogeneous temperature field at a lower level that, the maximum (adiabatic) temperature. Therefore there is a reduction of the waste gas emission. A low weight of the porous medium means a low heat capacity. In the start-up phase the burner is less indolent. The start-up time is shorter and the waste emission is lower. So it was developed some new materials and new shapes of the porous media at the Institute of Fluid Mechanics at the University of Erlangen-Nürnberg.

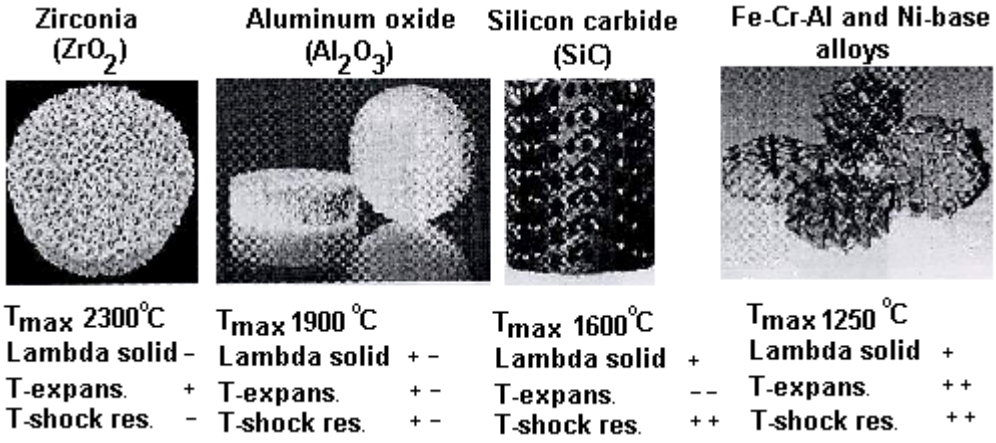

Figure 2.6. Porous materials [24]

In general metallic materials are not useful, as they are not quite stable with high temperature. Iron-chromium-aluminum alloys and nickel-base alloys can only be used in special application where the temperature is below 1300 ºC. But they have very good thermal properties: high heat conductivity, a very low thermal expansion and a very high thermal shock resistance.

Thermal expansion describes the material volume at changing temperature. If the material wants to expand, but cannot do this freely because of its shape, it causes a mechanical stress on the material. This shortens the life span of the structure.

The thermal shock resistance describes the behavior of material, not of volume. If a substance is not shock resistant, there can be cracks and other modifications in the material due to a fast or slow changing temperature. In a household burner the resistance is very important, the higher the better.

As the maximum temperature in the porous medium is normally between 1400 and 1600 ºC Zirconia can be used as it has a maximum temperature of 2300 ºC. Another possible material is Al_2O_3. It can stand principally a working temperature of 1900 ºC. The last material is the silicon carbide SiC that can stand a maximum temperature of 1600 ºC. But not only the material but also the geometrical shape influences the physical properties e.g. heat transport, start-up behavior, radiation, dispersion and pressure loss.

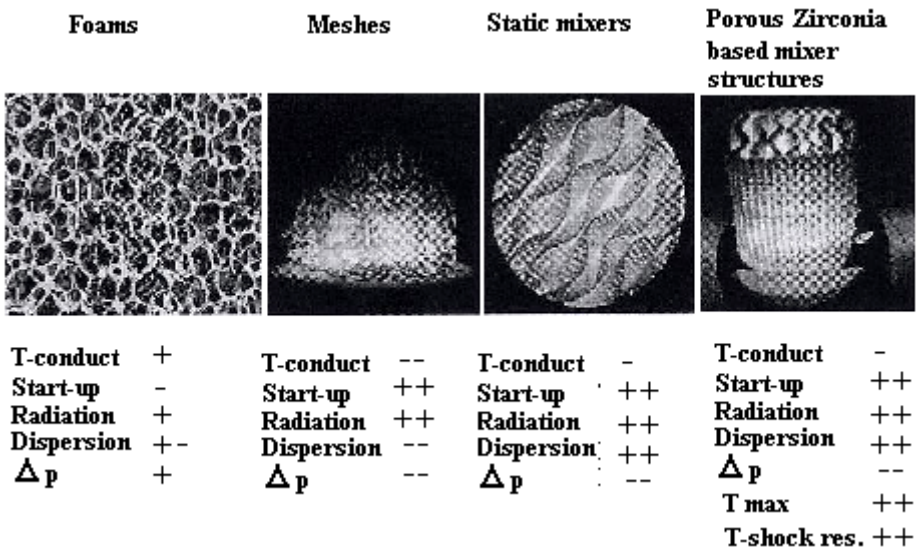

Figure 2.7. Geometrical shape of the porous materials [24]

The foams have good properties except for the start-up behavior. They are irregular so that the flow provides many eddies and therefore a good heat transfer. They are mostly made of Silicon carbide.

The meshes, mostly metallic and alloy meshes have a very good start-up and radiation, but very bad thermal conductivity, dispersion and pressure loss. The static mixers are regularly arranged which causes a very good flow property, very good radiation and dispersion. Only the pressure loss and the heat conductivity are not ideal due to the larger cavity dimension and therefore the larger boundary layer in comparison to the SiC foams.

In general a higher porosity (which means more and smaller pores) improves the resistance to thermal shock and decreases the maximum temperature due to the high inner surface. A combination of static mixer shape and zirconia results in very good properties also of the thermal shock resistance and the high maximum temperature [24].

There are several different materials of different geometry and execution forms that are suitable as porous media. The quintessential point is the fulfillment of some important characteristics;

- The oxidizing atmosphere and high operation temperatures require materials of temperature and corrosion resistance.
- The high spatial and temporal temperature gradients occurring with the operation, particularly with on and driving off processes require a good resistance to temperature changes, i.e. the porous body must indicate suitable

geometry, low thermal coefficients of expansion, a high heat conductivity and good mechanical characteristic values, in order to withstand the demands.

- Good heat transport characteristics of the porous body are necessary, in order to produce homogeneous temperature field and diminish point temperatures. These characteristics are essentially determined by heat conductivity, radiation emission coefficient and void structure.

Alumina, silicon carbide and zirconium oxide are the most frequently selected ceramic materials for porous bodies. They have different advantages and fields of application; Alumina is economical, possesses middle heat conductivity and is suitable for very high temperatures. Silicon carbide has a very high resistance to temperature changes, high heat conductivity and indicates high radiation emission coefficients. Stabilized zirconium oxide has an extremely high application temperature and a good resistance to temperature changes [26].

The combustion temperatures of PIM burners can be made relatively low through lean operation however; they are still high enough to cause the rapid degradation of fine porous metal structures. The recent availability of porous ceramic foams and discrete ceramic matrices has allowed the field to advance. While porous ceramic foam has good temperature resistance, their durability suffers from cracking caused by the stresses of differential expansion experienced during start-up and shutdown.

2.1.5. Heat Transfer in Porous Media

The heat transport in porous media is very effective due to two reasons:

The effective heat conductivity of the porous matrix is by the factor 10^2-10^3 higher than that of the pure gas.

The heat transfer coefficient to the wall is ten times higher than without porous media.

These effects originate from the fact that in porous media only a thin thermal boundary layer exists. So no thick laminar boundary films can develop that would be a very high resistance for the heat transport. The presence of a solid phase inside the combustion region causes the following advantages compared to combustion with free flames:

The heat transport from the reaction mixture to the porous media is very effective due to the high inner surface. So a nearly perfect equilibrium between the gas and the solid phase is possible. The significantly better heat transport properties of the porous matrix lead to a higher heat transport by conduction and radiation, also against the flow direction. This

causes very high flame propagation velocities compared to free flame combustion. These higher flame speeds create about two times wider reaction area. Reasons are the longer reaction time due to the lower temperature and the greater flame propagation speeds, which allow a higher incoming gas flow. The presented stabilization concept result in a high variability of the power rate from very low gas flows up to the maximum gas velocity above which the reaction would be extinct.

High power rate densities can be realized by easily increasing the gas mixture flow as soon as the temperatures in the porous medium are high enough over the whole area needed for a complete combustion. Reaction time, incoming flow speed and the temperature field define the length of this area. Very large reaction areas at low temperatures and high power densities can be reached.

Due to the very effective heat transport the gas mixture has not been pre-heated, which results in higher flame propagation speeds. Secondly the reaction area can be cooled, if desired, which causes lower temperatures in the reaction zone compared to free flame combustion. This measure implies strongly reduced NO_X emissions. By the use of porous media with different heat transport properties and different heat exchangers the temperature field can be widely controlled and optimized in respect to a minimum pollutant production.

The combustion process behaves very insensitive to quick fluctuations of excess-air ratio and power rate, because the great heat capacity of the ceramic material leads to a big thermal inertia. The basic heat transport mechanisms of the porous medium combustion technique are shown in Figure 2.8 [26].

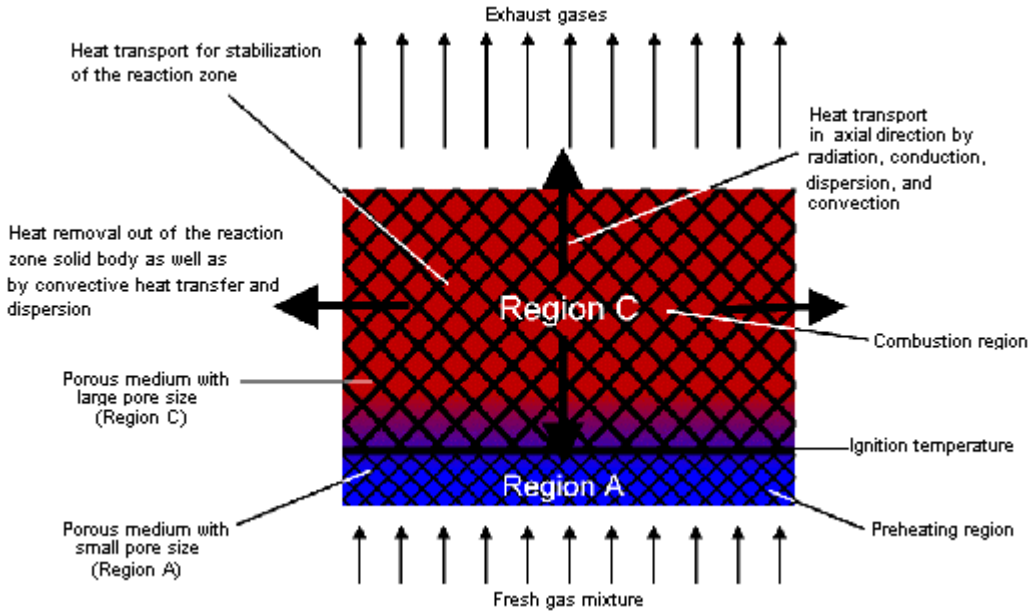

Figure 2.8. The basic heat transport mechanisms of the PM [11]

The heat convection describes the heat transfer from hot gas to porous medium and also from hot PM to cold gas.

$$\dot{q} = \alpha \left(T_{gas} - T_{PM} \right) \tag{2.7}$$

α : heat transfer coefficient

If there is no solid medium like in the free flame there is only heat convection to the wall.

The law of Fourier describes the heat conduction.

$$\dot{q} = \lambda \left(\frac{\partial T}{\partial s} \right) \tag{2.8}$$

λ : heat conductivity

As the heat conduction coefficient of the porous medium is much larger than of the gas of a free flame, also the heat conduction in a porous medium is larger than in a free flame.

Also the radiation is larger in the PM than in a free flame.

$$\dot{q} = \varepsilon \sigma T^4 \tag{2.9}$$

ε : emission coefficient

σ : Stefan-Boltzmann constant

As the emission coefficient of the porous medium is much larger than that of the gas, there is also more radiation in a porous medium than in a free flame.

There are no hot spots, which can destroy the materials like in a free flame. The most heat energy remains not in the products but is lead away by the porous medium to preheat the reactant and to enlarge the combustion zone. Therefore the temperature does not reach the adiabatic temperature and the products are cooled down fast. It can be described as equilibrium between gas and porous medium so that PM and gas has the same temperature [24].

2.1.6. Combustion Products and Emission Measurements of the PMB

The waste gas emission can be divided into primary and secondary air polluting substance:

The nitrous oxides NO_X belong to the primary group. Both NO and NO_2 are built at high temperatures above 1300 ºC in the combustion of fossil fuels with the molecular nitrogen of air.

Also the product of an uncompleted combustion, mainly the CO belongs to this group.

In the secondary group there is the carbon dioxide. It can be reduced in a more efficient combustion.

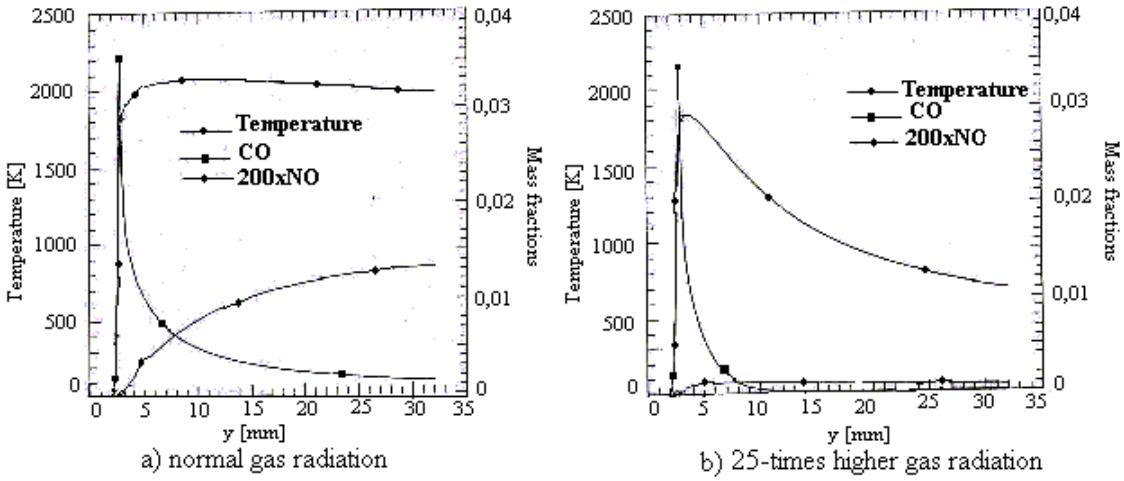

Figure 2.9. Comparison of emission products between free flame without radiation and with radiation [24]

In Figure 2.9.a shows the temperature, the concentration of NO_X and CO in respect to the distance y to the free flame. It is a numerical simulation. At the beginning the gas reaches very fast the adiabatic temperature of 2000 K and keeps it, as there is no heat conductivity to the wall. Therefore much NO_X is build. As the production of NO_X needs much oxygen, the CO cannot oxides completely to CO_2.

In Figure 2.9.b shows not a realistic flame but simulates a 25 times higher radiation of gases can be compared with a heat transfer in PM. The temperature peak is at a lower level, the products cool down fast, and there is almost no NO_X. Therefore all CO can oxides to CO_2.

It also has to be prevented inhomogeneous conditions as high temperature peaks causes high NO_X concentration, low temperature areas causes flame quench or/and high concentrations of unburned hydrocarbons and CO [24].

Since CO is being emitted at low process temperatures, while NO_X is produced at higher temperatures, measures to minimize both pollutants have to operate in a process temperature window between 1100 and 1400 ºC. Furthermore, the homogeneity of the temperature distribution is very important, since hot spots can produce large amounts of NO_X and cold spot result in incomplete combustion with high CO and CH emissions.

The thermal (Zeldovich) mechanism or the prompt (Fenimore) mechanism can produce NO_X. Both mechanisms are temperature dependent, lower temperatures resulting in lower NO_X levels. Although the thermal mechanism is a "slow" mechanism, it contributes most of the NO_X. Therefore, the formation of NO_X depends on mainly on the maximum temperatures reached in the center of the combustion region and on the residence time in the hot regions assuming that hot spots in the porous medium are avoided and the temperature distribution is uniform, then the NO emissions depend mainly on the heat load and the excess-air ratio of the burner. In the case of the porous burner, a non-typical insensitive NO emission behavior is observed with respect to the heat load. This can be explained with the decreased residence times at higher heat loads and decreased temperatures at lower heat loads. The excess-air ratio, however, affects the NO_X level very strongly, since with increasing excess-air ratio the residence time and the temperature in the combustion region decrease. Experiments with various combustion region shapes and porous materials have shown that configurations with smaller burner dimensions or higher heat transport properties of the combustion zone, resulting in a better cooling of the region C, are characterized by lower NO_X emissions.

A typical emission curve for CO and NO is presented in Figure 2.10 and Figure 2.11, respectively. The measurements were performed in a 10 kW porous burner prototype equipped with an Al_2O_3 fiber structure in the combustion region C and a packed bed of Al_2O_3 spheres in region A.

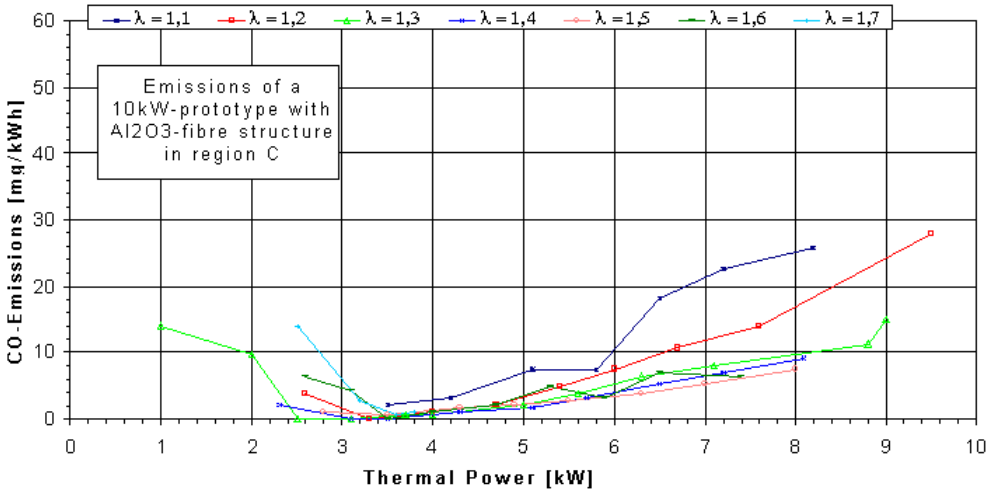

Figure 2.10. CO-emission concentration as a function of thermal power and Excess-air ratio for the 10 kW prototype [27]

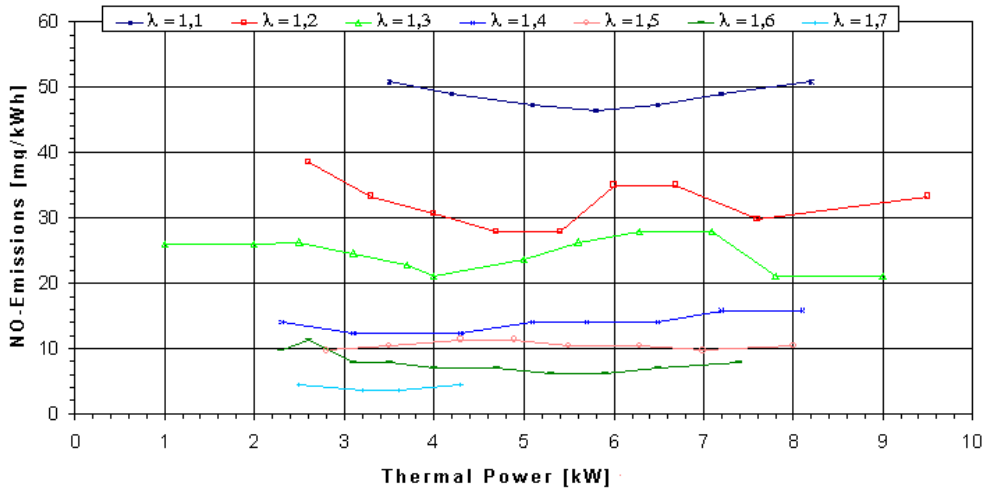

Figure 2.11. NO_X-emission concentration as a function of thermal power and Excess-air ratio for the 10 kW prototype [27]

The emissions of NO_X and CO are clearly below the most current European emission standards as indicated in the Figure 2.12 (Blauer Engel and Hamburger Förderprogramm are German emission standards, but are even more stringent than the general European ones).

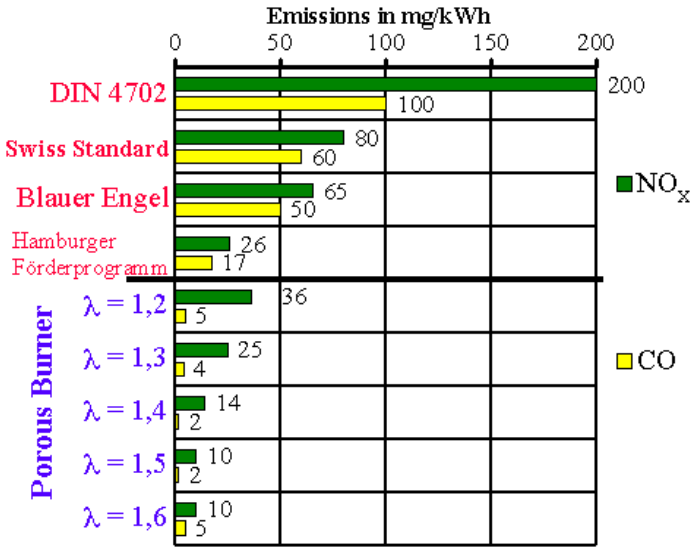

Figure 2.12. Emission of a 30 kW porous media burner in comparison to European standards [25, 11]

2.2. Basic Construction of the Porous Medium Burner

It is a general practice to build gas combustors in such a way that they contain free burning flames in an enclosure acting as a combustion chamber (Figure 2.13.).

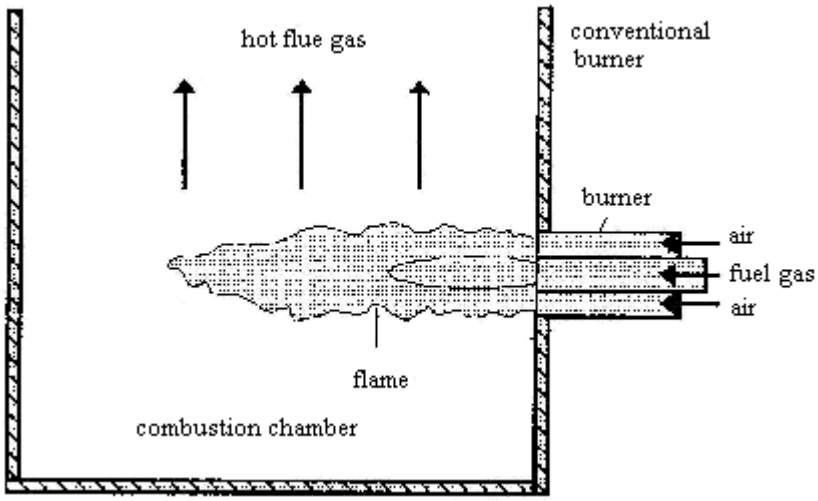

Figure 2.13. Conventional Combustors [28]

The hot gases from the combustion chamber are subsequently fed through heat exchangers to heat up water or produce steam. Combustors of this kind are characterized by high NO_X formation in the hot combustion region of the flame and by high temperatures of the emission gases leaving the heat exchangers or steam generators [9]. It is shown in Figure 2.14.

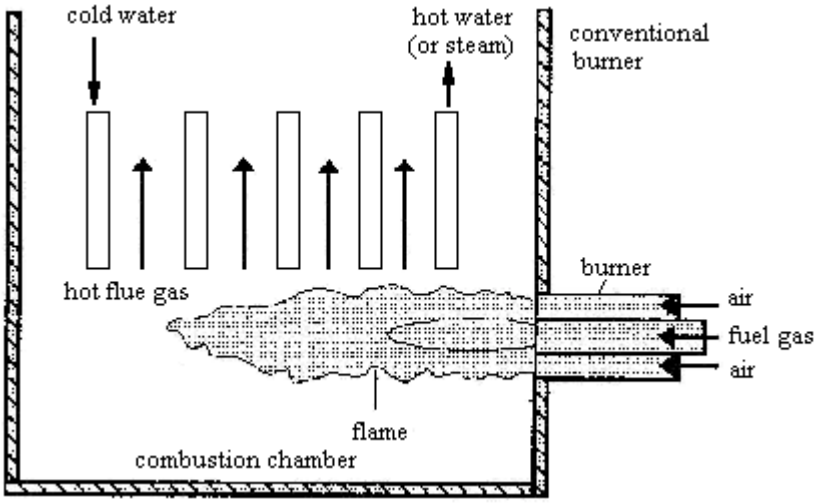

Figure 2.14. Conventional Combustors-Heat exchanger [28]

A complete different mechanism is one of the porous medium combustion. In this case the flames are not free, but they are burning in the pores of a porous medium formed from pebbles.

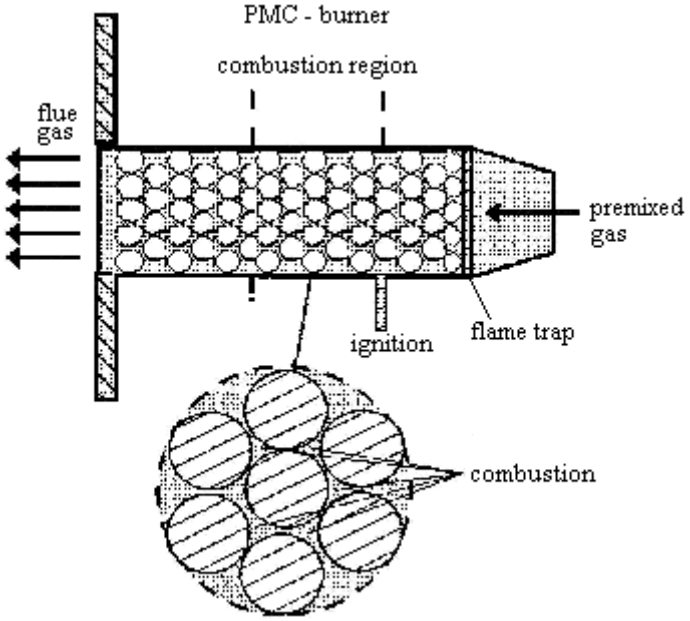

Figure 2.15. Porous Medium Combustors [28]

Combustion in porous media has some unique features:

- The flow is highly turbulent and combustion velocities 1-50 times higher than the normal ones have been reported
- The heat transfer from the combustion zone to the porous medium itself, where the flame front is located, is very effective, because of the very large surface

available between them. This results in cold exhaust gases, since the energy is directly transferred after its production to the porous medium (solid)

- The flame temperature is low because of the cooling through the porous medium and thus NO_X formation is reduced, if not eliminated.

The idea was to use the unique features of the porous medium combustion in a compact burner unit, filled with ceramic pebbles. This unit acts at the same time as a combustor and heat exchanger, in which the porous medium inside the burner is cooled with water in the porous medium combustor a compact unit with a high power density, high efficiency (low exhaust gas temperature) and low NO_X emissions can be realized.

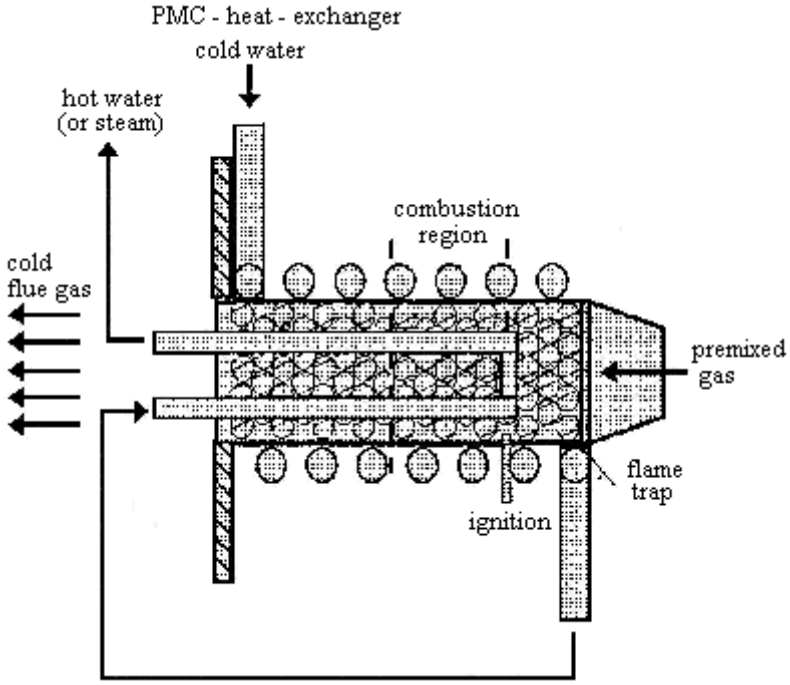

Figure 2.16. Porous Medium Combustor and Heat Exchanger [28]

Preliminary tests helped solve several problems concerning the porous medium combustion:

- Stabilization of the flame in the porous medium
- Quenching effects of the porous medium
- Effects of porosity and heat transfer coefficient of the porous medium on the combustion and cooling process

These preliminary investigations resulted in a burner-heat exchanger unit of about 2 liters volume with a power of 5 kW, an efficiency of 95% and an exhaust gas temperature of 60 ºC.

The geometry of the inside of the burner-heat exchanger still has to be optimized (mainly the cooling process) and parametric studies have to be performed in order to make a scale up of the unit possible, without losses in efficiency. The water vapor condensation energy from the combustion products can also be used in further development [28].

The concept of the Porous Burner is the following:

A stabilized premixed flame inside or near a non-combustible PM heats the porous matrix, which then emits thermal radiation to a heat load. The main advantages of this burner technology are higher efficiencies, lower NO_X emissions and more uniform heating. Porous Burner's operating with a reaction region completely in the inner porous medium has the main problem of stabilization of the reaction region in the PM. The main advantages of the Porous Burner's can be achieved, if the flame front region is in the middle of the porous medium.

The scientists have developed a Porous Medium Combustor, which solves the problem of flame stabilization in the PM. Also a practical application of the burner as a water heater or steam generator has been developed. In the latter cases the concept of the burner function is no longer that of the PB's i.e. the porous matrix is not heated until thermal radiation to the heat load occurs. Instead the heat load is the porous matrix itself, which is cooled and with a conductive-convective mechanism the heat is transported to the heat load. This results in small dimensions of the whole burner with integrated heat exchanger apparatus.

The Porous Medium Combustor (PMC) is built from a cylindrical tube of 60 mm inner diameter. At the inlet of the PMC a flame trap is placed, consisting of a 4 mm steel plate with 1000 holes of 1 mm diameter. The interior of the PMC is filled with pebble sizes were tested preliminary experiments. The ignition is performed at the wall of the PMC with a spark plug.

The experiments were performed in closed tubes, where the quiescent gas was ignited from one end of the tube and the maximum steady propagation velocity was recorded. In the case of the PMC the design requirements are different, i.e. the reaction region must remain at a definite location, while the premixed gas and the cold reaction products flow through the PM. In order to stabilize the reaction region the following design was realized.

The premixed gas flows after the flame trap through a PM region A with an equivalent diameter d_m of the PM cavity space, which is less than the quenching diameter for these flow-conditions. At the position where the flame front should be located, a

gradient in the d_m of the PM is realized resulting in PM cavity space diameters larger than the quenching ones. In other words a PM region B with a gradient in d_m leads to a region C with a d_m, which is larger than the quenching diameter. This construction results in a reaction zone that is self-stabilized depends on the flow conditions (p, T, stoichiometry) at a position within the zone B.

One can understand this phenomenon also from the creation developed by Babkin et al. In the region A, Péclet number is smaller than 65 (Pe<65), while in the region C, Pe>65. Flame propagation reaches the position in region B, where local quenching stabilizes the flame front.

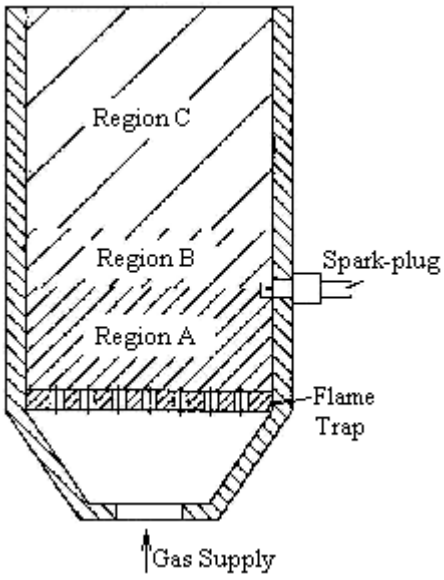

Figure 2.17. Schematic diagram of the Porous Medium Combustor (PMC) [29]

Another possible design omits the region B and lets the gas flow directly to region C. In this case the reaction zone is stabilized at the outlet of region A and burns in the region C, in which much larger flame velocities could be achieved. So a change in the load of the PMC does not affect the flame front location but only changes its length, starting always from the edge of region A. In the design with three regions a change in load of the PMC shifts the flame front location to a position in region B, where it is self-stabilized. For practical applications it is desirable to know the exact location of the flame front in order to design the cooling, select the materials etc. On the other hand self-stabilization with a gradient region B has the advantage, that the flame front is located at the smallest possible PM cavity size diameters d_m with the advantage of better heat transport to the porous matrix.

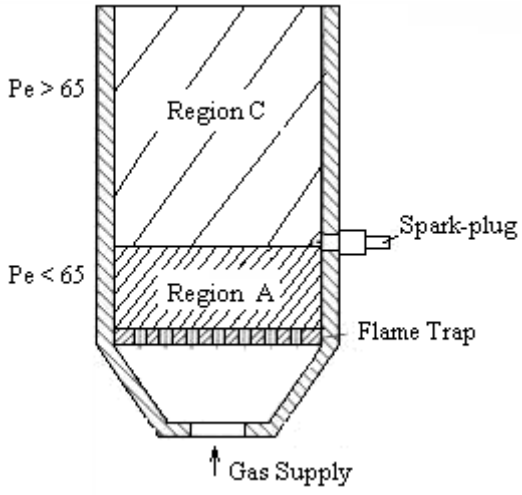

Figure 2.18. Schematic diagram of the PMC with two porous region (PMC) [29]

The spark plug for ignition is located in the sidewall of the burner at the height of the region B or at the edge of region A.

Another ignition possibility involves igniting the premixed gas at the outlet of the burner and then letting the flame front propagate through region C, till it is self-stabilized in the PM. This method has proved to be less satisfactory than the spark-plug ignition in the PM. Because the flame front velocity of the free flame is relatively low compared to the flame velocity in the PM, flashback occurred; the mean gas velocity (and consequently the load) had to be again increased without blow-off of the flame front. This is a tricky procedure and hence the spark-plug ignition was preferred.

The critical pebble diameter, for which flame propagation couldn't be established, was found experimentally to be 9 mm. The experimental conditions were p=1 atm at the outlet of the burner and t=20 ºC. The gas used was stoichiometric premixed methane with air. The criterion of Pe=65 used in fits well with the experimentally found critical pebble diameter of 9 mm. The Pe number was calculated for stoichiometric laminar flame velocity S_L=0.4 m/s. For the region A pebbles of 5 mm diameter were used and for the region C pebbles of 11 mm diameter. In the preliminary experiments the solution of two-region flame stabilization was preferred. The region A can replace in practice the flame trap used at the entrance of the burner. Nevertheless the flame trap was used in order to be safer against flashback. The flame trap acted also as a distributor of the premixed gas supplying a homogeneous mixture to the PM.

Different pebble materials were used in preliminary tests. These included steel polished balls of different diameters and ceramic pebbles of different compositions and

sizes (steatit, stemalox, pure Al_2O_3). The void fraction ε was determined by the amount of liquid required to fill the entire PM; it resulted in values of about 0.44 for the larger pebbles (>11 mm) and 0.38-0.42 for the smaller pebbles.

The basic construction of a porous medium burner with heat exchanger has been developed at the LSTM-Erlangen. Figure 2.19 shows the principle construction of a porous burner device. The integration of the heat exchanger in the compact burner results in a very compact construction. A ceramic insulation layer insulates the combustion region C, in order to prohibit CO-formation due to low wall-temperatures. An extra region D is exclusively used for heat exchange purposes. This region D is placed adjacent to the end of the combustion region C, since no after burning is necessary. The exhaust gases can be cooled below the water condensation temperature [30].

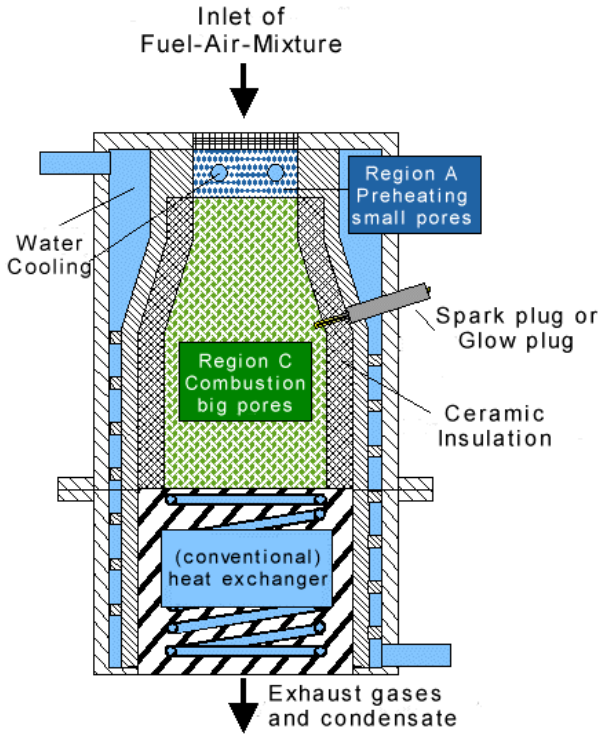

Figure 2.19. Schematic diagram of the Porous Burner with integrated heat exchanger [27,30]

By cooling the porous medium with water, i.e. at the walls and within the porous matrix, the unit acts as combustor and heat exchanger at the same time. Because of the effective heat exchange, the water vapor produced by combustion condenses, giving its latent heat to the heat exchanger. The burner is mounted so that the gas flows from the top to the bottom in order to enable the condensed water to flow out of the burner. The 10 kW porous medium burners with integrated heat exchanger are subdivided into three regions,

the preheating zone (region A), the combustion zone (region C) and an additional heat exchanger region D. In region A, due to the small pore diameters, no flame propagation is possible. In this area, the fuel-air mixture is pre-heated. The burner cross-section has been reduced in the region A in order to increase the power modulation region. To enable a steady, complete combustion, the region C is insulated from the cold walls by ceramic ring, which provides a controllable heat flux to the mantle cooling and a high inner surface temperature. Thus, the formation of CO due to the contact of reaction radicals with the cold surface is avoided almost completely. As a consequence, the CO-emissions are hardly measurable over a wide range of the thermal load. The region D is attached to the combustion region to transfer the produced heat to the water circulation. This region can also be filled with porous material. The heat transfer rate is high enough to condense the vapor from the exhaust gases. By this condensation the latent heat of the vapor can be used additionally. A part of the heat is already transferred to the water-cooled double jacket. To let the condensed water flow off freely, the burner-heat exchanger system is supplied with the gas mixture from the upper side. It should be noted that the cooling region is no part of the porous medium burner concept itself. Whether a cooling area is added or not is only dependent on the respective application and does not affect the operation of the porous medium burner technology [11,25].

CHAPTER 3

APPLICATIONS OF THE POROUS BURNER TECHNOLOGY

Due to its outstanding properties, such as the wide operation area with regard to the thermal power, the small dimensions and the low pollutant emissions, the porous burner technology may be advantageously applied to many different industrial branches. The presented work provides a survey of already realized porous medium burners for applications in power plants and automobile industry as well as for household heating devices and various industrial applications.

In the domain of household heating systems a prototype of a natural gas water heating system, which is based on the combustion in porous media, has been developed in Erlangen. Further on fundamental works on the utilisation of the porous medium burner technology have been done.

- for the catalytic assisted combustion,
- in gas turbine combustion chambers,
- for radiation burners,
- for power and heat cogeneration units,
- for the combustion of liquid fuel (e. g. fuel oil),
- as independent vehicle heaters for automobiles,
- for heat pumps,
- for generators of process vapour,
- as reactors for HCl synthesis,
- for co-combustion of HFCC/HFC and
- as component for fuel cells.

Some of these applications will soon be introduced to the market.

Various other applications are possible, e.g.:

- as heat generator for chemical reactors,
- for the simultaneous heat and CO_2 generation in greenhouses
- as dual-fuel burner (gas- and liquid fuels),
- as burner for the power generation from mineral oil, liquid, pyrolysis or coke plant gas,

- as burner for the power generation out of regenerative energy carriers, e. g. gasified bio-mass, hydrogen (from solar energy), wood gas, bio-gas, dump or sewer gas,
- for the thermal exhaust cleaning.

Other applications are possible, e. g.:

The porous medium burner concept is especially suitable for low-calorific gas mixtures (mixtures with a high inert gas part) and shows advantages compared to conventional combustion concepts, which use free flames due to the high combustion stability of a porous medium burner [11,25].

3.1. Application in Household Burners for Air and Warm Water Heating Systems

An important aspect for the development of new gas burners for household applications is the fact that the power requirement for the heating operation decreases more and more, due to the improved insulation of the buildings. This can be related to the trend of lowering energy costs by energy-saving buildings. However, for hot water production the energy requirement remains unchanged, since high comfort is strongly requested in this field. On account of this discrepancy, burners for heating systems are required to have a wide power modulation range. This also relates directly to the number of burner starts. As the highest emissions occur during the warm up phase, a higher power modulation automatically leads to a decrease of waste gas emissions. Also in stationary operation, emissions of porous media burners are minimized in comparison to many domestic gas appliances working with free flames because it is possible to control the combustion temperature with the porous material in the combustion region. Solid materials have extremely good thermal properties in comparison to gases; thus heat can be efficiently transported out of the combustion region leading to a significant decrease of the NO_X formation, which is strongly temperature dependent.

Another aspect that makes the use of porous media combustion especially interesting for household applications is the high compactness of porous media burner units. Maximum power densities of 3500 kW/m^2 can be realized with various gases and air ratios in comparison to conventional systems which densities are 300 kW/m^2. Resulting from small burner sizes separate heating rooms is no longer necessary. Instead the porous burner units can be installed in small wall niches or even outside the houses. Figure 3.1 shows a schematic sketch and a photograph of a complete heating system for household applications

on porous burner basis. It is about half as large as a conventional heating system for the same nominal power output [25].

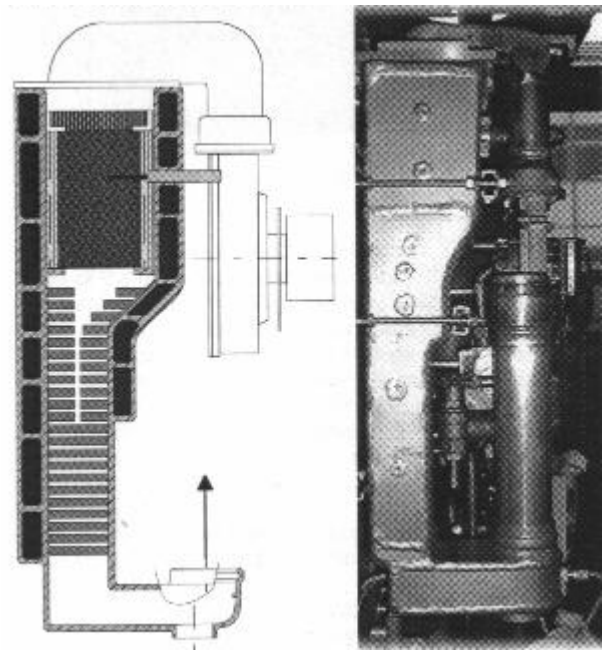

Figure 3.1. Porous burner and integrated heat exchanger unit for household applications [25]

3.2. Combined Usage of Porous Medium Combustors and Premixed Industrial Burners

When porous medium burners are combined with conventional premixed industrial burners, new possibilities arise in the application of the combined burner system to provide thermal energy. Conventional premixed burners can only modulate in a power range of about 1:2.5. When they are combined with ring-type porous burners, as indicated in the Figure 3.2, a combined burner system arises which can modulate from 1/50 of the maximum power of the burner system to its full power without any negative effects on the emission behavior. Such high power modulations can usually only be reached if industrial burners are operated over a part of the power range in diffusion flame mode. In this mode, however, the emission values of the burner are very poor. If a combined premixed conventional and a porous medium burner is used, very good emission rates are obtained for the entire combustion range. In addition, burner systems arise that are compact, especially if the conventional burner is used with high swirl. A ring-type porous burner is shown in Figure 3.2, in the center of which a conventional premixed burner could be integrated allowing the complete system to be operated over a modulation range of about 1:50 [25].

Figure 3.2. Ring-type porous medium combustor [25]

3.3. Air-Heating Systems for Dryers

In the process industry, dryers are used to remove moisture from agricultural products, food, textiles, chemicals, leather, wood, paper, and many other goods. For this purpose, hot-air streams are often applied to evaporate the water and to remove the moisture. The systems, which are used for hot air, supply often use flue gas from gas burners, which is mixed with fresh cold air to adjust the correct temperature for the drying process. In many dryers, the heat of the mixed gas is transferred directly to the product, which needs to be dried. If direct contact with the flue gas is not allowed or not desirable, a heat exchanger is mounted in between.

The industrial gas burners used in these applications allow a reliable operation, but they operate with free, partially premixed or diffusion flames which have lengths between 1 and 3 meters. The large combustion chambers needed are often undesirable. Small and compact hot air heating systems can be realized if porous media combustors are used. The porous medium burners have a burning length in the range of 10 cm. Thus, very small hot-air heating systems for industrial drying are possible, as indicated in Figure 3.3. Together with the other considerable advantages, the low emissions and the high modulation range, the porous media combustion has very good prospects to gain an interest in this market [25].

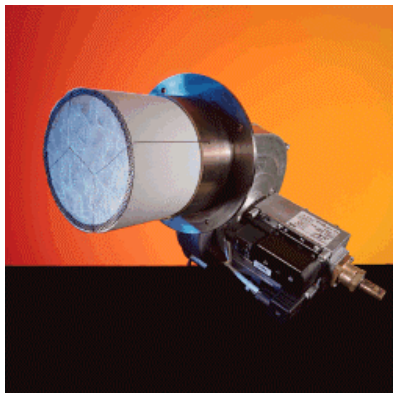

Figure 3.3. Air cooled porous medium burner with a maximum thermal power of 25 kW for the use in air-heating systems [25]

3.4. Gas Turbine Combustion Chambers

State-of-the-art gas turbines work with premixed combustion to achieve very low NO_X emissions. However, if the power decreases below 50% of the nominal maximum power, the combustion inside of the gas turbine becomes unstable. In that case the burners must either operate with diffusion combustion or produce high NO_X and CO emissions or alternatively, a certain number of burners have to be switched off. This results in an inhomogeneous temperature load of the turbine blades, which decreases the life span of the turbine significantly. Both problems could be overcome by applying porous medium burning chambers with high power turndown ratios in gas turbines. The adiabatic combustion temperature is situated for most fuels with the stoichiometric combustion with air with approximately 2000 ºC. With some industrial applications because of the small heat conductivity of gases and the high velocity rate, with which combustion runs, the adiabatic combustion temperature is almost achieves. In order to be able to measure the potential of the attainable improvements, attempts were executed for combustion in porous media under adiabatic conditions. In order to supply flame stabilization and adiabatic combustion processes, as they occur in gas turbine combustion chambers, in porous inert media experimentally, a high-pressure porous burner chamber was built, in which the behaviour of different porous media over temperature and pollutant emission measurements could be observed. Special attention with the experiments was put on the stability behaviour of the combustion within the area of high air numbers as well as on the influence of an air preliminary heating. By analysis of the received results of measurement it was possible to determine the flame rate of a methane air mixture in porous media. The flame rate is influenced by the effective heat conductivity of the gases or of the porous medium. Since

the heat conductivity of the porous medium is about 60 to 100 times larger than the heat conductivity of the gas, the flame rate in the porous medium can be for instance eight to ten times higher than with free flames. It lies due to the executed theoretical estimation for a stoichiometric methane air mixture with approximately 4 m/s. In this test rig the behavior of different porous media are investigated, under gas turbine conditions by measuring the temperature and the emission profiles. Figure 3.4, indicates a sketch of this special adiabatic burning chamber.

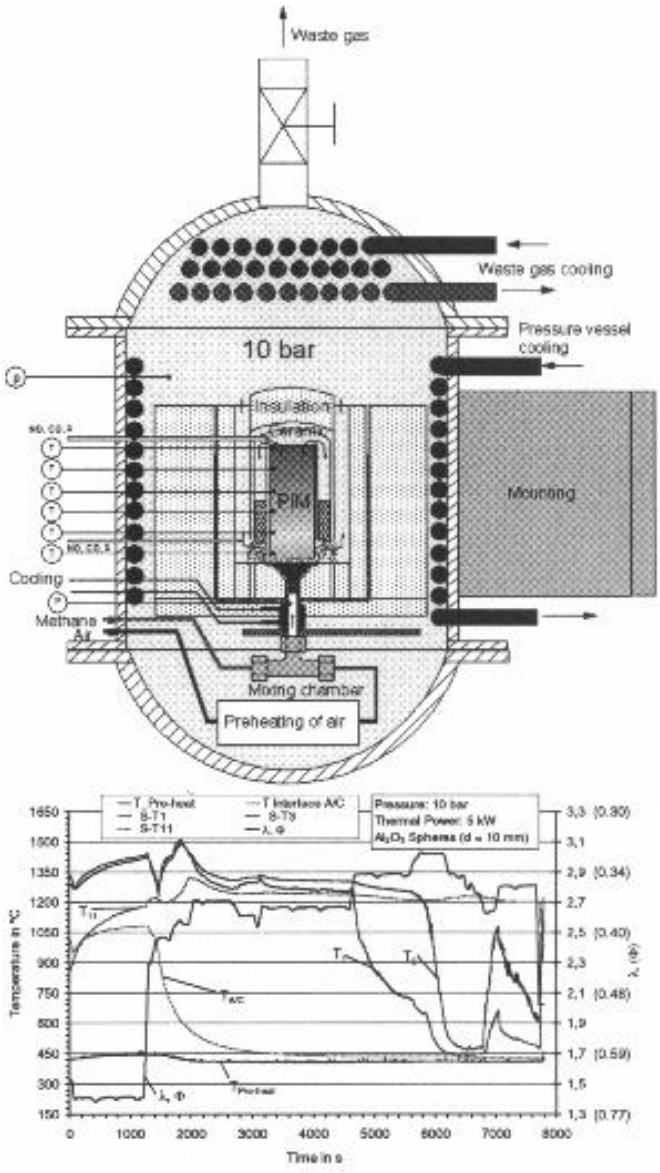

Figure 3.4. Schematic layout, and temperature profile of the experimental facility for adiabatic combustion processes in porous media under high pressure [25]

Attention was focused on the stabilizing behavior of the combustion wave in the range of low equivalence ratios ϕ (i.e. high excess-air ratiosλ) and the influence of air preheating. In experiments it could be shown that the use of a porous medium leads not only to a substantial enlargement of the flame rate but also to an extension of the stability area of the before-mixed combustion. The admissible air number area is extended by the application of porous media in the combustion chamber by a factor of 0.3. The results indicate that stabilized porous medium combustion leads to a significant rise of the thermal heat load, e.g. the flame velocity, and to a larger stability range of premixed combustion.

The potential of this burner technology with respect to applications like gas turbines at partial load, incinerators, etc. is an interesting task for future investigations. In this respect, experiments dealing with adiabatic combustion processes in porous inert media under pressure (up to 10 bars) are being carried out at present [25].

3.5. Application in Caravan Heating Systems and Pre-Heaters for Cars

The trend in vehicles for the near future will go in the direction of more comfort, life span, and safety, particularly in cars and caravans. Therefore, new heating systems for cars and caravans become more and more important. They offer several advantages apart from the consequence of more comfort. Pre-heaters prevent the formation of ice and condensate on windows with safety advantages. Furthermore, the preheating of the engine leads to less wear out and lower emissions of the engine during the starting phase. Also, heating systems for the passenger cabin are of great interest because of the high efficiency of modern engines and their small waste heat production. The first heaters for this application had the problem that the pollutants were too high for operation in closed garages and particularly in subterranean parking garages. These problems resulted from the necessary compact design of the combustion chamber although conventional burner technique had to be applied.

The aim of a better acceptance of these heating systems can be achieved with the porous medium burner technology. With this principle, it is possible to obtain low pollutant emissions with even a better space usage. Figure 3.5 shows a schematic drawing a), a photograph of the porous medium burner being operated with the heat exchanger removed b), and an exploded view of the complete independent vehicle heating system on porous burner basis c) [25].

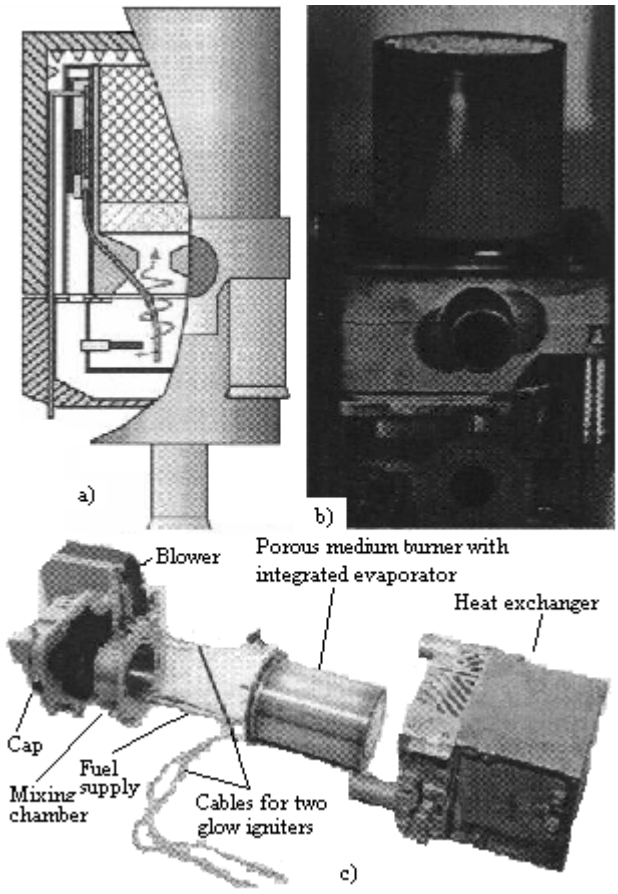

Figure 3.5. Independent vehicle heating system on porous burner basis [25]

3.6. Porous Medium Burners for Steam Generation

Steam generators are used for steam turbines, industrial processes, hospitals, laundries, or even in ships. Conventional devices are usually very large in size due to the necessary length of the free flames for a complete conversion of the fuel. This fact requires long flame tubes for burners for steam generation. Additionally, a very large diameter of the combustion chamber is required because of the limited radiation heat transfer from the combustion region to the working fluid. Applying the porous burner technology can reduce both the length and the diameter of combustion chambers for steam generation devices. Figure 3.6, shows a conception for the generation of steam on porous medium basis. As a consequence of the counter flow based heat exchange, the heat is transferred very effective. After preheating the feed water, the water is evaporated in two operation stages. By using the high temperature level in the superheating stage, the steam can be heated up to temperatures of 4000 ºC.

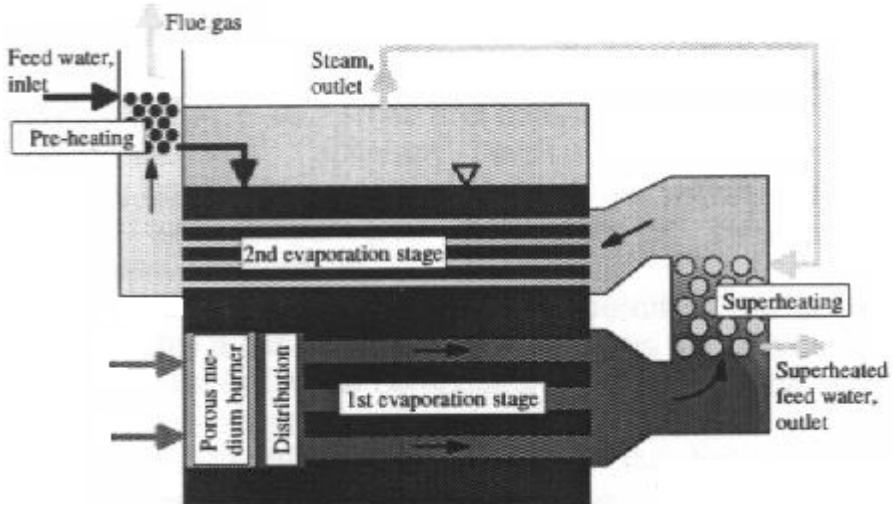

Figure 3.6. Highly effective steam generator using a PM combustor [25]

The large necessary flame tube as described above mostly causes the huge dimensions of conventional steam generators. By replacing the huge flame tubes of conventional steam generators by a compact porous burner, extra space for the heat exchanger is made available resulting in a much smaller design of the complete system. In this application, the modulation range of the porous burner is less important because the whole systems shows a very large time constant due to the massive steel construction. However, with the modulation range of the porous burner the system may always be operated at its point of maximum efficiency regardless of the actual load of the steam generator [25].

3.7. Porous Medium Oil Burners

The porous medium burner concept is not only limited to gaseous fuels; it is also possible to burn liquid fuels. At the LSTM-Erlangen, prototypes of burners for the combustion of oil, e.g. fuel oil, have been realised. A main field of application will be in the household and automobile sector.

In principle it could be shown that there is no fundamental difference between a pre-mixed natural gas / air combustion and a pre-mixed oil vapour / air combustion. The latter requires a strict separation of the part processes vaporisation, mixing and combustion. In experimental studies different vaporiser-mixer-principles are examined with respect to their applicability on the porous medium burner technology. Other studies deal with the vaporisation performance of fuel oil with the aim to optimise the conditions for a complete and a residue-free vaporisation. As a result it was possible to develop satisfying porous oil

burner prototypes that show an optimised emission performance with a low need of auxiliary energy during the starting phase [26].

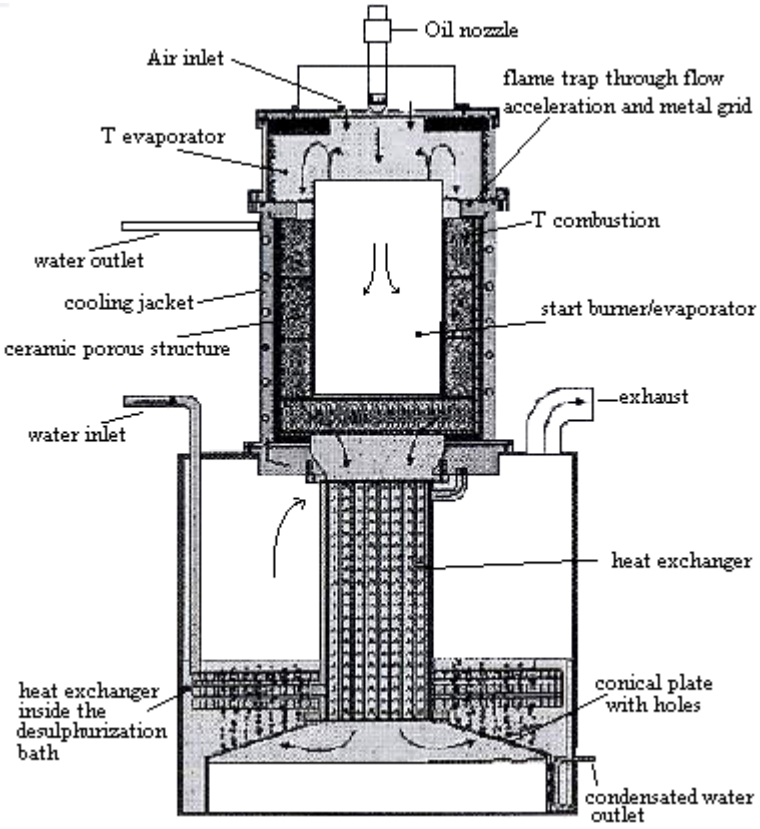

Figure 3.7. Oil burners [26]

3.8. Radiation Burners

In industrial process engineering applications, like glass melting furnaces, surface treatment, metal treatment, etc. a uniform heating with a fast response is required. Radiation heating is the best solution for such applications and many different concepts are used, depending on the necessary power density and required temperatures. The potential of the developed burner technology with regard to the more efficient heat transport due to the high radiation rate of the solid surfaces was examined in a theoretical study. Furthermore different prototypes of a high-temperature oxygen radiation burner were built and studied experimentally. These burners can be operated with either oxygen-enriched air or pure oxygen. The heat produced by the combustion process can be delivered immediately to the outer burner surface by the high thermal conductivity of the porous medium if the burner is designed suitably. This can handle the high adiabatic combustion temperature. The amount of heat delivered to the heated medium via radiation is not only dependent on the radiation properties of the burner's surface, but also on these of the oven itself and the heated

medium. An important field of application are industrial furnaces, in which the oven atmosphere must not get in contact with the combustion gases. Oxy-fuel burners are increasingly applied in such applications because of the primary high efficiency without recuperation (low investment cost) and the reduced NO_X emissions due to the very low nitrogen concentration in the furnace environment [22, 25].

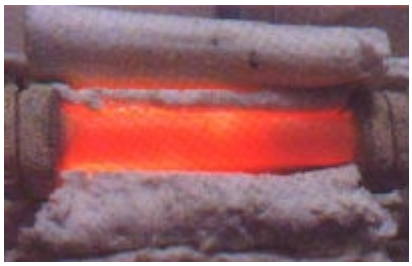

Figure 3.8. Radiant burner with pure oxygen on porous burner basis [22]

3.9. Catalytic and Catalytic Assisted Combustion in Porous Media

As shown before, very low emissions can be realised with the porous medium burner technology. A further big potential of a reduction of emissions offers combustion processes under the influence of catalysts. They cannot only be used for a subsequent treatment of exhaust gases, but also to control the combustion process in a way that the production of pollutants is prevented. It can be distinguished between catalytic assisted and complete catalytic combustion. In a complete catalytic combustion process, the fuel is exclusively transformed by catalytic reactions without the existence of homogeneous reactions. This concept could lead to operation failures and fuel slip when not enough catalytic material is offered. The catalytic assisted combustion is technology that uses the catalytic effect of some precious metals without being dependent on it. The combustion room is divided into two sections.

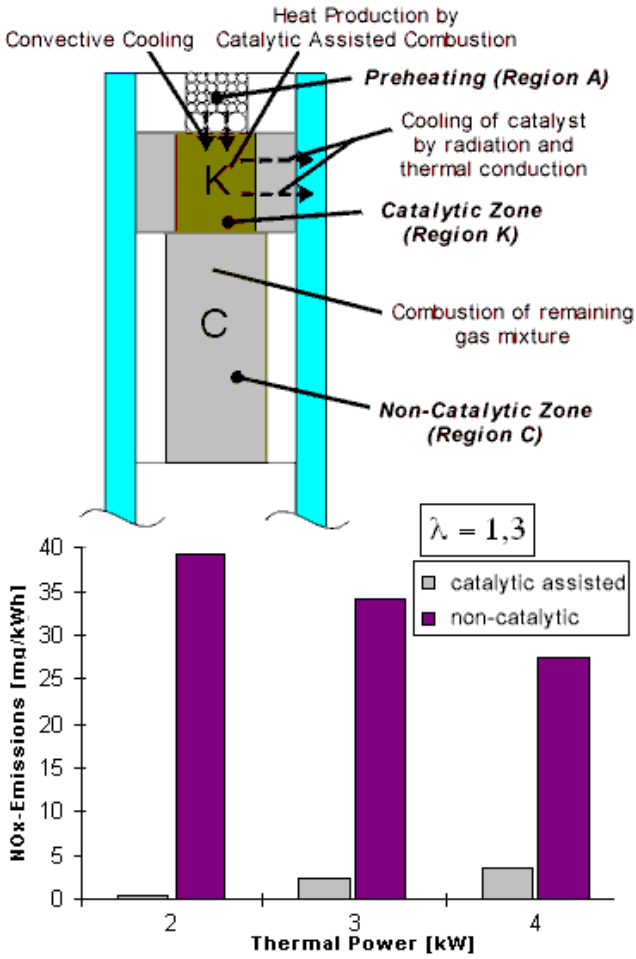

Figure 3.9. Catalytic and catalytic assisted combustion in porous media [26]

The first comprises a catalytically coated porous medium in which catalytic assisted (big pore diameters) or complete catalytic reactions (small pore diameters) can take place. In this part a part of the fuel gas is converted. Due to the activating effect of the catalyst the reaction can run at much lower temperatures. So the production of thermal nitrogen oxide can prevent almost completely. In the following section that consists of an uncoated porous medium the rest of the fuel gas reacts. When the burner is started, the reaction initially takes place in this part of the burner, until the catalytic zone is heated to operation temperature by heat conduction effects. So installations for pre-heating of the catalyst are needless. This concept guarantees a maximum of operation reliability because even with a fully disactivated catalyst a complete reaction is ensured. The accessible power modulation of the developed test device with a maximum power of 5 kW is at 1:3, which can be increased by an appropriate design of the burner.

In initial studies at the LSTM-Erlangen, possibilities of an application of the catalytic concept for porous medium burners have been investigated. Various porous media have been coated and tested. Experiments have shown that NO_X emissions can be lowered [26].

3.10. Porous Media Engine

The engine in a car could be applied a PM to improve the combustion. In conventional Diesel engines, the fuel is injected with high pressure to disperse the liquid fuel in the combustion chamber. As there is only a short time before ignition, the combustion is not homogeneous as the fuel doesn't mix completely with the air and isn't evaporated totally.

There is like in conventional burners a temperature gradient. That causes the production of NO_X in these high temperature regions. With an applied porous medium a homogenous combustion can be realised. There are no single flames, but the reaction takes place in the whole PM. There are no temperature peaks, therefore less emission and a complete combustion as the fuel is evaporated and mixed faster with the air due to the heat capacity of the PM which accumulates the released heat energy and due to the pores which influence the mixing in a positive way due to turbulence. One example of installing the PM is in the head of the cylinder. In the 4-stroke engine, in the first stroke the airflows into the cylinder. In the second, the piston compresses the air into the PM, where then the fuel is injected, mixed, evaporated and ignited (not by spark as in conventional Otto engines and also not by compression alone as in conventional Diesel engines but) by 3D thermal ignition. The third stroke is the combustion and expansion. The fourth stroke is the exhaust output.

The application of PM in Otto engines is also in research due to the excellent results in reduction of NO_X, CO, unburned hydrogen carbons and soot [24].

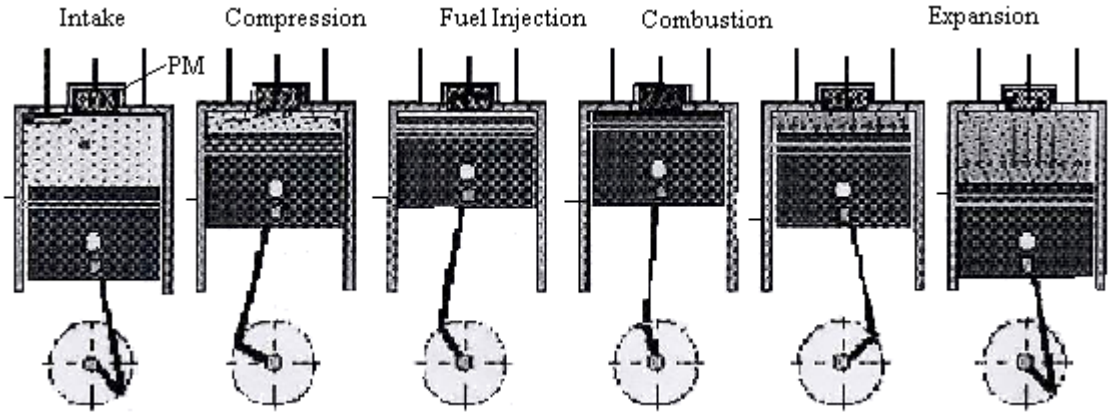

Figure 3.10. PM Engine [24]

CHAPTER 4

EXPERIMENTAL

This study had been performed in two main parts. One of them was carried out in the Combustion Laboratory of the Institute of Fluid Mechanics of the Technical Faculty, University of Erlangen-Nürnberg. Methane was used for 25 kW porous burner. The second was carried out at Izmir Institute of Technology and Liquefied Petroleum Gas was used as a fuel. The experimental work for 25 kW porous burner includes two series of measurements, A series obtained from burner running at 100, 70, 40% power ranges and B series obtained while working at 100, 70, 30% power ranges, at the same porous medium burner with a nominal capacity of 25 kW. These series were obtained different adjustments that were done by changing of blower revolution. Experiments were carried out in order to determine the behaviour of the burner at different power generations between about 28 down to 7 kW in experiments A, and 25 down to 4.5 kW in B. The experimental work, which was made in Izmir, performed to evaluate 10 kW porous burner behaviour and determine the possibility of the process water production. The experimental results and their discussions are given in Chapter 5.

4.1. Experimental Set-up for 25 kW Porous Burner

The experimental set-up consists of three parts, a steal gas bottle as a fuel source, a porous medium burner and measuring devices, such as: gas analysers, temperature reader and recorder, and gas flow meter, Figure 4.1.

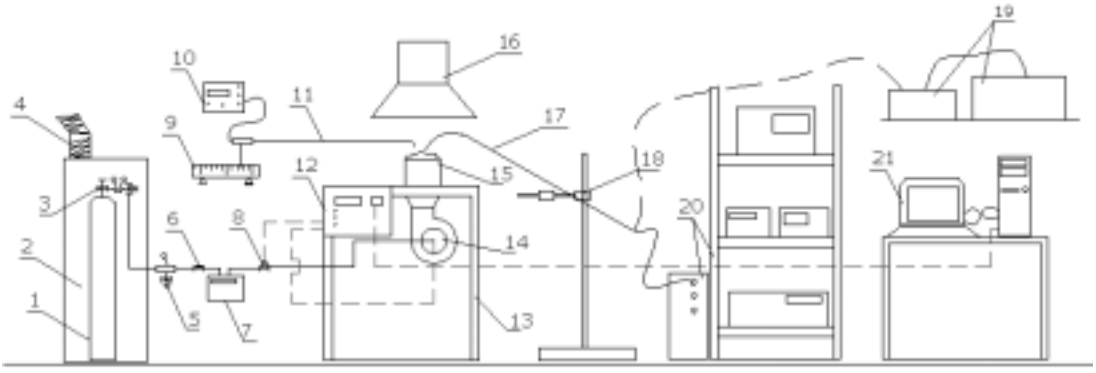

Figure 4.1. Experimental set-up for 25 kW porous burner

In Figure 4.1, the following positions are shown:

1. Methane bottle with pressure regulation valves,
2. Cupboard with a gas bottle,
3. Valve I,
4. Ventilation hose for the cupboard,
5. Pressure regulator,
6. Valve II,
7. Gas flow meter,
8. Valve III,
9. Traverse mechanism,
10. Digital device for temperature reading,
11. Pt-Rh-Pt, S-type-temperature sensor,
12. Control unit for the burner,
13. Test desk,
14. Air blower,
15. Porous medium burner,
16. Ventilation hose for flue gases,
17. Emission measurements probe,
18. Probe holder,
19. Flue gas analyser I with a dryer of flue gases,
20. Flue gas analyser II with a dryer of the flue gases,
21. Computer system for parameter adjustments.

The necessary devices for the fuel gas pressure regulation, volume flow rate readings and temperature measurements are also shown in Figure 4.1. The pressure of the fuel after the regulation device (Figure 4.1, component 1) was 34 mbar above the atmospheric pressure. The measurement devices and their specifications are as follows:

a) DUNGS control unit with microprocessor for controlling the burner operation, Figure 4.2,
b) IMR 3000P combustion gas analyser, Figure 4.3,
c) Pt -Rh-Pt, S-type thermocouple probe, Figure 4.4,
d) Data-logger-ALMEMO 3290-8, Figure 4.5,
e) Traverse mechanism for the measurement of the local exhaust gas temperature, Figure 4.6,
f) Adaptive 2000 domestic gas meter, Figure 4.7,

g) Combined gas analyzer, Figure 4.8,

h) Methane gas bottle with pressure regulation valves, Figure 4.9,

i) Digital chronometer.

The combined gas analyser consists of 4 components i.e. 4 different devices for emission measurements described as follows:

1. Instruments Inc.; 42 C NO-NO_2-NO_x High Level Analyser
2. Rosemount; BINOS 1002M; O_2-CO_2 Analyser
3. Rosemount; NGA 2000; CH_4 Analyser
4. Thermo Environmental Instruments Inc. CO Analyser, Model 48.

This advanced gas analyser has an air conditioner, so that it measures much more precise than the gas analyser without air conditioner does.

Figure 4.2. DUNGS electronic unit with microprocessor for controlling the burner operation

Figure 4.3. Combustion gas analyser IMR 3000P

Figure 4.4. Pt-Rh-Pt, S-type thermocouple probe

Figure 4.5. Data-logger ALMEMO 3290-8

Figure 4.6. Traverse mechanism

Figure 4.7. Adaptive 2000 domestic gas meter

Figure 4.8. Combined gas analyser

Figure 4.9. Methane gas bottle with pressure regulation valves

4.2. Experimental Set-up for 10 kW Porous Burner

Experimental set-up in Izmir mainly consists of air preparation section, Liquefied Petroleum Gas vessel, data acquisition system and computer, combustion gas analyzer and 10 kW Porous Medium Combustor test rig. It is shown in Figure 4.10. Screw compressor, air tank, air filters and air drier were used in air preparation section and each of devices are shown in Figure 4.11, Figure 4.12, Figure 4.13, Figure 4.14. Liquefied Petroleum Gas vessel, gas flow meter, data acquisition system and computer are respectively shown in Figure 4.15, Figure 4.16, and Figure 4.17. MRU Vario plus combustion gas analyzer was used for emission measurements, Figure 4.18. 10 kW Porous Medium Combustor test rig consists of air and fuel mass flow controllers, which were able to control by data acquisition system and also computer, alto-meter used for cooling water and porous burner itself, Figure 4.19.

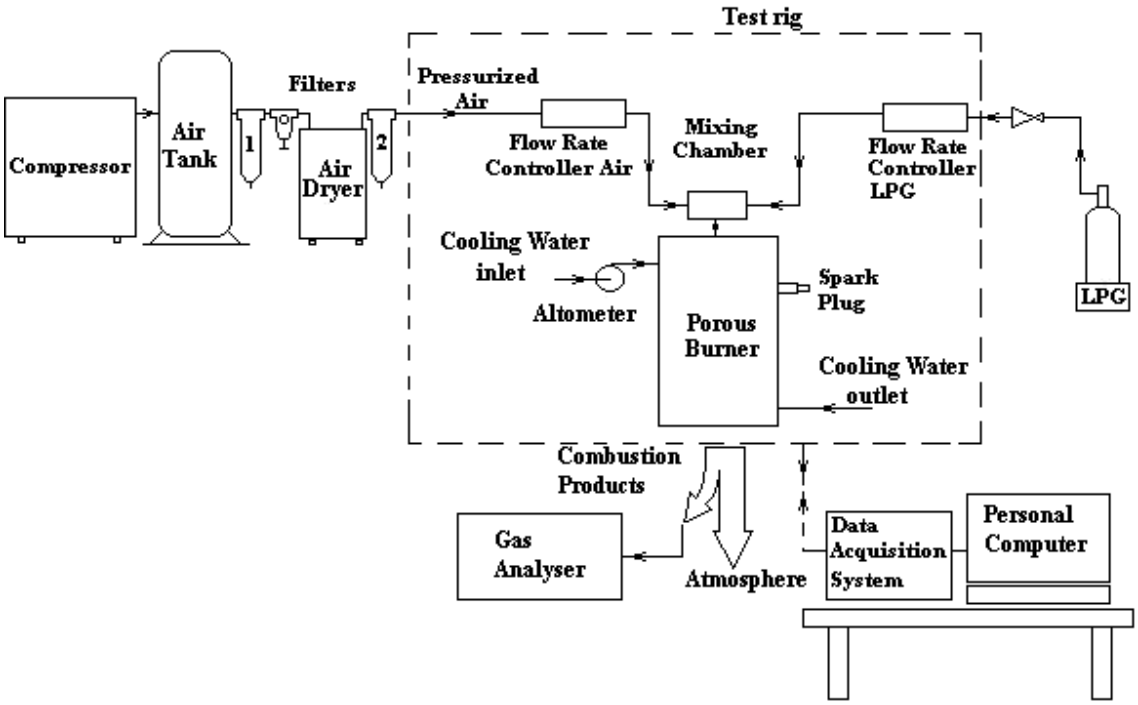

Figure 4.10. Experimental Set-up for 10 kW porous burner

Figure 4.11. Screw compressor

Figure 4.12. Air tank

Figure 4.13. Air filter

Figure 4.14. Air drier

Figure 4.15. Liquefied Petroleum Gas vessel

Figure 4.16. Gas flow meter

Figure 4.17. Data acquisition system and computer

Figure 4.18. MRU Vario plus Combustion gas analyzer

Figure 4.19. 10 kW Porous Medium Combustor test rig

4.3. Experimental Work for 25 kW Porous Burner

The aim of the experimental work was to investigate the temperature profile within the Region C along the centre axis (in z direction) starting with a height of 5 mm above the region A of the 25 kW porous medium (Figure 4.20).

In addition, the simultaneous emission and temperature measurements were carried out immediately above the burner, 1-3 mm in the x- and y-direction (Figure 4.21.) in order to show the change in emission and temperature values as a function of the power of the burner.

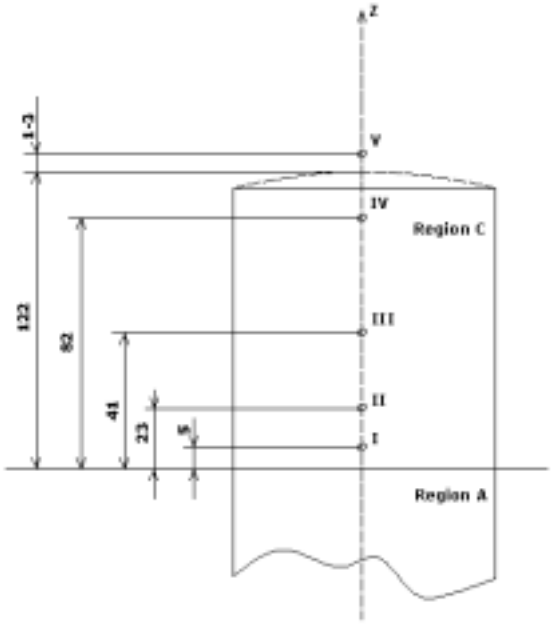

Figure 4.20. Heights in (mm) of the temperature measurements along the central axis of the 25 kW porous medium burner (schematic)

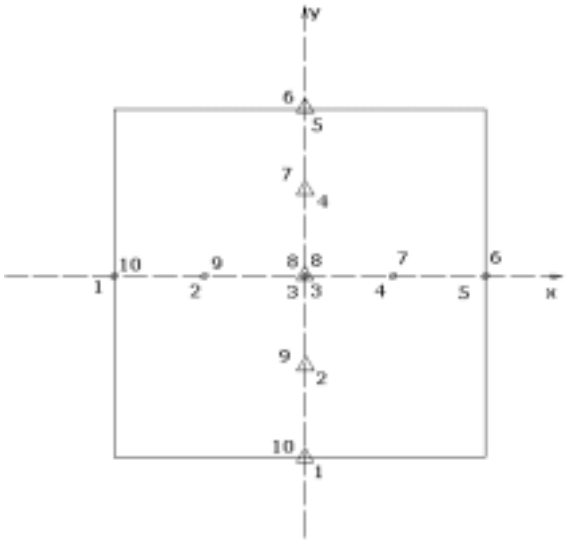

Figure 4.21. Emission and temperature measurement points

During the experiments, the power of the burner was regulated from 27.71 down to 7.49 kW and from 25.06 down to 4.60 kW. Using the measured Oxygen concentration values the corrected excess air ratio numbers, λ_{corr} were calculated by using Equation 4.1. The amount of air needed for the actual combustion processes is called excess air ratio number. Excess air ratio numbers are always higher than the stoichiometric air in order to increase

the chances of complete combustion or to control the temperature of the combustion chamber.

$$\lambda_{corr} = 0{,}895\left(\frac{O_{2,corr}}{20{,}9 - O_{2,corr}}\right) + 1 \qquad (4.1)$$

$O_{2,corr}$: Corrected O_2 values [%]

The results show that the excess air ratio numbers in the positions 1 and 10, 5 and 6 are higher than the values in all other positions. Namely, in the positions 1 and 10, the excess air ratio numbers were 1.56 and 2.36 respectively, and in the positions 5 and 6, the excess air ratio numbers were 1.91 and 1.96 respectively in the x-direction. In all other positions the values of λ were between 1.39 and 1.42. It is caused by the additional excess air coming from the atmosphere due to the jet effect of the exhaust gases above the burner. Therefore, in diagrams and discussions the data of the measurements at positions 1 and 10, 5 and 6 are not taken into account for the residence time.

The experimental work includes two series of measurements, A and B, at the same porous medium burner with a nominal capacity of 25 kW (Figure 4.22). Experiments were carried out in order to determine the behaviour of the burner at different power generations between about 28 down to 7 kW in experiments A, and 25 down to 4.5 kW in B.

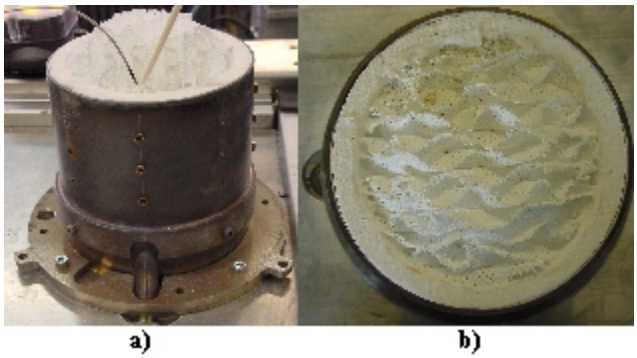

Figure 4.22. a) 25 kW burner **b)** The top view of the burner

First of all each component of the experimental set-up has been check-up in it's functioning before starting the experiments. These are:

- The pressure level of the methane-bottle,
- The range of the pressure reducer, e.g. 20-70 mbar above the atmospheric pressure,

- Gas meter.

Afterwards, the microprocessor of the control unit has been reset and the experiments have been carried out, starting with the maximum power generation of the burner, for instance, in the experiments A with a starting power (100%) of 27.71 kW and in series B 25.06 kW. The fine regulation of the burner has been done using two regulation valves at the inlet of the burner. The stabilisation of the burner has been reached through these fine regulation valves. For the porous burner, a stable flame is defined as one entirely within the burner. If any part of the flame leaves the burner, the flame is considered unstable. After waiting for steady state conditions to be reached, the measurements were performed. First, the emission values measured by using combined gas analyser were taken from the computer. Second, the readings at the gas meter were taken within about 1 min time intervals and recorded in order to calculate the power of the burner. Third, the composition of the exhaust gases and the excess air ratio numbers λ were read at the combustion gas analyser and recorded as well. Then, the temperature values along the centre axis of the burner were read by using Data-logger. After completed the measurements for one position, the positions of the emission and temperature probe were changed by traverse mechanism. The temperature and emission measurements were carried out locally at 10 points in the x-direction (direction of the structure) and 10 points in the y-direction (orthogonal direction to the structure). One measurement at one power range took about 2 hours.

4.4. Experimental Work for 10 kW Porous Burner

This project made in Izmir will demonstrate the new burner technology of combustion in porous media for the first time in Turkey. Furthermore, the burner with integrated heat exchanger will be investigated as well.

The aim of the experiments in Izmir is to measure emissions at different power ranges and excess air ratio numbers by using 10 kW porous medium burner, which was denoted by the "Alexander von Humboldt-Stiftung" to the Izmir Institute of Technology. It was manufactured by the "Lehrstuhl für Strömungsmechanik" of the University Erlangen under the supervision of Prof.Dr.Dr.h.c. Franz Durst. In addition, process water production possibility will be determined.

After installing the porous medium burner in the Energy Laboratory of the Izmir Institute of Technology, a screw compressor with an air preparation unit and a storage tank, a gas analyser, and fuel vessel were supplied by the Faculty of Engineering and gas flow meter denoted by ELSEL Gas Equipment Co in order to complete the experimental set-up.

Experiments were carried out using Liquefied Petroleum Gas as a fuel. The burner has been running at 100, 50, 25% power ranges and 1.4, 1.6, 1.8 excess air ratio numbers which were chosen according to previous experimental works [27]. Furthermore, they have shown that porous burner gives us good results excess air ratio numbers between 1.4 and 2.0. Therefore, measurements were performed in three categories, starting with 25% power ranges going up to 50, 100% at different excess air ratio numbers. At first, screw compressor and fuel vessel were controlled in order to determine that we had enough air and fuel. Second, combustion gas analyser was turned on, because it took time to get ready for measurements. Third, the data acquisition system and computer program were checked. The computer program enabled us to change power ranges and excess air ratio numbers. Before the burner had been running at 25% power range, excess air ratio numbers were entered. Then, the mixture was ignited by spark plug. After waiting for steady state conditions to be reached, measurements were performed. The readings at the gas flow meters were taken within about 1-minute intervals and recorded, so that the porous burner power could be calculated during the experiments. Having recorded data, the composition of the exhaust gases, its temperature, and excess air ratio numbers λ were read at the gas analyser and recorded in experiment sheet as well. Emission measurements and exhaust gas temperatures were carried out immediately below the burner. Cooling water inlet and outlet temperatures were read and recorded by using thermocouples, which were controlled by data acquisition system and computer.

CHAPTER 5

RESULTS AND DISCUSSIONS

5.1. Evaluations of Measured Data for 25 kW Porous Burner

In the present work the results of experimental investigations on 25 kW porous medium burners are given. Experiments were carried out using methane gas as a fuel at different power ranges and excess air ratio numbers. The burner has been running at 100, 70, 40% power ranges for emission and temperature measurements in order to find out the relation between the emission concentrations and the power ratio during the experimental research the burners were allowed enough time to enter steady state conditions for all chosen operating conditions. The thermal power of 25 kW burner for first adjustment (series A) systematically varied between 27.71 kW and 7.49 kW, for second adjustment (series B) between 25.06 kW and 4.60 kW.

The results have been evaluated in three categories, residence time, temperature profiles in x, y, and z direction and emission measurements.

The measured temperatures along the centre axis of the burner at the heights (z =5); 23; 41 and 82 mm and immediately above the exit surface of the burner in position 3, in the x- and y- direction (Figures 4.20 and 4.21) at different powers for the experiments, series A and B are shown in Figure 5.1. It is obvious that a similarity between the temperature profiles exists. The lowest temperature of all profiles is at the height z = 82 mm and the highest one at z = 23 mm. After the height 23 mm the temperature decreases within the burner in order to drop about 400 ºC immediately above 1-3 mm of the exit surface of the burner. In all experiments, series A and B, the temperature within the burner, along the central axis, increases up to the height 23 mm. Afterwards it decreases continuously in all other heights. This means at the point z = 23 mm there is a temperature gradient equal to zero, $\left(\frac{dT}{dz}\right)_{z=23\,mm} = 0$.

In other words, at the height z = 23 mm there is an invisible insulation plane, which distributes heat fluxes in two different regions, downwards, from z = 23 mm down to 5 mm, and upwards from z = 23 mm up to z = 82 mm.

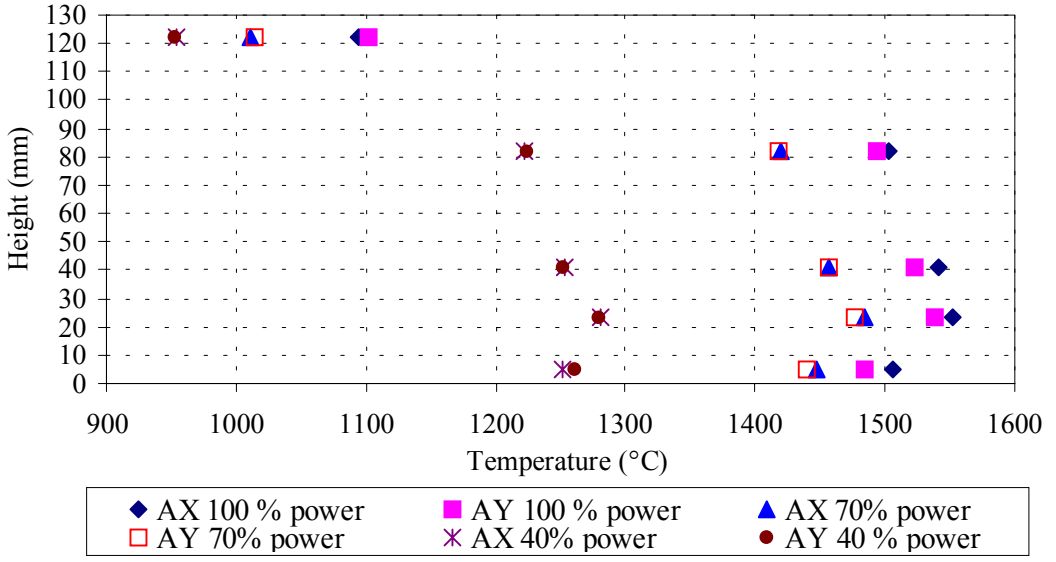

(a)

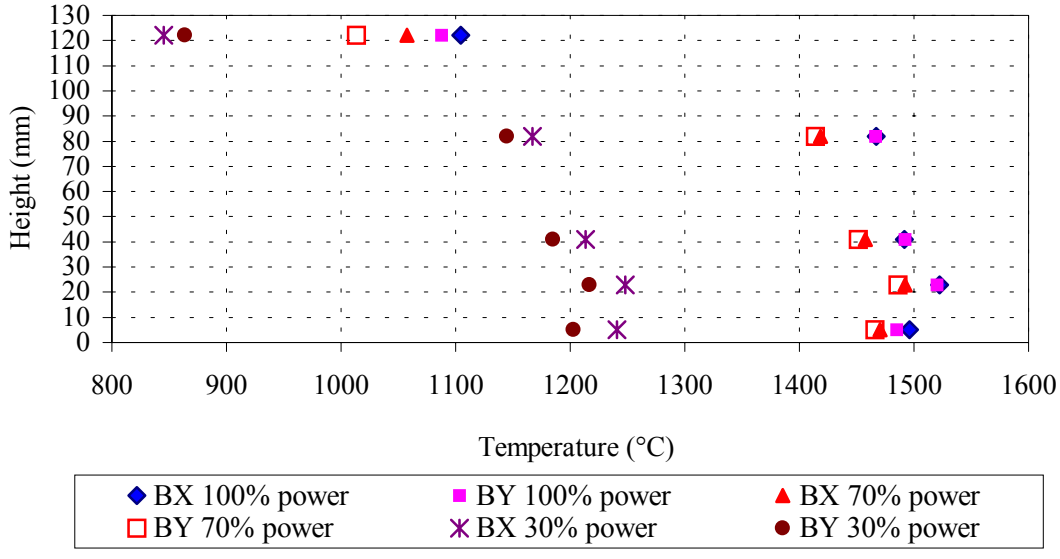

(b)

Figure 5.1. Temperature profiles along the central axis of the burner:

a) Temperature profiles in position 3; measurements for series A

b) Temperature profiles in position 3; measurements for series B

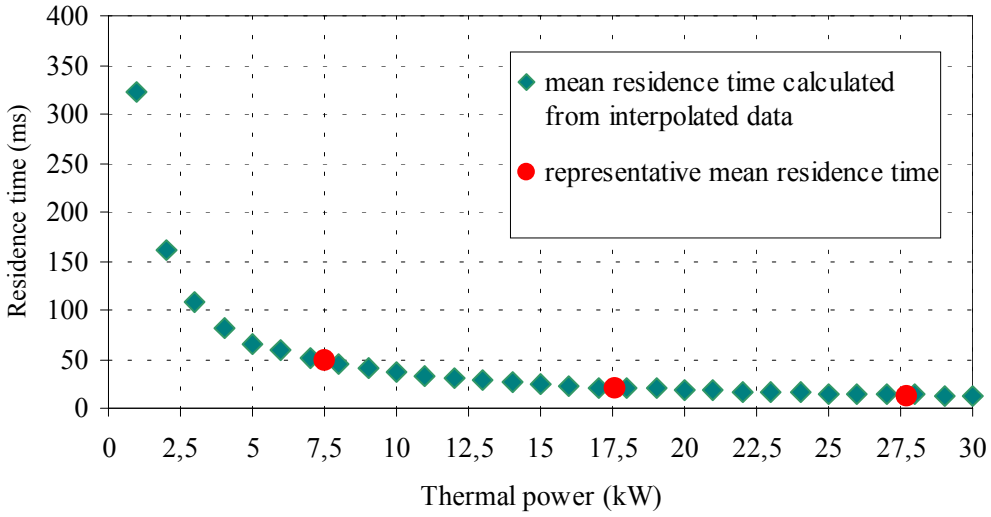

(a)

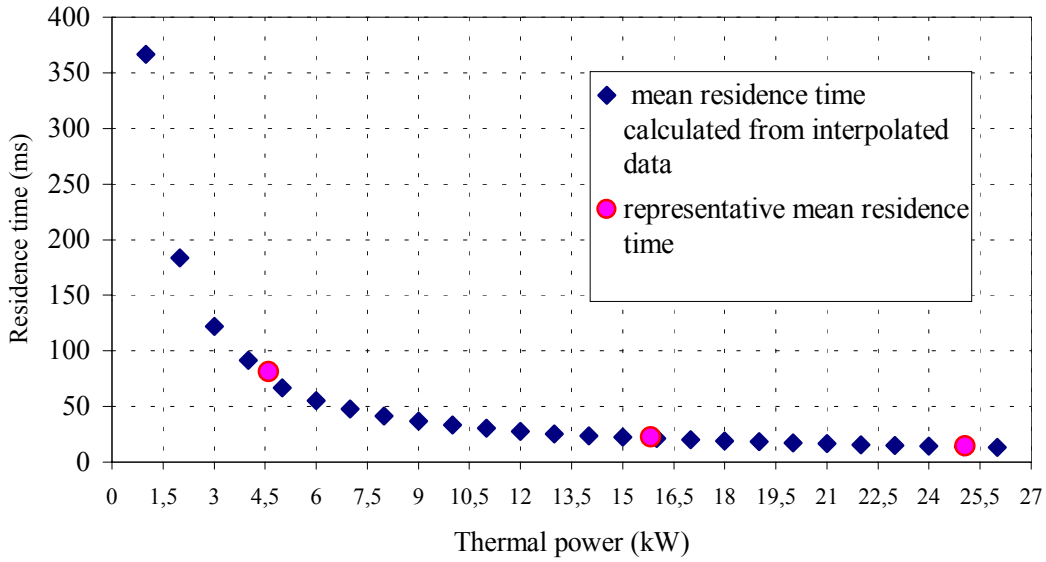

(b)

Figure 5.2. Mean residence times versus the thermal power of the burner, calculated from the data given in Tables A.1, A.2 and A.3:

a) Residence time for different powers; measurements for series A

b) Residence time for different powers; measurements for series B

There are several reaction mechanisms, which are responsible for the production of NOx in the combustion processes. These are thermal NOx mechanisms, prompt NOx mechanisms and fuel dependent NOx production. The first one plays a major role in the

flame zone and depends on the temperature of the exhaust gas and the residence time inside the combustion chamber. An effective way to reduce the emission of thermal NOx is by reducing the exhaust gas temperature and minimizing the residence time. In order to be able to calculate the residence times using the measured data, given in Tables A.1, A.2 in Appendix and the temperature profiles in Figure 5.1 are necessary. Residence times were calculated by using Equation 5.1 and Equation 5.2.

$$t = \frac{V_{burner}}{\dot{v}_{exhaust}} \tag{5.1}$$

t : Residence time [s]

$V_{burner} = 0{,}0008478\, m^3$

$\dot{v}_{exhaust}$: Exhaust gas flow rate [m^3/s]

$$\dot{v}_{exhaust} = \left(1 + \frac{2}{0{,}21}\lambda_{corr}\right)\frac{T_{mean}}{T_{room}}\dot{v} \tag{5.2}$$

T_{mean} : Mean temperature in z-direction [K]

T_{room} : Room temperature [K]

$\dot{v}$: Cold gas flow rate [m^3/s]

The analysis of the temperature profiles shows that there are three different temperature regions according to the power range, namely 100, 70 and 40 % or 30 %. Therefore, three mean residence times for three power ranges are calculated and given in Table A.4 in Appendix. For this purpose, the mean temperature within the burner of the experiments in series A and B was calculated using the temperature profiles given in Figure 5.1, and taking as arithmetic mean of the mean temperatures in the planes x - z and y - z (Figures 4.20, 4.21 and 4.6). Through the traverse mechanism it was possible to read temperatures at the same locations from 1 to 10 in the x- and y- direction (Figure 4.21). The corresponding excess air ratio numbers at 100, 70 and 40 or 30 % power ranges from Tables A.1 and A.2 with the arithmetic mean temperatures gave the mean residence times (Figure 5.2). In Figure 5.2 these, from measured data, calculated mean residence times are given as “representative residence time” and pointed out with dots. In Figure 5.2, other mean residence times are also given, which are calculated by using Equation 5.3 for the whole power range 1-30 kW for series A and 1-26 kW for series B, taking 1 kW power steps and using interpolated data given in Tables A.1 and A.2. These mean residence times

in Figure 5.2 are called as "mean residence time calculated from interpolated data" and calculated by using Equation 5.3. From Figure 5.2, it can be easily seen that the representative mean residence times lie on the curve of the mean residence time from the interpolated data.

$$\dot{t} = \left(\frac{V_{burner}}{1 + 9{,}524\lambda} \left(\frac{T_{mean}}{T_{room}} \right) \frac{P}{35880} \right) 10^3 \qquad (5.3)$$

$\dot{t}$: mean residence time calculated from interpolated data [ms]

P : Power [kW]

Figure 5.3 illustrates the theoretically calculated and measured representative mean residence time as a function of the thermal power of the burner. Theoretical curves are calculated for the highest and lowest temperatures, which are measured during the experiments for series A and B with corresponding excess air ratio numbers (Tables A.1 and A.2). The excess air ratio numbers and the temperatures for the series A are taken as follows: λ = 1.3 – 1.5 and 2.0 and T = 1700 and 1400 K. For the series B they are: λ = 1.5 – 1.7 and 2.0 and T = 1700 and 1400 K.

The measured representative mean residence times are also plotted versus the thermal power of the burner in Figure 5.3. From Figure 5.3 it is obvious that the measured representative mean residence time for the series A, t_{mean} = 13.21 ms (100%), 21.13 ms (70%) and 47.99 ms (40%) lie exactly in the field given by the theoretical mean residence time curves. The measured representative mean residence times are respectively 13.82 ms (100%), 21.61 ms (70%) and 76.99 ms (30%) for the series B.

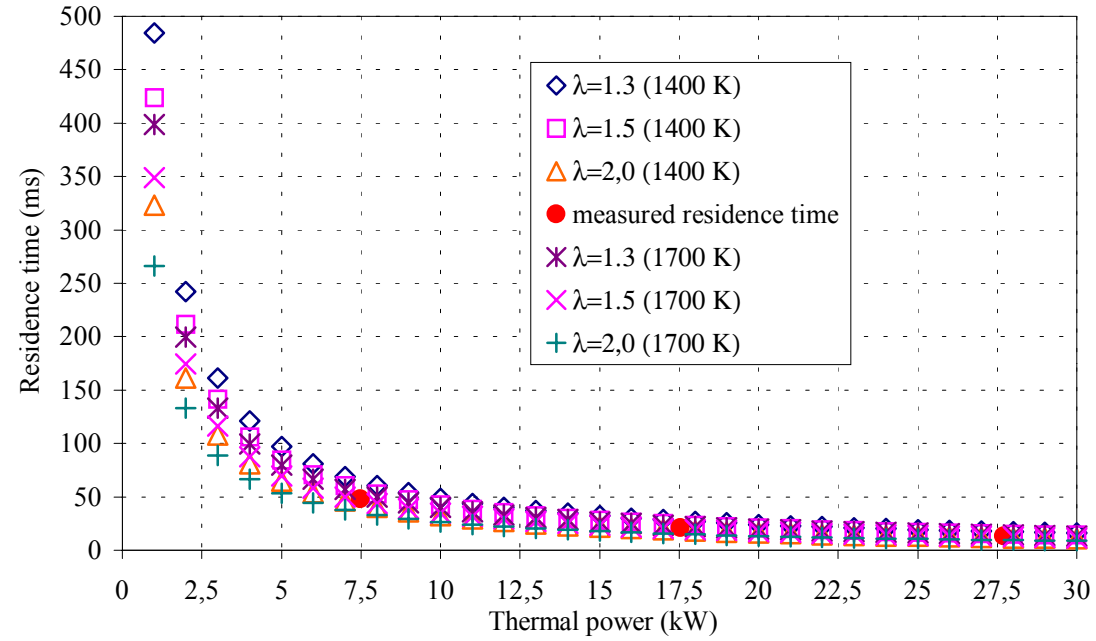

(a)

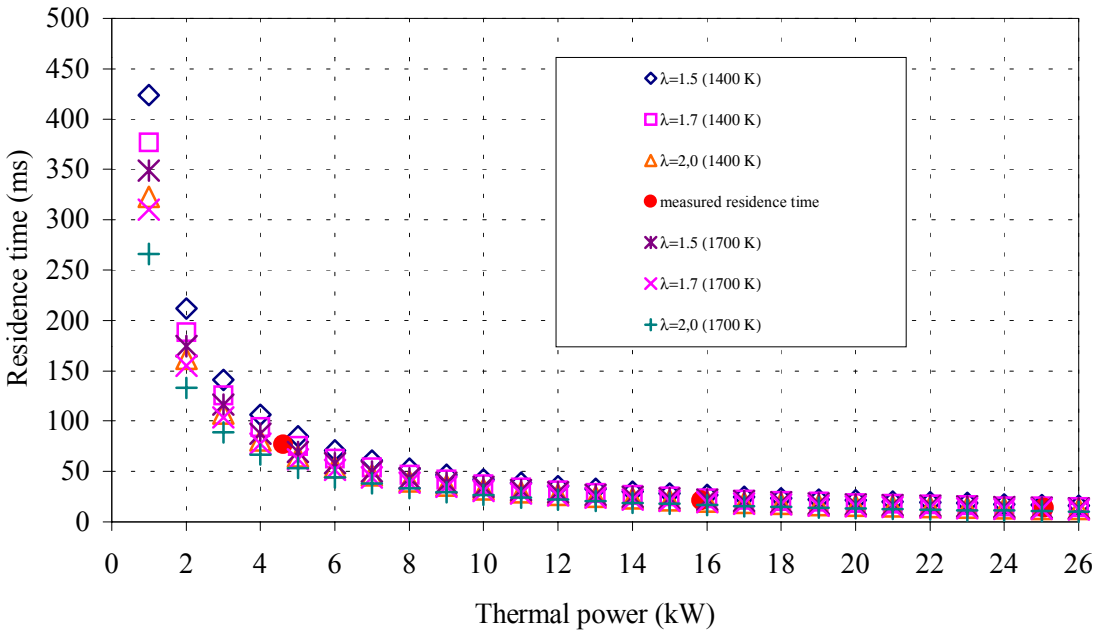

(b)

Figure 5.3. Theoretical and measured mean residence time versus thermal power of the burner

a) Residence time for different powers; measurements for series A

b) Residence time for different powers; measurements for series B

Temperatures above 1 - 3 mm of the exit surface of the burner were measured in positions 1 to 10 in the x- and y- direction (Figure 4.21). This means, at the same location

the temperature was read twice. Therefore, temperatures at the positions 3 and 8, 2 and 9, or 4 and 7 should be compared to check the reproducibility of the experiment. For instance, in Figure 5.4 the comparison gives that the temperatures are close to each other: in position 3 and 8: 1093.8 and 1113.5 °C; in position 2 and 9: 1211.1 and 1195 °C; in position 4 and 7: 1055.1 and 1054 °C respectively. These temperatures were taken in the direction of the structure of the matrix.

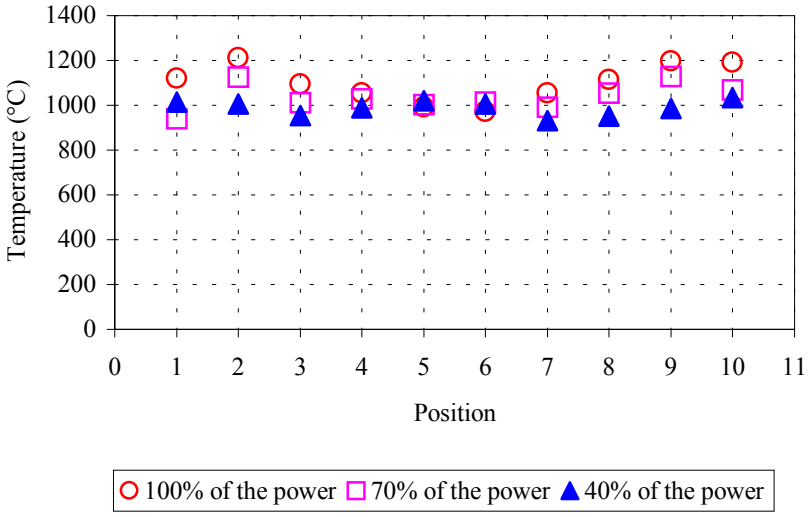

Figure 5.4. Temperature profile above 1 – 3 mm of the exit surface of the burner for the experiments series A in the x-direction

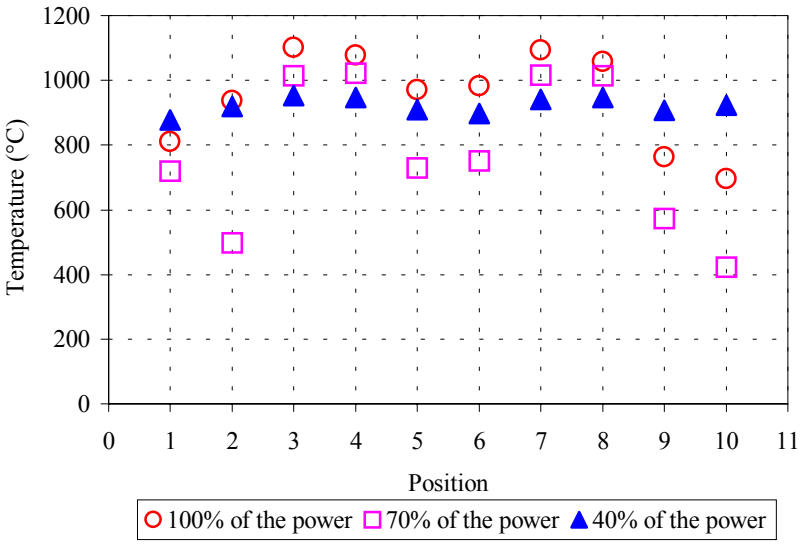

Figure 5.5. Temperature profile above 1 – 3 mm of the exit surface of the burner for the experiments series A in the y-direction

The temperatures in the orthogonal direction to the structure are given in Figure 5.5. The temperature distribution in the y-direction has entirely different picture from that in the x-direction (Figure 5.4) because of the porous structure.

Temperature profiles for the experiments, series B, given in Figures 5.6 and Figure 5.7 show the same character like in Figures 5.4 and Figure 5.5 for the experiments, series A.

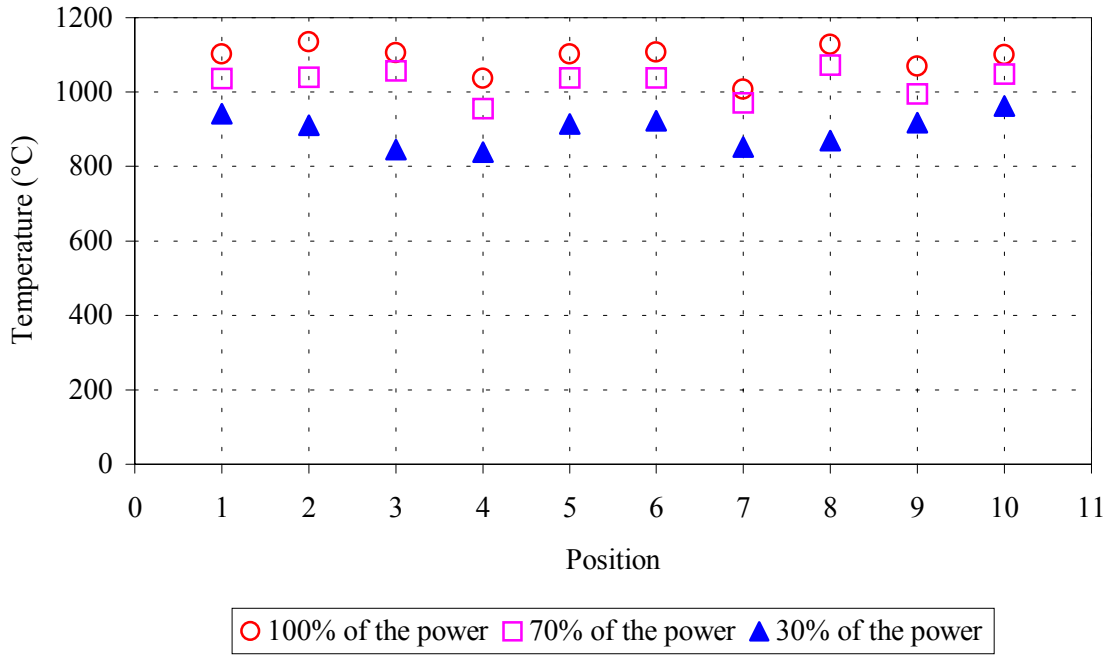

Figure 5.6. Temperatures above 1 – 3 mm of the exit surface at different power ranges in the x direction of the matrix within the burner, series B

Emissions were measured simultaneously with the temperatures at the same position, 1 to 3 mm above the exit surface of the burner. Figure 5.8 gives the carbon monoxide emissions at the power ranges 100, 70 and 40 %. From Figure 5.8 it is seen that the higher the power is the higher also carbon monoxide emissions are. But it is not linearly depending on the power, because at the power range 40 % it goes down to 5 mg/kWh from 120 mg/kWh at 100 % power range. All CO and NOx emission values were measured in ppm unit and their values were converted to mg/kWh unit by using Equation 5.4 and Equation 5.5.

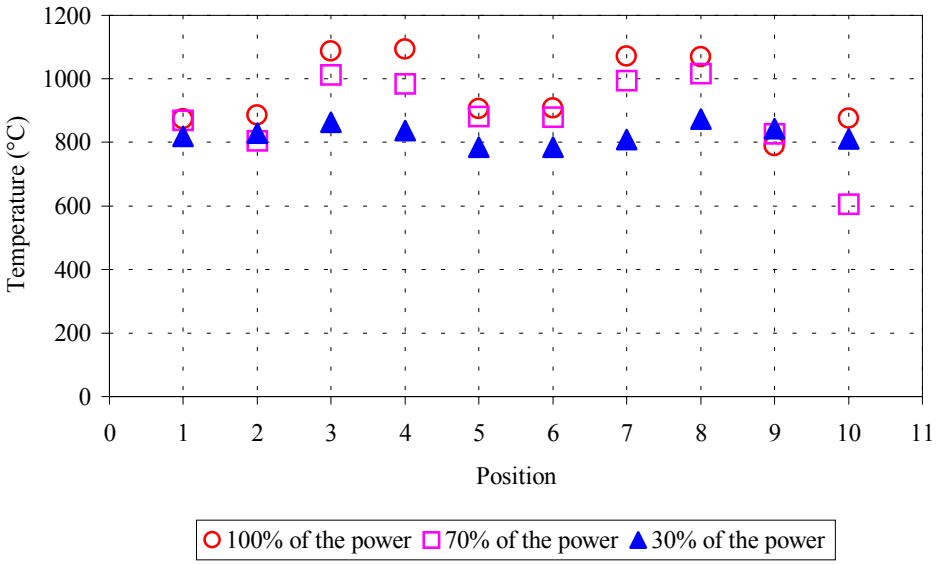

Figure 5.7. Temperatures above 1 – 3 mm of the exit surface at different power ranges in the y direction of the matrix within the burner, series B

$$\dot{E}_{CO} = \frac{8{,}524 + (\lambda_{corr} - 1)9{,}524}{9{,}9675} 1{,}25 (E_{CO}) \tag{5.4}$$

$\dot{E}_{CO}$ **:** CO emission value [mg/kWh]

E_{CO} : Corrected CO emission value [ppm]

$$\dot{E}_{NOx} = \frac{8{,}524 + (\lambda_{corr} - 1)9{,}524}{9{,}9675} 2{,}05 (E_{NO} + E_{NO2}) \tag{5.5}$$

$\dot{E}_{NOx}$: NO_X emission value [mg/kWh]

$E_{NO} + E_{NO2} = E_{NOx}$: Measured NO and NO_2 values [ppm]

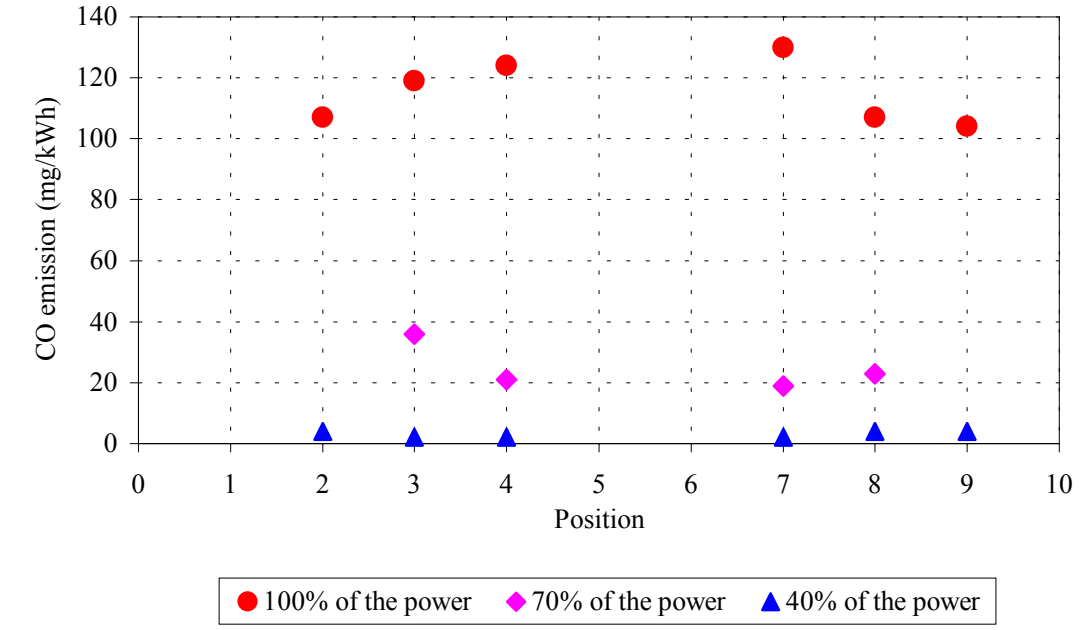

Figure 5.8. Carbon monoxide emissions at different power ranges in the x-direction, series A

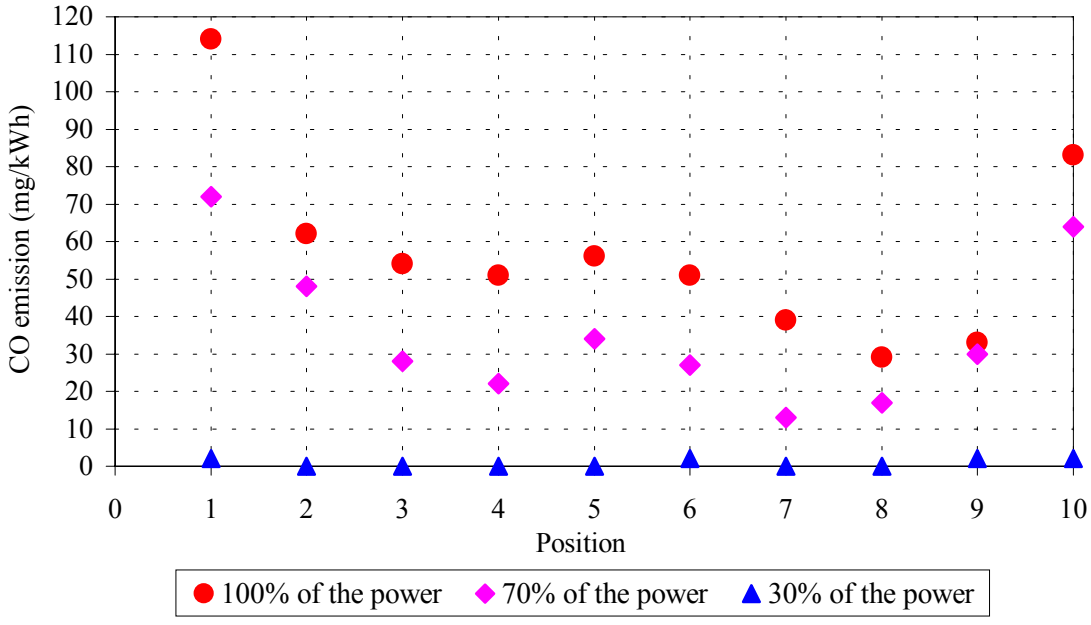

Figure 5.9. Carbon monoxide emissions at different power ranges in the x-direction, series B

The same tendency is to be seen also in Figure 5.9, in experiments, series B. Although these experiments started with a maximum power of 26 kW instead of 28 kW (at series A), carbon monoxide emissions go down from 60 immediately to about 1 - 2 mg/kWh at the

power range 30 %. In addition, it means that 30 times less emission by 1/3 power reduction. This behaviour does not change with the directions, x or y, (Figures 5.10 and Figure 5.11) but, the absolute values of the CO changes with changing direction. This means, the absolute CO emission changes with the power and the structure of the matrix.

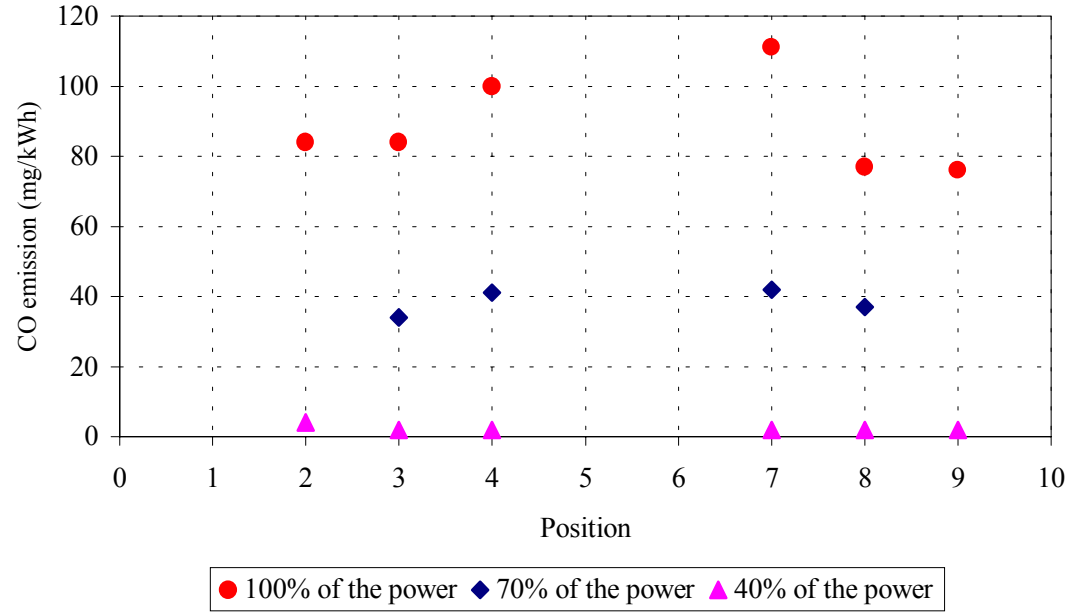

Figure 5.10. Carbon monoxide emissions at different power ranges in the y-direction, series A

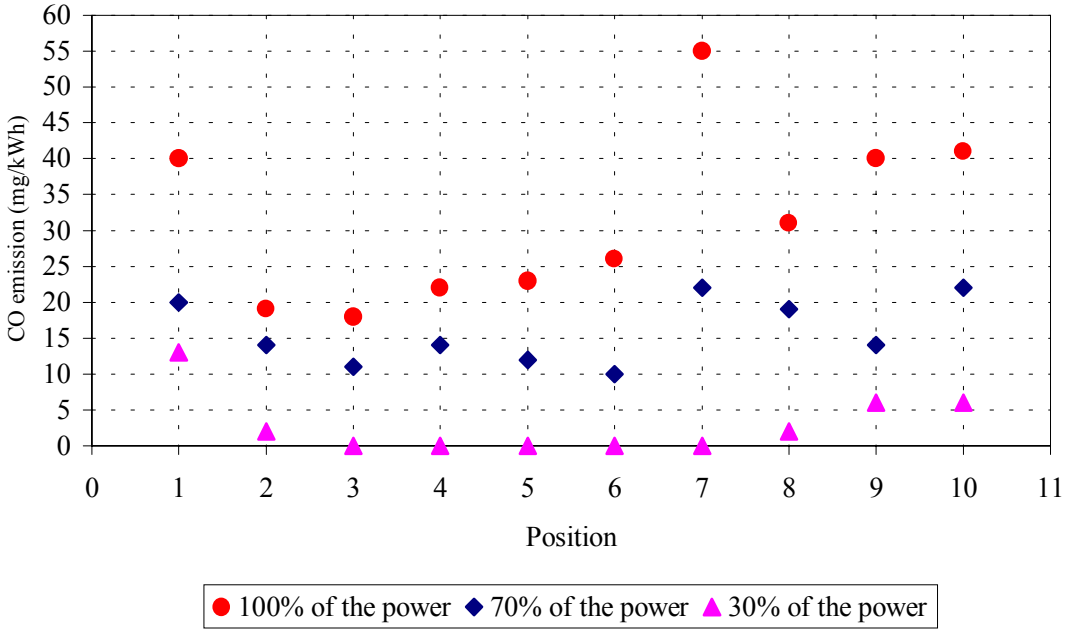

Figure 5.11. Carbon monoxide emissions at different power ranges in the y-direction, series B

In Figure 5.12, nitrogen oxides are given at different power ranges in the x-direction for the series A and in Figure 5.13 in the y-direction. In both directions the highest value appear at 100% range and the lowest ones at 40%.

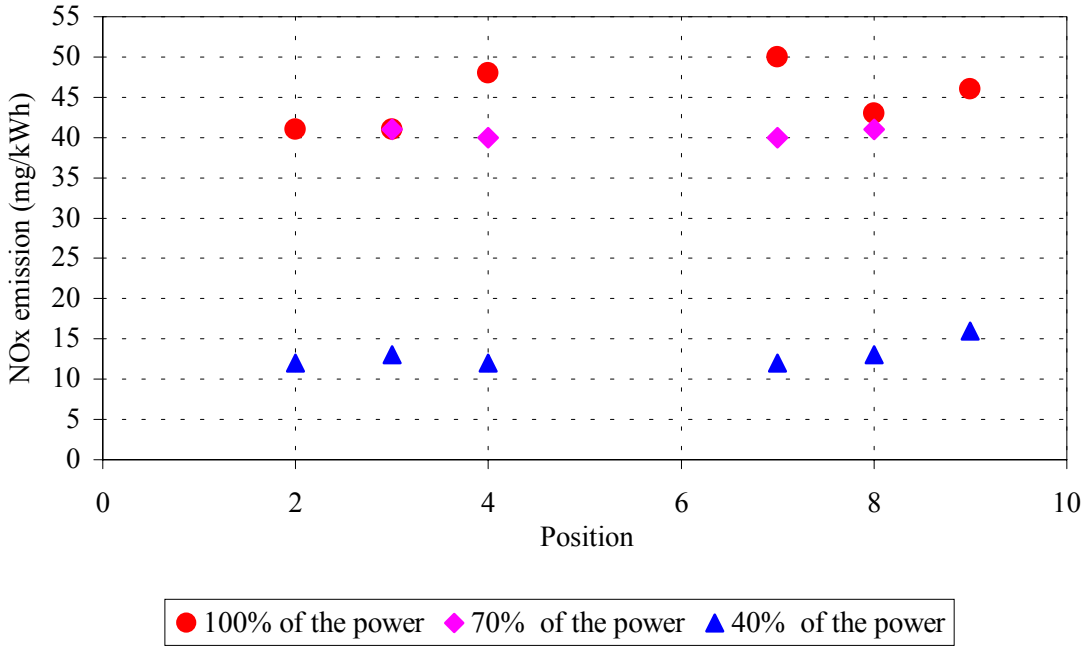

Figure 5.12. Nitrogen oxides emissions at different power ranges in the x-direction, series A

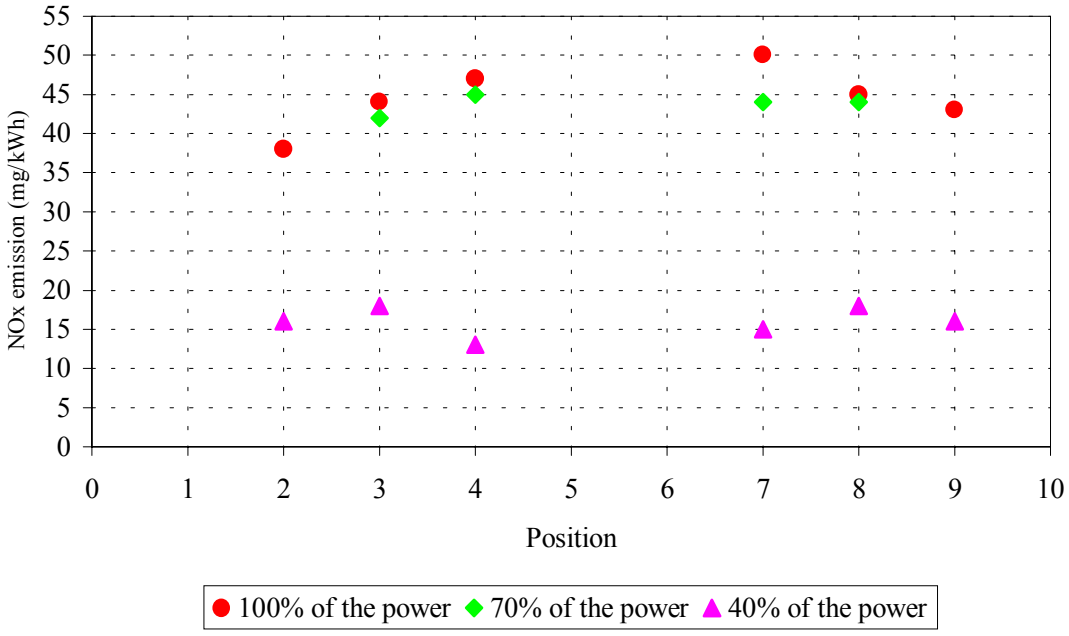

Figure 5.13. Nitrogen oxides emissions at different power ranges in the y-direction, series A

According to the emission distribution in both cases, the structure direction has no influence on the emission concentration. Figures 5.14 and 5.15 show similar character like Figures 5.12 and 5.13. In series B, the highest NOx emission values occur at 70% power ranges because of the porous structure.

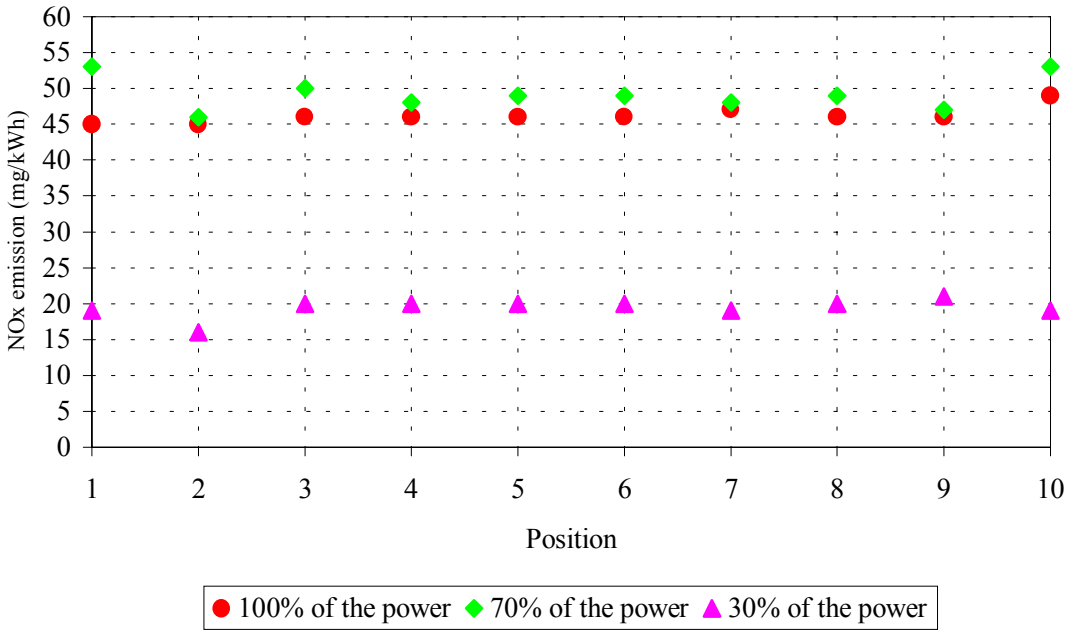

Figure 5.14. Nitrogen oxides emissions at different power ranges in the x-direction, series B

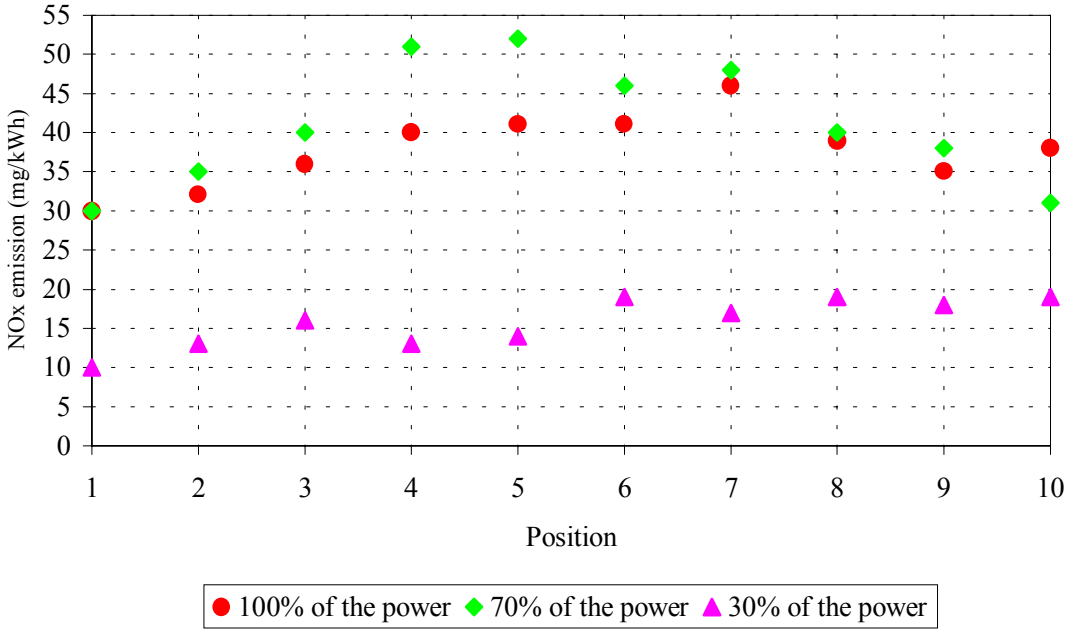

Figure 5.15. Nitrogen oxides emissions at different power ranges in the y-direction, series B

In order to compare CO- and NO_X- emissions of the burner with the European limits of emissions are given in Table 5.1.

Table 5.1. European limits of emissions [24,30]

	German Norm DIN 4702	Swiss Norm	Blue Angel
NO_X (mg/kWh)	200	80	60
CO (mg/kWh)	100	60	50

Although some CO values are above the German Norm DIN values, one can keep in mind that these values will decrease after installing heat exchanger part. From Table 5.1, it can easily be seen that CO- and NO_X- emissions at all power ranges lie lower than the values given by the German Norm DIN 4702.

5.2. Evaluations of Measured Data for 10 kW Porous Burner

The thermal power of 10 kW porous burner varied between 9.43 and 2.44 kW. The burner showed that it had extremely high turns down ratio capabilities of over 4:1. In view of this large modulation range, the present burners are far ahead of any state-of-the-art burners in the markets. Collected data have been evaluated in three categories; relationship between power and excess air ratio numbers, emission measurements, exhaust gas and cooling water temperatures.

Experiments show us that there is a strong relationship between thermal power and excess air ratio numbers. This relationship is drawn in Figure 5.16. One can easily see that the Figure 5.16 depicts decrease of excess air ratio numbers with the increase of thermal power. It was also considerable result that the measured excess air ratio numbers remained between selected excess air ratio numbers.

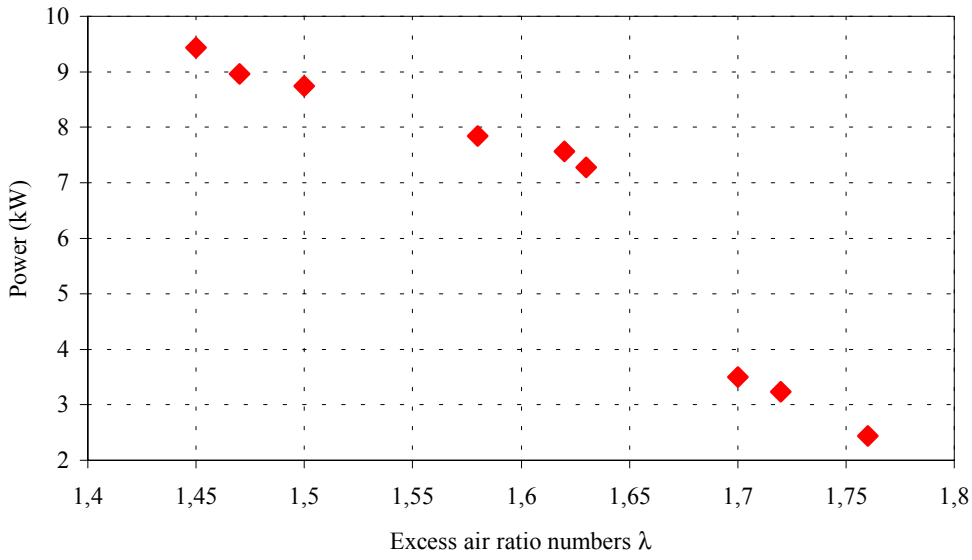

Figure 5.16. Burner power as a function of the excess air ratio numbers

Both measured values of CO emission and emission of NO_X as a function of the thermal power are given in Figure 5.17 for 10 kW burner. In general, a CO emission increases with the thermal power of the burner. The CO gradient is steeper than NO_X gradient, which can be explained by the higher ratio of the surface to the volume of 10 kW burner. All measured emission values are in ppm unit. In figures all these values are converted in mg/kWh unit by using Equation 5.6 and Equation 5.7.

$$\dot{E}_{CO} = \frac{26{,}460 + (\lambda - 1)28{,}809}{31{,}87} 1{,}25 (E_{CO}) \tag{5.6}$$

$\dot{E}_{CO}$ **:** CO emission value [mg/kWh]

E_{CO} : Corrected CO emission value [ppm]

$$\dot{E}_{NOx} = \frac{26{,}460 + (\lambda - 1)28{,}809}{31{,}87} 2{,}05 (E_{NO} + E_{NO2}) \tag{5.7}$$

$\dot{E}_{NOx}$: NO_X emission value [mg/kWh]

$E_{NO} + E_{NO2} = E_{NOx}$: Measured NO and NO_2 values [ppm]

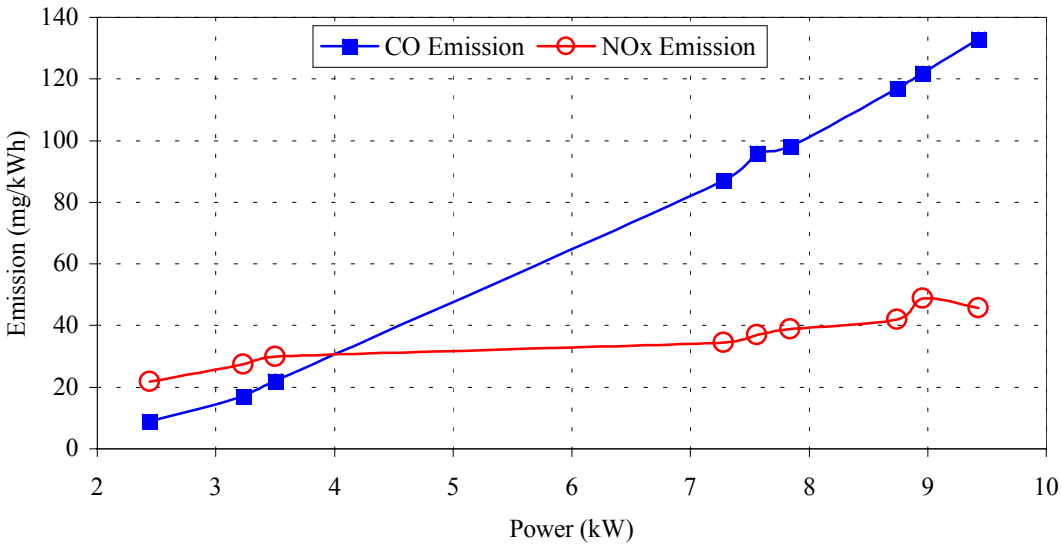

Figure 5.17. CO and NO_X emissions as a function of the burner power

Figure 5.18 shows CO emission as a function of the excess air ratio numbers. European standards are given in both figures. CO emission values at minimum air ratios are higher than the values that are given in all standards because of the cracked material. The emissions decrease for the excess air ratio numbers increase, similarly emissions of NO_X are decreasing with the excess air ratio numbers, as shown in Figure 5.19. All NOx values are lower than the all standards values.

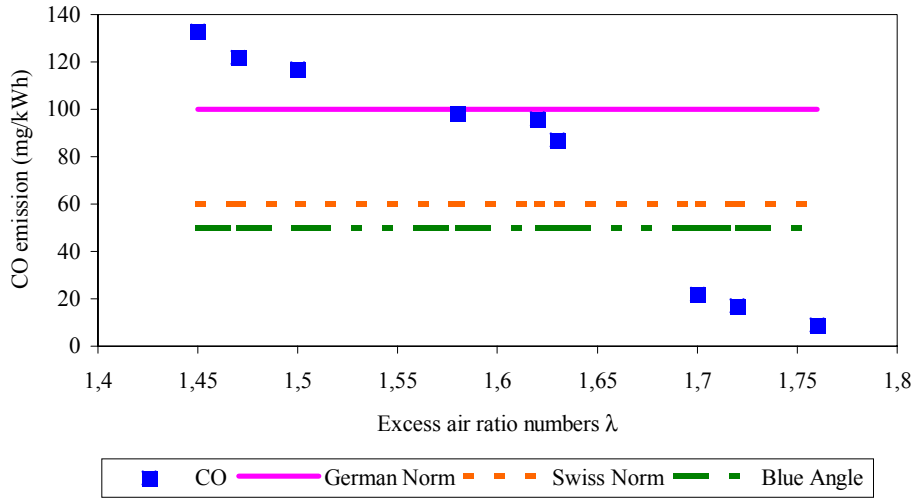

Figure 5.18. CO emissions as a function of the excess air ratio numbers

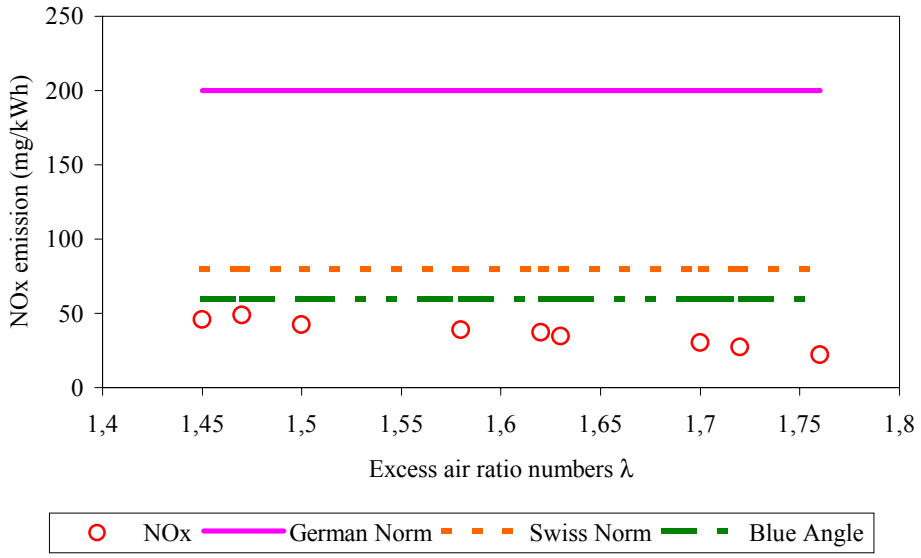

Figure 5.19. NO_X emissions as a function of the excess air ratio numbers

In addition, CO and NO_X emission values are given with respect to power ranges at 25, 50, 100% respectively Figure 5.20 and Figure 5.21. From figures, it is seen that the higher the power is the higher emissions are.

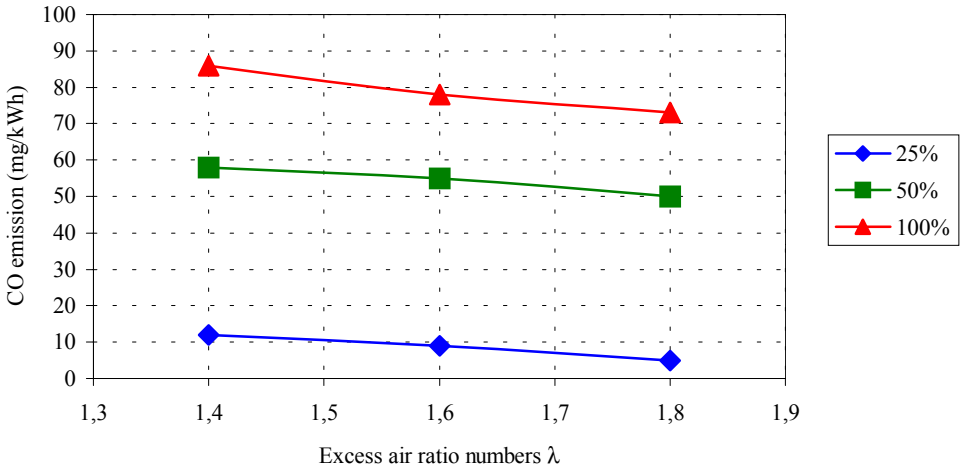

Figure 5.20. CO emissions with respect to power ratios

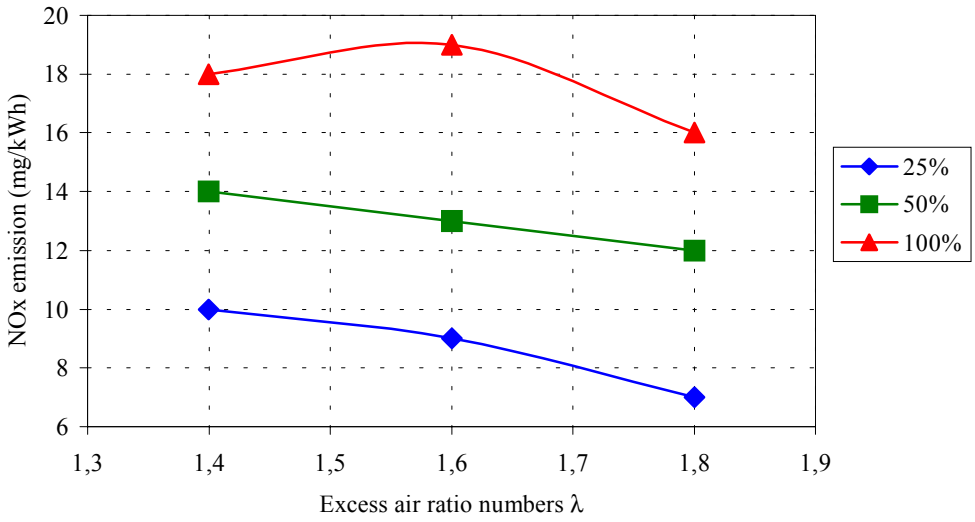

Figure 5.21. NO_X emissions with respect to power ratios

It is well known that emission regulations for energy facilities can be in the form of a prescriptive requirement for a particular control technology, the prescription that best available technologies have to be used, or a maximum allowable emission limit or rate which must be achieved. Some countries that favour emission limits have sets, which vary according to fuel and facility types. Air emission limits for large combustion facilities in Turkey are given in Table 5.2.

Table 5.2. Emission limits for large new combustion facilities in Turkey [33]

Fuel	CO Limits	NO_X Limits
	mg/kWh	mg/kWh
Solid	250	800
Liquid	175	800
Gas	100	500

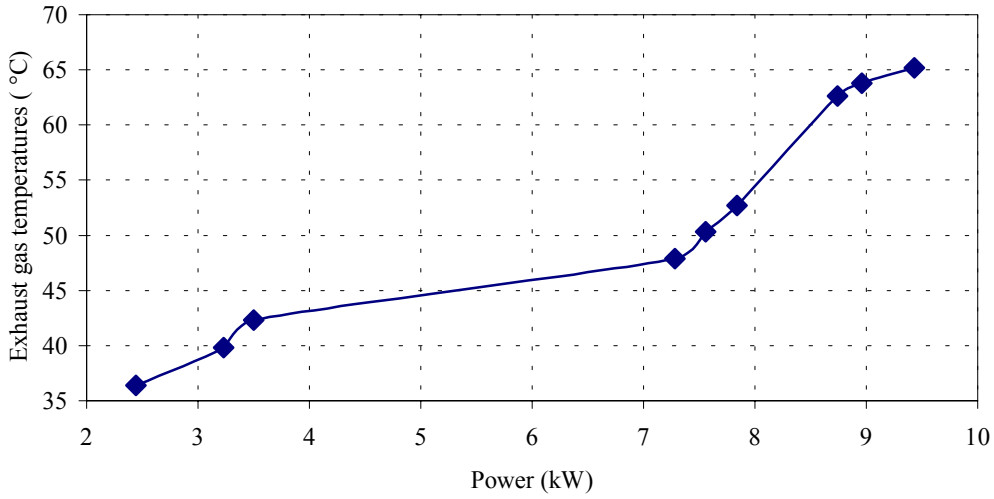

Figure 5.22. Exhaust gas temperatures as a function of the burner power

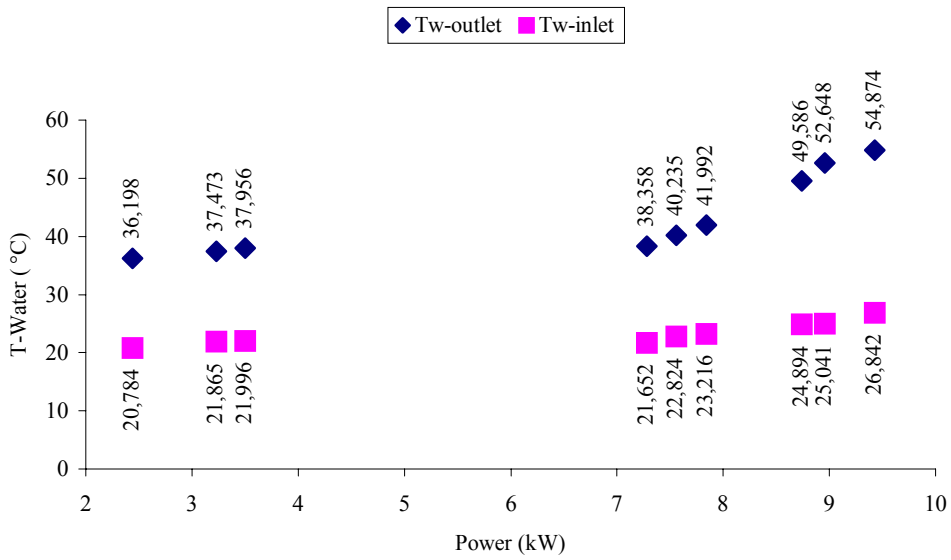

Figure 5.23. Inlet and outlet water temperatures according to burner power

From Figure 5.22, it can be seen that exhaust gas temperatures, which were measured immediately after the heat exchanger unit, goes up while increasing the thermal power. Hence, porous burner doesn't have a special equipment to throw away the exhaust gases from where located. There is a strong relationship between water temperatures and thermal power. This relationship is also shown in Figure 5.23. This figure shows us that temperature differences increase with power. Thus, the greater the power is the higher the temperature differences are, which means that the more heat we get. All calculated and measured data for 10 kW porous burner are given in Appendix Table A.5.

CHAPTER 6

CONCLUSIONS

An experimental investigation on 25 kW porous medium burner was performed in order to determine the turndown ratio, which can be defined as a ratio of obtained maximum power to obtained minimum power while working with maximum and minimum power ratios, exhaust gas temperature distribution at the exit surface, temperature distribution along the centre axis of the burner measured at different heights and emission profiles of carbon monoxide CO and nitrogen oxides NO_X. An estimation of the residence time, necessary for the quality checking of the burner, was also performed. The following conclusions could be drawn for 25 kW porous burner;

- It was found that the burner allows very stable combustion with turn down ratio of around 6:1, and excess air ratio numbers in the range 1.40 – 2.0. The exhaust gas temperature could easily reach 1100°C with a more and less uniform distribution over the burner's exit surface area.
- It was also noticeable that the emission values at different measurement positions and at all power ranges, lies lower than the values given by German Norm 4702 and International Energy Agency, IEA [31, 32].
- The turn down ratio and the emissions obtained during the experiments confirmed the excellent performance of the porous medium burner technology compared with classical free flame burners.

High level of environmental protection becomes a basic factor characterizing the economical and technological potential of country. It becomes a necessary priority in the European Union. More countries in Europe, which have set emission standards, have introduced the strict emission requirements for energy facilities. Furthermore stringent requirements on CO and NO_X emission are important for our country as a new potential member of E.U. An experimental investigation on 10 kW porous medium burner was performed to determine the turn down ratio capabilities, relationship between power and excess air ratio numbers, carbon monoxide CO and nitrogen oxides NO_X emission measurements, exhaust gas and cooling water temperatures.

The following conclusions could be drawn;

- CO and NO_X emissions linearly depend on the power, whereas they are inversely proportional to the excess air ratio numbers. Also it is concluded that emissions increase while the power goes up. It can easily be seen that NO_X emissions at all power ranges are quite smaller than the values given in both Table 5.2 and all European norm. The highest CO emission value at 100% power range for 25 kW porous burner is about 135 mg/kWh, at the same power range for 10 kW porous burner CO emission value is about 140 mg/kWh. While NOx values at 100% power range for 25 kW porous burner varied between 35 and 55 mg/kWh, NOx values for 10 kW porous burner varied between 40 and 60 mg/kWh because of the fact that experimental works for 10 kW burner carried out by using LPG.
- It is also considerable result that excess air ratio numbers are related with thermal power. Namely, one can be observed that the decrease of power with the increase of excess air ratio numbers.
- Temperature differences show us that there is enough heat to produce process water for various fields of heat and energy engineering applications.
- It was found that the 10 kW porous burner enable very stable combustion with turndown ratio of around 4:1 and excess air ratio numbers in the range of 1.4-2.0.

In the future, more efficient heat exchanger will be constructed and made experiments in order to examine porous burner behaviours. Besides, porous material can be changed in view of the fact that temperature differences are investigated. Temperature profiles along the centre axis of 10 kW porous burner may easily be measured by making holes from outside of the burner.

REFERENCES

[1] O.Pickenäcker, K.Pickenäcker, D.Trimis, W.E.C. Pritzkow, C.Müller, P.Goedtke, U.Popenburg, J.Adler, G.Standke, H.Heymer, W.Tauscher, and F.Jansen, "Innovative Ceramic Materials for Porous Medium Burners ," *Intercream.* **5&6**, (1999).

[2] R.Viskanta, "Interaction of Combustion and Heat Transfer in Porous Inert Media, " The 8th International Symposium on Transport Phenomena in Combustion, (San Francisco, 1995).

[3] P.H.Bouma, "Methane-Air Combustion on Ceramic Foam Surface Burners," PhD. Thesis, (Eindhoven, 1997).

[4] M.D. Rumminger, "Numerical and Experimental Investigation of Heat Transfer and Pollutant Formation in Porous Direct-Fired Radiant Burners," PhD. Thesis, (California, Berkeley ,1996).

[5] D.Trimis and F.Durst, "Combustion in Porous Medium Advances and Application," *Combustion Science and Technology.* **121**, (1996), 153-168.

[6] G.Brenner, K.Pickenäcker, D.Trimis, K.Wawrzinek and T.Weber "Stabilized Combustion and Heat Transfer in Porous Media-An Experimental and Numerical Study," The 5th Int. Conference on Technologies and Combustion for a Clean Environment, (Lisbon, Portugal, 1999).

[7] I.Malico, X.Y.Zhou, and J.C.F.Pareira, "Two Dimensional Numerical Study of Combustion and Pollutants Formation in Porous Burners," *Combustion Science and Technology.* **152**, (2000), 57-79.

[8] I.Malico, X.Y.Zhou, and J.C.F.Pareira, "Porous Burner Combustors for Household Application: Modelling and Simulation," The 2nd European Conference on Small Burner and Heating Technology, (Stuttgart, 2000).

[9] "Low Emission, High Efficiency, Compact Porous Medium Burner and Heat Exchanger for Household Applications," *Joint Turkish-German Project Proposal*, (1996).

[10] C.J.Tseng, and J.R.Howell, "Combustion of Liquid Fuels in a Porous Radiant Burner," *Combustion Science and Technology.* **112**, (1996), 141-161.

[11] "Compact Porous Medium Burner and Heat Exchanger for Household Applications," *European Commission-Non Nuclear Energy JOULE-Project Proposal*, (European Commission, Brussels, 1995).

[12] I.Malico and J.C.F.Pareira, "Numerical Predictions of Porous Burners with Integrated Heat Ex-changer for Household Application," *Journal of Porous Media.* **2(2)**, (1999), 153-162.

[13] G.De Soete, " Stability and Propagation of Combustion Waves in Inert Porous Media, " The 11th International Symposium on Combustion, p.959-966.

[14] T.Takeno, and K.Sato, "An Excess Enthalpy Flame Theory," *Combustion Science and Technology.* **20**, (1979), 73-84.

[15] T.Takeno, K.Sato, and K.Hase, "A Theoretical Study on an Excess Enthalpy Flame," The 18th International Symposium on Combustion, (1981), p.465-472.

[16] V.S. Babkin, .A.Korzhavin, and V.A. Bunev "Propagation of Premixed Gaseous Explosion Flame in Porous Media," The 22nd International Symposium on Combustion (1988).

[17] L.D.Pfefferle and S.W.Churchill "The Stability of Flames inside a Refractory Tube," *Combustion and Flame.* **56**, (1984), 165-174.

[18] R.Echigo, Y.Yoshizawa, K.Hanamura, and T.Tomimura, "Analytical and Experimental Studies on Radiation Propagation in Porous Media with Internal Heat Generation," Proceedings of the 8th International Heat Transfer Conference, (1986), p.827.

[19] D.K.Min, and H.D.Shin, "Laminar Premixed Flame Stabilized inside a Honeycomb Ceramic," *International Journal Heat Mass Transfer.* **34(2)**, (1991), 287-338.

[20] S.B.Sthe, E.Peck, and T.W.Tong, "A Numerical Analysis of Combustion and Heat Transfer in Porous Radiant Burners," National Heat Transfer Conference, ASME HTD-106, (1989), 461-468.

[21] P.F.Hsu, W.D.Evans, and J.R.Howell, "Experimental and Numerical Study of Premixed Combustion within Non-Homogenous Porous Ceramic," *Combustion Science and Technology.* **90**, (1993), 149-172.

[22] A.Kesting, O.Pickenäcker, D.Trimis, and F.Durst "Development of Radiation Burner for Methane and Pure Oxygen Using the Porous Burner Technology," The 5th Int. Conference on Technologies and Combustion for a Clean Environment, (Lisbon, Portugal, 1999).

[23] J.R.Howell, M.J.Hall, and J.L.Ellzey, "Combustion of hydrocarbon fuels within porous inert media," *Progress in Energy and Combustion Science*, **22**, (1996), 121-145.

[24] J.Wanka, "The Porous Medium Combustion Technique and its Application for stationary Burners and Porous Medium Engines," Izmir Summer Academy, (2001).

[25] S.Möβbauer, O.Pickenäcker, K.Pickenäcker, and D.Trimis, "Application of the Porous Burner Technology in Energy and Heat Engineering," The 5th Int. Conference on Technologies and Combustion for a Clean Environment, (Lisbon, Portugal, 1999).

[26] "The Porous Medium Burner Technology," http://www.lstm.uni-erlangen.de/

[27] D.Trimis, F.Durst, and K. Pickenäcker, "Porous Medium Combustor versus Combustion Systems with Free Flames," (ISHTEEC, Guanngzhou, China 1997).

[28] F.Durst, D.Trimis, and G.Dimaczek, "Porous Medium Combustor and its Application as Water Heater or Steam Generator," (1996).

[29] F.Durst, G.Dimaczek, and D.Trimis, "Burner Having Porous Material of Varying Porosity" (US Patents Office, 1996), US5522723.

[30] D.Trimis, "The Porous Burner Technique and its Application,"(Lausanne, Swiss,1998).

[31] "Emission Controls in Electricity Generation and Industry," International Energy Agency, (Publication Service, OECD, 1988), p.44-47.

[32] T.Godish, "Air Quality" (Lewis Publishers, Inc., 1985), p.216-217.

[33] Hava Kalitesinin Korunması Yönetmeliği, Resmi Gazete, s19269, 1986.

APPENDIX

Table A.1. Measured and corrected values of the experiments; series A in the x- and y-direction

	P.N.	Temperature values in z-direction				t [^{0}C]	λ (O_2)	P_A kW	IM3000P				$\lambda_{corr.}$	Corrected values		E NOx [mg/kWh]	E CO [mg/kWh]
		I	II	III	IV				CO [ppm]	NO [ppm]	NO_2 [ppm]	O_2 [%]		CO [ppm]	O_2 [%]		
in x-Direction 100 %	1	1510.5	1555.5	1546.5	1508	1118.9	1.55	28.3	97	16	0	6.7	1.56	204.90	8.02	46	355
	2	1507.5	1552.2	1543.2	1505	1211.1	1.41	27.438	69	16	0	6.9	1.42	67.96	6.66	41	107
	3	1506.5	1552.4	1540.8	1503.6	1093.8	1.4	27.907	74	16	0	6.8	1.41	76.58	6.52	41	119
	4	1505.5	1551.7	1540.7	1504.8	1055.1	1.38	27.794	72	19	0	6.7	1.39	80.87	6.31	48	124
	5	1507.4	1551	1539	1503.8	991.1	1.89	27.258	115	18	0	7.5	1.91	203.06	10.52	64	437
	6	1508.8	1552	1539.5	1504.8	971.9	1.95	27.438	93	19	0	7.4	1.96	155.13	10.84	69	344
	7	1507	1549.1	1535.8	1501.4	1054	1.38	27.907	73	20	0	6.6	1.39	84.78	6.32	50	130
	8	1506	1548.5	1534.7	1501.3	1113.5	1.4	27.219	68	17	0	6.8	1.41	68.77	6.53	43	107
	9	1505.5	1548.3	1533.6	1500.8	1195.9	1.41	27.438	66	18	0	6.9	1.42	66.70	6.63	46	104
	10	1505	1549.2	1534.9	1501.5	1191.2	2.34	28.383	145	17	0	9	2.36	288.53	12.61	75	778
in x-Direction 70 %	1	1447.5	1482.4	1455.5	1418.4	940.1	4.8	17.396	30	3	0	19.4	4.85	25.73	16.96	28	146
	2	1446.5	1484.3	1456.4	1419.7	1124.4	1.63	17.807	21	14	0	9	1.64	37.48	8.69	42	69
	3	1446.9	1484.4	1457.2	1420.3	1010.8	1.48	17.707	20	15	0	7.6	1.49	22.09	7.36	41	36
	4	1446.7	1484.3	1456.5	1420.4	1027.3	1.48	17.298	14	15	0	7.4	1.48	13.05	7.31	40	21
	5	1447.4	1484.5	1456.4	1420.3	1001.9	2	17.464	24	15	0	7.7	2.02	34.38	11.13	56	79
	6	1445.7	1483.5	1456.2	1420.1	1013	1.93	17.369	21	14	0	8.7	1.94	36.30	10.71	50	80
	7	1446.4	1484.3	1456.4	1419.4	991.9	1.47	17.307	8	15	0	7.5	1.48	11.78	7.28	40	19
	8	1446.9	1483.7	1455.8	1418.9	1053	1.48	17.781	14	15	0	7.6	1.49	13.94	7.39	41	23
	9	1446.6	1483.3	1455.7	1419	1129	1.56	17.664	19	14	0	8.5	1.56	17.04	8.07	40	30
	10	1447.4	1483.4	1454.7	1418.4	1068.9	2.91	17.707	26	5	0	16.7	2.96	37.57	14.35	28	128

	P.N.	Temperature values in z-direction				t [^{0}C]	λ (O_2)	P_A kW	IM3000P				$\lambda_{corr.}$	Corrected values		E NOx [mg/kWh]	E CO [mg/kWh]
		I	II	III	IV				CO [ppm]	NO [ppm]	NO_2 [ppm]	O_2 [%]		CO [ppm]	O_2 [%]		
in x-Direction 40 %	1	1250.3	1279.7	1251.2	1219.8	1013.4	1.74	7.4997	6	4	0	10.1	1.74	7.12	9.46	13	14
	2	1250.9	1279.3	1250.8	1219.6	1004.9	1.68	7.5803	3	4	0	9.5	1.68	2.04	9.05	12	4
	3	1252.3	1281.4	1252.8	1221.5	953.3	1.78	7.28	3	4	0	10.1	1.78	1.15	9.71	13	2
	4	1251.2	1281.6	1253.3	1221.8	987.3	1.67	7.176	2	4	0	9.5	1.67	1.12	8.95	12	2
	5	1253.3	1280.9	1252.4	1221.2	1020.9	1.82	7.176	5	4	0	10.5	1.82	4.07	10.01	13	8
	6	1252.4	1279.9	1252.1	1220.8	1006.1	1.83	7.5803	5	4	0	10.3	1.83	3.29	10.08	14	7
	7	1253.7	1281.1	1252.4	1221.2	930.8	1.68	7.8	2	4	0	9.5	1.68	1.12	9.04	12	2
	8	1255.8	1281.5	1254.1	1222.1	952.6	1.72	7.634	2	4	0	10	1.72	1.98	9.31	13	4
	9	1254.6	1280.5	1253.4	1221.6	986.6	1.71	7.5803	2	5	0	9.6	1.71	2.18	9.23	16	4
	10	1255.3	1281.9	1253.6	1221.7	1035	1.68	7.8641	6	5	0	9.8	1.68	5.19	9.01	15	10
in y-Direction 100 %	1	1487.8	1541.4	1524.8	1494.4	811.4	4.06	28.122	28	2	1	18.6	4.04	28.77	16.15	23	135
	2	1486.4	1542	1525.4	1494.9	936.3	1.58	28.159	26	13	0	8.9	1.58	47.64	8.20	38	84
	3	1483.6	1537.6	1523	1493.8	1101.6	1.37	27.04	25	18	0	6.5	1.36	55.60	6.05	44	84
	4	1485.5	1539.4	1521.8	1493.6	1078.2	1.38	28.3	72	19	0	6.5	1.38	65.64	6.22	47	100
	5	1482.8	1538.5	1523.5	1493	971	3.01	27.408	31	10	2	11.5	3	23.55	14.43	68	81
	6	1483.9	1539.3	1523.7	1493.7	982.3	3	27.438	27	11	1	11.8	2.99	13.64	14.42	68	47
	7	1483.4	1538.6	1521.2	1492.5	1094.1	1.37	27.994	84	20	0	6.4	1.37	73.29	6.12	50	111
	8	1485.7	1539.4	1521.4	1493.8	1057.7	1.37	27.794	26	18	0	6.6	1.37	50.70	6.12	45	77
	9	1484.3	1538.9	1520.8	1492	763.4	1.67	27.794	24	14	0	9.4	1.66	40.75	8.90	43	76
	10	1485.8	1539.3	1519.6	1491.3	695.9	11.57	27.382	28	13	0	9.5	11.4	12.74	19.25	288	172

	P.N.	Temperature values in z-direction				t [^{0}C]	λ (O_2)	P_A kW	IM3000P				$\lambda_{corr.}$	Corrected values		E NOx [mg/kWh]	E CO [mg/kWh]
		I	II	III	IV				CO [ppm]	NO [ppm]	NO_2 [ppm]	O_2 [%]		CO [ppm]	O_2 [%]		
in y-Direction 70 %	1	1439.1	1476.1	1457.5	1418.7	720.5	5.75	17.672	29	4	0	18.9	5.7	28.75	17.56	44	192
	2	1439.8	1476.2	1456.8	1418	497.4	1.92	17.762	34	11	0	10.2	1.91	44.80	10.56	39	97
	3	1439.4	1477.4	1456.2	1417.7	1014.2	1.44	17.396	21	16	0	7.2	1.44	21.60	6.90	42	34
	4	1440.2	1478.9	1457.2	1418.5	1022.6	1.45	17.687	35	17	0	7.1	1.45	25.61	7.01	45	41
	5	1444.4	1480.4	1459.3	1420.6	729.8	2.26	17.513	11	14	2	9	2.25	9.52	12.18	67	24
	6	1441.3	1479.6	1457.8	1419.1	750.5	2.22	17.396	11	13	1	8.6	2.22	7.79	12.06	58	20
	7	1442.4	1480.3	1458.7	1419.8	1016.6	1.44	17.707	34	17	0	7.1	1.44	26.56	6.89	44	42
	8	1441.5	1480.7	1456.7	1419.3	1013.8	1.44	17.513	23	17	0	7.1	1.44	23.51	6.84	44	37
	9	1442.6	1481.8	1456.4	1419.2	572.9	2.05	17.476	37	11	0	10.2	2.05	35.48	11.28	42	82
	10	1441.8	1481.4	1456.6	1418.5	422.5	4.69	17.724	23	5	0	17.1	4.66	22.71	16.79	45	124
in y-Direction 40 %	1	1256.2	1274.4	1247.2	1219.4	11.51	877.5	8.07	27	4	0	11.2	2.12	51.31	11.60	16	123
	2	1256.6	1277.5	1250.2	1222.2	9.11	919.9	7.28	2	5	0	9.6	1.7	1.94	9.18	16	4
	3	1260.3	1279	1251	1223.4	8.94	952.4	7.66	2	6	0	9.3	1.68	1.05	9.01	18	2
	4	1262.6	1280.3	1252.5	1224.2	9.79	946.2	7.58	2	4	0	10.3	1.8	0.99	9.86	13	2
	5	1262.3	1281.4	1253.4	1223.8	10.27	909.9	7.80	0	5	0	10.6	1.88	0.00	10.35	17	0
	6	1262.2	1281.2	1253.1	1224.4	10.41	897.4	7.48	0	5	0	10.7	1.9	0.00	10.49	18	0
	7	1262.4	1280.9	1253	1223.9	8.76	942	7.69	1	5	0	9.3	1.65	1.05	8.83	15	2
	8	1262.6	1281.7	1253.4	1225.4	8.86	946.3	7.49	2	6	0	9.3	1.67	0.96	8.93	18	2
	9	1263.7	1281.3	1252.8	1224.3	9.1	906.9	7.18	0	5	0	9.6	1.7	1.06	9.17	16	2
	10	1261.5	1280.3	1251.9	1223.9	10	922.8	7.18	21	5	0	10.6	1.83	19.69	10.08	17	41

Table A.2. Measured and corrected values of the experiments; series B in the x- and y-direction

	P.N.	Temperature values in z-direction				t [^{0}C]	λ (O_2)	P_A kW	IM3000P				$\lambda_{corr.}$	Corrected values		E NOx [mg/kWh]	E CO [mg/kWh]
		I	II	III	IV				CO [ppm]	NO [ppm]	NO_2 [ppm]	O_2 [%]		CO [ppm]	O_2 [%]		
in x-Direction 100 %	1	1493.5	1522.8	1492.6	1468.3	1101.6	1.53	25.228	32	16	0	7.9	1.532	66.84	7.79	45	114
	2	1493.4	1521.7	1492.5	1467.5	1134.2	1.64	24.799	48	15	0	8.5	1.641	33.65	8.72	45	62
	3	1496.3	1522.5	1491.6	1466.8	1104.5	1.56	25.17	16	16	0	8.4	1.56	30.83	8.04	46	54
	4	1495.7	1522.6	1490.5	1466.2	1036.8	1.5	24.774	33	17	0	7.9	1.499	30.75	7.48	46	51
	5	1495.6	1521.8	1490.3	1466.3	1101.5	1.49	24.84	22	17	0	7.9	1.493	33.66	7.43	46	56
	6	1493.7	1521.2	1489.4	1465.7	1107.1	1.5	25.387	14	17	0	7.9	1.5	30.64	7.49	46	51
	7	1496.1	1521.5	1489.7	1465.8	1007.3	1.51	24.799	11	17	0	8.1	1.513	23.42	7.62	47	39
	8	1496.8	1521.7	1490.5	1466.4	1127.7	1.58	25.234	7	16	0	8.8	1.583	16.57	8.24	46	29
	9	1495.4	1520.5	1488.2	1465.3	1069.3	1.59	56.458	10.16	16	0	8.9	1.587	18.47	8.28	46	33
	10	1496.4	1521.3	1489.5	1465.2	1099.8	1.59	25.17	30	17	0	8.3	1.586	46.80	8.27	49	83
in x-Direction 70 %	1	1470.8	1492.6	1457.8	1418.3	1037	1.71	15.89	15	17	0	8.6	1.71	37.58	9.25	53	72
	2	1469.3	1491.4	1457.3	1417.6	1040.7	1.69	15.771	16	15	0	9.8	1.686	25.22	9.07	46	48
	3	1470.2	1492.3	1457.6	1418.2	1057.8	1.6	15.947	9	17	0	8.6	1.599	15.47	8.38	50	28
	4	1470.5	1492.4	1457.8	1418.3	956.1	1.54	15.947	8	17	0	8.4	1.539	12.80	7.86	48	22
	5	1471.6	1492.5	1458.3	1418.4	1038.2	1.59	15.728	10	17	0	8.7	1.585	19.43	8.26	49	34
	6	1470.7	1491	1456.8	1417.2	1038	1.59	15.765	9	17	0	8.7	1.591	15.47	8.31	49	27
	7	1469.6	1491.5	1456.6	1417.4	971	1.53	15.448	6	17	0	8.2	1.532	7.70	7.79	48	13
	8	1469.5	1490.8	1455.4	1416.4	1072.6	1.57	15.947	6	17	0	8.5	1.571	9.45	8.14	49	17
	9	1468.7	1489.9	1455.5	1416.5	995.9	1.71	16.008	29	15	0	9.9	1.713	15.42	9.27	47	30
	10	1469.3	1490.3	1455.2	1416	1048.8	1.7	15.863	10	17	0	8.4	1.702	33.59	9.19	53	64

	P.N.	Temperature values in z-direction				t [^{0}C]	λ (O_2)	P_A kW	IM3000P				$\lambda_{corr.}$	Corrected values		E NOx [mg/kWh]	E CO [mg/kWh]
		I	II	III	IV				CO [ppm]	NO [ppm]	NO_2 [ppm]	O_2 [%]		CO [ppm]	O_2 [%]		
in x-Direction 30 %	1	1192.4	1206.9	1175.1	1137.9	818.7	1.86	4.6	6	3	0	10.6	1.699	0.97	9.17	19	2
	2	1195.6	1210.2	1178.3	1139.6	828.9	1.77	4.7653	0	4	0	10.2	1.747	0.00	9.51	16	0
	3	1203	1216.6	1184.9	1144.8	863.8	1.73	4.7284	0	5	0	9.9	1.765	0.00	9.63	20	0
	4	1213	1224.9	1191.9	1150.1	836.6	1.79	4.7576	0	4	0	10.1	1.798	0.00	9.85	20	0
	5	1221.2	1231.5	1198.3	1155.1	785.2	1.95	4.7056	0	4	0	10.9	1.841	0.00	10.12	20	0
	6	1221.5	1232.1	1198.5	1155.2	785.1	2.03	4.485	0	5	0	10.9	1.778	0.91	9.72	20	2
	7	1228.7	1239.2	1204.3	1159.8	808.3	1.79	4.485	0	5	0	9.9	1.727	0.00	9.37	19	0
	8	1230.2	1240.3	1206.5	1162.3	872.3	1.68	4.5804	2	6	0	9.3	1.834	0.00	10.08	20	0
	9	1233	1242.6	1208.3	1163.5	842.9	1.91	4.4346	3	5	0	11	1.857	1.05	10.22	21	2
	10	1236.6	1246.3	1212.3	1166.3	810.8	1.76	4.3593	3	6	0	9.9	1.682	1.02	9.04	19	2
in y-Direction 100 %	1	1484.5	1520.7	1492.2	1467.2	873.6	1.64	25.355	8	10	0	8.7	1.639	21.76	8.70	30	40
	2	1485.3	1520.6	1492.3	1467.9	885.9	1.46	25.551	2	12	0	7.8	1.463	11.64	7.13	32	19
	3	1484.9	1520.2	1491.9	1466.7	1087.9	1.43	24.905	3	14	0	7.2	1.426	11.60	6.74	36	18
	4	1486.9	1520.7	1492.8	1466.5	1094	1.47	25.773	5	15	0	7.7	1.474	13.72	7.24	40	22
	5	1486.7	1520.1	1491.6	1466.7	905.2	1.59	24.592	17	14	0	8.4	1.592	12.69	8.32	41	23
	6	1488.5	1520.3	1491.4	1465.9	906.9	1.61	25.327	22	14	0	8.4	1.609	14.55	8.46	41	26
	7	1490.3	1520.8	1491.8	1466	1071.8	1.47	25.088	24	17	0	7.5	1.472	33.77	7.22	46	55
	8	1489.8	1520.4	1491.5	1465.6	1068.2	1.42	24.917	4	15	0	7.2	1.422	19.55	6.69	39	31
	9	1489.7	1520.6	1491.6	1465.8	788.7	1.5	24.799	3	13	0	7.7	1.498	24.34	7.47	35	40
	10	1490.1	1520.1	1490.2	1465.1	875.8	1.74	24.873	9	12	0	8.9	1.741	20.82	9.47	38	41

	P.N.	Temperature values in z-direction				t [^{0}C]	λ (O_2)	P_A kW	IM3000P				$\lambda_{corr.}$	Corrected values		E NOx [mg/kWh]	E CO [mg/kWh]
		I	II	III	IV				CO [ppm]	NO [ppm]	NO_2 [ppm]	O_2 [%]		CO [ppm]	O_2 [%]		
in y-Direction 70%	1	1464.3	1484.1	1449.2	1412.3	869.6	1.65	15.947	4	10	0	8.8	1.649	10.67	8.78	30	20
	2	1465.8	1486.7	1451.9	1414.1	804.8	1.48	15.947	3	13	0	7.7	1.475	8.72	7.25	35	14
	3	1466.1	1486.1	1451.5	1414	1013.2	1.48	15.947	3	15	0	7.6	1.48	6.98	7.30	40	11
	4	1465.5	1484.9	1449.6	1412	983.3	1.55	15.87	6	18	0	8.2	1.545	7.91	7.91	51	14
	5	1466.1	1484.5	1449.3	1412.5	881.1	1.76	16.093	5	16	0	8.6	1.756	5.95	9.57	52	12
	6	1466.2	1485.2	1449.9	1412.4	880.1	1.79	15.829	7	14	0	8.8	1.793	5.08	9.82	46	10
	7	1465.3	1485.4	1449.8	1412.7	994.5	1.54	15.714	14	17	0	8.4	1.544	12.74	7.90	48	22
	8	1467	1486.1	1450.6	1413	1017.2	1.48	15.765	4	15	0	7.5	1.48	11.41	7.30	40	19
	9	1466.7	1485.7	1450.3	1413.1	826.2	1.47	15.614	3	14	0	7.3	1.474	8.72	7.24	38	14
	10	1466.3	1486.2	1450.2	1412.8	604.5	1.68	15.947	4	10	0	9.1	1.676	11.58	8.99	31	22
in y-Direction 30%	1	1231.8	1241.3	1206.8	1159.4	941.2	1.7	4.5203	0	6	0	9.6	1.86	5.99	10.24	10	13
	2	1233.8	1242.8	1208.4	1162.2	910.6	1.75	4.8486	0	5	0	10.4	1.772	1.11	9.68	13	2
	3	1240.9	1248.2	1213.5	1167.2	845.1	1.76	4.485	0	6	0	10.5	1.729	0.00	9.38	16	0
	4	1245.8	1253	1217.7	1170.3	838	1.8	4.6433	0	6	0	10.4	1.787	0.00	9.78	13	0
	5	1246.6	1253.4	1218.9	1172.2	914.8	1.84	4.6986	0	6	0	9.7	1.937	0.00	10.69	14	0
	6	1248.3	1255.9	1221.3	1173.8	923	1.78	4.7488	0	6	0	10.1	2.027	0.00	11.17	19	0
	7	1251.8	1258.4	1223.4	1175.4	852.1	1.73	4.8927	0	6	0	9.6	1.795	0.00	9.83	17	0
	8	1252.1	1259.4	1224.2	1175.6	869.6	1.83	4.485	0	6	0	10.2	1.682	1.05	9.04	19	2
	9	1252.8	1260.4	1224.5	1176	918.2	1.86	4.4346	0	6	0	11.4	1.906	2.98	10.52	18	6
	10	1254.3	1260.3	1225.2	1176.5	962	1.68	4.485	0	6	0	9.7	1.762	3.00	9.61	19	6

Table A.3. Example of the measured and recorded values of the experiments. series A in the x- direction

Series A	Pos.N.	(Txz)mean (°C)	(Tyz)mean (°C)	Tmean (°C)	Tmean (K)	Troom (K)	Vxy (m^3/s)	Pmean(kW)	Res.t.(ms)
% 100	2	1463.8	1397	1430.4	1703.55	298.15	0.00155	27.8091	12.52205
	3	1439.42	1427.92	1433.67	1706.82	298.15	0.00153	27.44938	13.65823
	4	1431.56	1423.7	1427.63	1700.78	298.15	0.001563	28.0385	13.41623
	7	1429.46	1425.96	1427.71	1700.86	298.15	0.001557	27.93438	13.50853
	8	1440.8	1419.6	1430.2	1703.35	298.15	0.001528	27.41382	13.65958
	9	1456.82	1359.88	1408.35	1681.5	298.15	0.00154	27.6291	12.47072
% 70	3	1363.92	1360.98	1362.45	1635.6	298.15	0.000979	17.56236	21.13469
	4	1367.04	1363.48	1365.26	1638.41	298.15	0.000975	17.49208	21.1576
	7	1359.68	1363.56	1361.62	1634.77	298.15	0.000976	17.50708	21.27232
	8	1371.66	1362.4	1367.03	1640.18	298.15	0.000983	17.6353	20.96961
% 40	2	1201.1	1185.28	1193.19	1466.34	298.15	0.000413	7.41034	48.79467
	3	1192.26	1193.22	1192.74	1465.89	298.15	0.000416	7.46182	47.50936
	4	1199.04	1193.16	1196.1	1469.25	298.15	0.000411	7.373	47.73171
	7	1187.84	1192.44	1190.14	1463.29	298.15	0.000431	7.73298	47.52563
	8	1193.22	1193.88	1193.55	1466.7	298.15	0.000422	7.57122	47.65677
	9	1199.34	1185.8	1192.57	1465.72	298.15	0.000411	7.37534	48.71308

Series A			**Series B**		
Power Range (%)	P_{mean} (kW)	Res.t. (ms)	Power Range (%)	P_{mean} (kW)	Res.t. (ms)
100	27.71	13.21	100	25.06	13.82
70	17.55	21.13	70	15.84	21.61
40	7.49	47.99	30	4.60	76.99

Series B	Pos.N.	(Txz)mean (°C)	(Tyz)mean (°C)	Tmean (°C)	Tmean (K)	Troom (K)	Vxy (m^3/s)	Pmean(kW)	Res.t.(ms)
% 100	1	1415.76	1367.64	1391.7	1664.85	298.15	0.001409	25.27746	13.39
	2	1421.86	1370.4	1396.13	1669.28	298.15	0.001403	25.16982	13.69
	3	1416.34	1410.32	1413.33	1686.48	298.15	0.001395	25.0263	14.12
	4	1402.36	1412.18	1407.27	1680.42	298.15	0.001408	25.25952	14.10
	5	1415.1	1374.06	1394.58	1667.73	298.15	0.001377	24.70338	14.03
	6	1415.42	1374.6	1395.01	1668.16	298.15	0.001411	25.31334	13.59
	7	1396.08	1408.14	1402.11	1675.26	298.15	0.00139	24.9366	14.27
	8	1420.62	1407.1	1413.86	1687.01	298.15	0.001397	25.06218	14.01
	9	1407.74	1351.28	1379.51	1652.66	298.15	0.001382	24.79308	14.11
	10	1414.44	1368.26	1391.35	1664.5	298.15	0.001394	25.00836	12.94
% 70	1	1375.3	1335.9	1355.6	1628.75	298.15	0.000887	15.91278	20.59
	2	1375.26	1324.66	1349.96	1623.11	298.15	0.000883	15.84102	21.98
	3	1379.22	1366.18	1372.7	1645.85	298.15	0.000888	15.93072	22.08
	4	1359.02	1359.06	1359.04	1632.19	298.15	0.000886	15.89484	22.28
	5	1375.8	1338.7	1357.25	1630.4	298.15	0.000886	15.89484	20.69
	6	1374.74	1338.76	1356.75	1629.9	298.15	0.00088	15.7872	20.59
	7	1361.22	1361.54	1361.38	1634.53	298.15	0.000868	15.57192	22.77
	8	1380.94	1366.78	1373.86	1647.01	298.15	0.000883	15.84102	22.38
	9	1365.3	1328.4	1346.85	1620	298.15	0.000881	15.80514	21.88
	10	1375.92	1284	1329.96	1603.11	298.15	0.000886	15.89484	20.83
% 30	1	1156.1	1106.2	1131.15	1404.3	298.15	0.000254	4.55676	78.93
	2	1151.56	1110.52	1131.04	1404.19	298.15	0.000268	4.80792	75.65
	3	1142.98	1122.62	1132.8	1405.95	298.15	0.000257	4.61058	79.36
	4	1144.96	1123.3	1134.13	1407.28	298.15	0.000261	4.68234	76.16
	5	1161.18	1118.26	1139.72	1412.87	298.15	0.000262	4.70028	71.93
	6	1164.46	1118.48	1141.47	1414.62	298.15	0.000257	4.61058	72.84
	7	1152.22	1128.06	1140.14	1413.29	298.15	0.000261	4.68234	77.18
	8	1156.18	1142.32	1149.25	1422.4	298.15	0.000252	4.52088	79.52
	9	1166.38	1138.06	1152.22	1425.37	298.15	0.000248	4.44912	75.58
	10	1175.66	1134.46	1155.06	1428.21	298.15	0.000246	4.41324	82.74

Table A.4. Calculated and measured representative mean residence time as a function of the thermal power of the burner

Series A							
Power kW	Mean Res.t.(ms)	T = 1400K			T = 1700K		
		λ =1.3	λ =1.5	λ =2.0	λ =1.3	λ =1.5	λ =2.0
1	323.1396395	484.1345	423.8062	323.1396	398.699	349.0169	266.115
2	161.5698198	242.0672	211.9031	161.5698	199.3495	174.5084	133.0575
3	107.7132132	161.3782	141.2687	107.7132	132.8997	116.339	88.705
4	80.78490988	121.0336	105.9515	80.78491	99.67474	87.25422	66.52875
5	64.6279279	96.82689	84.76124	64.62793	79.73979	69.80337	53.223
6	59.00749829	80.68908	70.63436	53.85661	66.44983	58.16948	44.3525
7	50.57785568	69.16207	60.54374	46.16281	56.957	49.85955	38.01643
8	44.94914107	60.51681	52.97577	40.39245	49.83737	43.62711	33.26437
9	39.95479207	53.79272	47.08958	35.9044	44.29989	38.77965	29.56833
10	35.95931286	48.41345	42.38062	32.31396	39.8699	34.90169	26.6115
11	32.69028442	44.01222	38.52784	29.37633	36.24536	31.72881	24.19227
12	29.96609405	40.34454	35.31718	26.9283	33.22491	29.08474	22.17625
13	27.66100989	37.24111	32.60048	24.8569	30.66915	26.84745	20.47038
14	25.68522347	34.58103	30.27187	23.0814	28.4785	24.92978	19.00821
15	23.97287524	32.27563	28.25375	21.54264	26.57993	23.26779	17.741
16	22.47457054	30.2584	26.48789	20.19623	24.91869	21.81355	16.63219
17	21.15253698	28.4785	24.92978	19.00821	23.45288	20.5304	15.65382
18	20.67818597	26.89636	23.54479	17.9522	22.14994	19.38983	14.78417
19	19.5898604	25.48076	22.30559	17.00735	20.98416	18.36931	14.00605
20	18.61036738	24.20672	21.19031	16.15698	19.93495	17.45084	13.30575
21	17.72415941	23.05402	20.18125	15.3876	18.98567	16.61985	12.67214
22	16.9185158	22.00611	19.26392	14.68817	18.12268	15.8644	12.09614
23	16.18292815	21.04932	18.42636	14.04955	17.33474	15.17465	11.57022
24	15.50863948	20.17227	17.65859	13.46415	16.61246	14.54237	11.08812
25	14.8882939	19.36538	16.95225	12.92559	15.94796	13.96067	10.6446
26	14.31566721	18.62056	16.30024	12.42845	15.33458	13.42373	10.23519
27	13.78545732	17.93091	15.69653	11.96813	14.76663	12.92655	9.856111
28	13.29311955	17.29052	15.13594	11.5407	14.23925	12.46489	9.504107
29	12.83473612	16.69429	14.61401	11.14275	13.74824	12.03506	9.176379
30	12.40691158	16.13782	14.12687	10.77132	13.28997	11.6339	8.8705

Series B							
Power kW	Mean Res.t.(ms)	T = 1400K			T = 1700K		
		λ =1.5	λ =1.7	λ =2.0	λ =1.5	λ =1.7	λ =2.0
1	366.6894537	423.8062	376.8471	323.1396	349.0169	310.3446	266.115
2	183.3447268	211.9031	188.4235	161.5698	174.5084	155.1723	133.0575
3	122.2298179	141.2687	125.6157	107.7132	116.339	103.4482	88.705
4	91.67236342	105.9515	94.21176	80.78491	87.25422	77.58616	66.52875
5	66.57875015	84.76124	75.36941	64.62793	69.80337	62.06893	53.223
6	55.48229179	70.63436	62.80784	53.85661	58.16948	51.72411	44.3525
7	47.55625011	60.54374	53.83529	46.16281	49.85955	44.33495	38.01643
8	41.61171885	52.97577	47.10588	40.39245	43.62711	38.79308	33.26437
9	36.98819453	47.08958	41.8719	35.9044	38.77965	34.48274	29.56833
10	33.28937508	42.38062	37.68471	32.31396	34.90169	31.03446	26.6115
11	30.26306825	38.52784	34.25882	29.37633	31.72881	28.21315	24.19227
12	27.7411459	35.31718	31.40392	26.9283	29.08474	25.86205	22.17625
13	25.6072116	32.60048	28.98824	24.8569	26.84745	23.87266	20.47038
14	23.77812505	30.27187	26.91765	23.0814	24.92978	22.16747	19.00821
15	22.19291672	28.25375	25.12314	21.54264	23.26779	20.68964	17.741
16	21.53455562	26.48789	23.55294	20.19623	21.81355	19.39654	16.63219
17	20.26781705	24.92978	22.16747	19.00821	20.5304	18.25557	15.65382
18	19.14182722	23.54479	20.93595	17.9522	19.38983	17.24137	14.78417
19	18.13436263	22.30559	19.83406	17.00735	18.36931	16.33393	14.00605
20	17.22764449	21.19031	18.84235	16.15698	17.45084	15.51723	13.30575
21	16.40728047	20.18125	17.9451	15.3876	16.61985	14.77832	12.67214
22	15.66149499	19.26392	17.12941	14.68817	15.8644	14.10657	12.09614
23	14.98056043	18.42636	16.38465	14.04955	15.17465	13.49324	11.57022
24	14.35637041	17.65859	15.70196	13.46415	14.54237	12.93103	11.08812
25	13.7821156	16.95225	15.07388	12.92559	13.96067	12.41379	10.6446
26	13.25203423	16.30024	14.49412	12.42845	13.42373	11.93633	10.23519

Table A.5. Measured and calculated values of experiments for 10 kW porous burner

% 25				% 50				% 100			
	λ=1,4	λ=1,6	λ=1,8		λ=1,4	λ=1,6	λ=1,8		λ=1,4	λ=1,6	λ=1,8
V_2	0,05	0,062	0,068	V_2	0,08	0,092	0,102	V_2	0,112	0,124	0,134
V_1	0,046	0,058	0,066	V_1	0,072	0,086	0,098	V_1	0,106	0,114	0,126
ΔV [m^3]	0,004	0,004	0,002	ΔV [m^3]	0,008	0,006	0,004	ΔV [m^3]	0,006	0,01	0,008
Δt [s]	131	142	94	Δt [s]	117	91	63	Δt [s]	73	128	105
υ' [m^3/s]	3,053E-05	2,817E-05	2,128E-05	υ' [m^3/s]	6,838E-05	6,593E-05	6,349E-05	υ' [m^3/s]	8,219E-05	7,81E-05	7,619E-05
P [kW]	3,50	3,23	2,44	P [kW]	7,84	7,56	7,28	P [kW]	9,43	8,96	8,74
$T_W$outlet [^{0}C]	37,956	37,473	36,198	$T_W$outlet [^{0}C]	41,992	40,235	38,358	$T_W$outlet [^{0}C]	54,874	52,648	49,586
$T_W$inlet [^{0}C]	21,996	21,865	20,784	$T_W$inlet [^{0}C]	23,216	22,824	21,652	$T_W$inlet [^{0}C]	26,842	25,041	24,894
ΔT [^{0}C]	15,96	15,608	15,414	ΔT [^{0}C]	18,776	17,411	16,706	ΔT [^{0}C]	28,032	27,607	24,692
CO [ppm]	12	9	5	CO [ppm]	58	55	50	CO [ppm]	86	78	73
CO [mg/kWh]	22	17	9	CO [mg/kWh]	98	96	87	CO [mg/kWh]	133	122	117
NO [ppm]	10	8	7	NO [ppm]	13	13	12	NO [ppm]	16	18	14
NOx [ppm]	10	9	7	NOx [ppm]	14	13	12	NOx [ppm]	18	19	16
NOx [mg/kWh]	30	27	22	NOx [mg/kWh]	39	37	34	NOx [mg/kWh]	46	49	42
NO_2 [ppm]	0	1	0	NO_2 [ppm]	1	0	0	NO_2 [ppm]	2	1	2
SO_2 [ppm]	0	0	0	SO_2 [ppm]	0	0	0	SO_2 [ppm]	0	0	0
λ	1,7	1,72	1,76	λ	1,58	1,62	1,63	λ	1,45	1,47	1,5
T-Gas [^{0}C]	42,3	39,8	36,4	T-Gas [^{0}C]	52,7	50,3	47,9	T-Gas [^{0}C]	65,2	63,8	62,6
O_2 [%]	8,9	9,1	9,4	O_2 [%]	7,9	8,3	8,4	O_2 [%]	6,7	6,8	7,1
Su υ' [m^3/h]	0,436	0,432	0,434	Su υ' [m^3/h]	0,432	0,43	0,38	Su υ' [m^3/h]	0,438	0,436	0,432

Table A.4. Calculated and measured representative mean residence time as a function of the thermal power of the burner

Series A							
Power kW	Mean Res.t.(ms)	T = 1400K			T = 1700K		
		λ =1.3	λ =1.5	λ =2.0	λ =1.3	λ =1.5	λ =2.0
1	323.1396395	484.1345	423.8062	323.1396	398.699	349.0169	266.115
2	161.5698198	242.0672	211.9031	161.5698	199.3495	174.5084	133.0575
3	107.7132132	161.3782	141.2687	107.7132	132.8997	116.339	88.705
4	80.78490988	121.0336	105.9515	80.78491	99.67474	87.25422	66.52875
5	64.6279279	96.82689	84.76124	64.62793	79.73979	69.80337	53.223
6	59.00749829	80.68908	70.63436	53.85661	66.44983	58.16948	44.3525
7	50.57785568	69.16207	60.54374	46.16281	56.957	49.85955	38.01643
8	44.94914107	60.51681	52.97577	40.39245	49.83737	43.62711	33.26437
9	39.95479207	53.79272	47.08958	35.9044	44.29989	38.77965	29.56833
10	35.95931286	48.41345	42.38062	32.31396	39.8699	34.90169	26.6115
11	32.69028442	44.01222	38.52784	29.37633	36.24536	31.72881	24.19227
12	29.96609405	40.34454	35.31718	26.9283	33.22491	29.08474	22.17625
13	27.66100989	37.24111	32.60048	24.8569	30.66915	26.84745	20.47038
14	25.68522347	34.58103	30.27187	23.0814	28.4785	24.92978	19.00821
15	23.97287524	32.27563	28.25375	21.54264	26.57993	23.26779	17.741
16	22.47457054	30.2584	26.48789	20.19623	24.91869	21.81355	16.63219
17	21.15253698	28.4785	24.92978	19.00821	23.45288	20.5304	15.65382
18	20.67818597	26.89636	23.54479	17.9522	22.14994	19.38983	14.78417
19	19.5898604	25.48076	22.30559	17.00735	20.98416	18.36931	14.00605
20	18.61036738	24.20672	21.19031	16.15698	19.93495	17.45084	13.30575
21	17.72415941	23.05402	20.18125	15.3876	18.98567	16.61985	12.67214
22	16.9185158	22.00611	19.26392	14.68817	18.12268	15.8644	12.09614
23	16.18292815	21.04932	18.42636	14.04955	17.33474	15.17465	11.57022
24	15.50863948	20.17227	17.65859	13.46415	16.61246	14.54237	11.08812
25	14.8882939	19.36538	16.95225	12.92559	15.94796	13.96067	10.6446
26	14.31566721	18.62056	16.30024	12.42845	15.33458	13.42373	10.23519
27	13.78545732	17.93091	15.69653	11.96813	14.76663	12.92655	9.856111
28	13.29311955	17.29052	15.13594	11.5407	14.23925	12.46489	9.504107
29	12.83473612	16.69429	14.61401	11.14275	13.74824	12.03506	9.176379
30	12.40691158	16.13782	14.12687	10.77132	13.28997	11.6339	8.8705

Series B							
Power kW	Mean Res.t.(ms)	T = 1400K			T = 1700K		
		λ =1.5	λ =1.7	λ =2.0	λ =1.5	λ =1.7	λ =2.0
1	366.6894537	423.8062	376.8471	323.1396	349.0169	310.3446	266.115
2	183.3447268	211.9031	188.4235	161.5698	174.5084	155.1723	133.0575
3	122.2298179	141.2687	125.6157	107.7132	116.339	103.4482	88.705
4	91.67236342	105.9515	94.21176	80.78491	87.25422	77.58616	66.52875
5	66.57875015	84.76124	75.36941	64.62793	69.80337	62.06893	53.223
6	55.48229179	70.63436	62.80784	53.85661	58.16948	51.72411	44.3525
7	47.55625011	60.54374	53.83529	46.16281	49.85955	44.33495	38.01643
8	41.61171885	52.97577	47.10588	40.39245	43.62711	38.79308	33.26437
9	36.98819453	47.08958	41.8719	35.9044	38.77965	34.48274	29.56833
10	33.28937508	42.38062	37.68471	32.31396	34.90169	31.03446	26.6115
11	30.26306825	38.52784	34.25882	29.37633	31.72881	28.21315	24.19227
12	27.7411459	35.31718	31.40392	26.9283	29.08474	25.86205	22.17625
13	25.6072116	32.60048	28.98824	24.8569	26.84745	23.87266	20.47038
14	23.77812505	30.27187	26.91765	23.0814	24.92978	22.16747	19.00821
15	22.19291672	28.25375	25.12314	21.54264	23.26779	20.68964	17.741
16	21.53455562	26.48789	23.55294	20.19623	21.81355	19.39654	16.63219
17	20.26781705	24.92978	22.16747	19.00821	20.5304	18.25557	15.65382
18	19.14182722	23.54479	20.93595	17.9522	19.38983	17.24137	14.78417
19	18.13436263	22.30559	19.83406	17.00735	18.36931	16.33393	14.00605
20	17.22764449	21.19031	18.84235	16.15698	17.45084	15.51723	13.30575
21	16.40728047	20.18125	17.9451	15.3876	16.61985	14.77832	12.67214
22	15.66149499	19.26392	17.12941	14.68817	15.8644	14.10657	12.09614
23	14.98056043	18.42636	16.38465	14.04955	15.17465	13.49324	11.57022
24	14.35637041	17.65859	15.70196	13.46415	14.54237	12.93103	11.08812
25	13.7821156	16.95225	15.07388	12.92559	13.96067	12.41379	10.6446
26	13.25203423	16.30024	14.49412	12.42845	13.42373	11.93633	10.23519